

Structure and Function of DNA Photolyase and Cryptochrome Blue-Light Photoreceptors

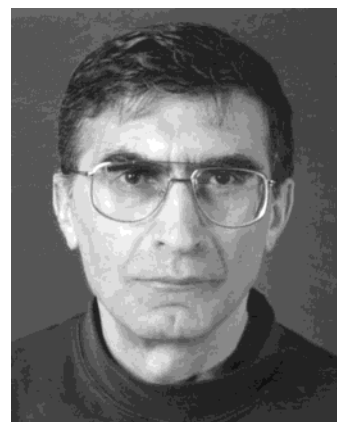
Aziz Sancar†

Department of Biochemistry and Biophysics, Mary Ellen Jones Building, CB 7260, University of North Carolina School of Medicine, Chapel Hill, North Carolina 27599

Received July 25, 2002

Contents

I. Introduction	2203
II. Photolyase	2204
A. Structure	2205
1. Primary structure	2205
2. Structures of chromophores	2205
3. Crystal structure of enzyme	2209
B. Reaction Mechanism	2210
1. Enzyme-substrate binding	2211
2. Catalysis	2213
3. Model Systems	2223
C. Photoreduction of Photolyase (Preillumination Effect)	2223
1. Electron Donor	2223
2. Electron Transfer Path	2225
3. Electron Transfer Mechanism	2226
4. Physiological Relevance	2226
D. Radical Reactions in Photolyase	2226
E. "Dark Function" of Photolyase	2227
F. Regulation of Photolyase	2227
III. (6–4) Photolyase	2228
IV. Cryptochromes	2230
A. Structure	2231
B. Function	2231
1. Circadian Rythm	2231
2. Mammalian Circadian System	2231
3. Cryptochromes and the Circadian Clock	2232
V. Perspectives	2234
VI. Acknowledgment	2235
VII. References	2235



Aziz Sancar is Distinguished Professor of Biochemistry and Biophysics at the University of North Carolina School of Medicine, Chapel Hill. He was born and raised in Turkey, where he received an M.D. degree in 1969 from the Istanbul University School of Medicine. He did his graduate work on DNA photolyase under the direction of Claud S. Rupert at the University of Texas at Dallas and obtained a Ph.D. degree in molecular biology in 1977. He did his postdoctoral work on DNA excision repair at Yale University in the laboratory of W. Dean Rupp. He joined the Department of Biochemistry of the University of North Carolina School of Medicine in 1982, where he has been conducting research on DNA repair mechanisms, DNA damage checkpoints, DNA photolyase, cryptochromes, and circadian photoreception.

reactions are the production of pyrimidine dimers in DNA by UV and the reversal of these photoproducts by photoreactivating enzyme (DNA photolyase, EC 4.1.99.3) using 350–450 nm light as an energy source or as a cosubstrate.⁵ The two major lesions in DNA induced by UV are the cyclobutane pyrimidine dimers (Pyr<>Pyr) and the pyrimidine–pyrimidone (6–4) photoproduct (Pyr [6–4] Pyr) (Figure 2). Both of these lesions are repaired by DNA photolyases of similar sequences and most likely similar structures and reaction mechanisms. However, a photolyase that repairs one cannot repair the other, and hence, the enzymes are often referred to as cyclobutane pyrimidine dimer (CPD) photolyase and (6–4) photolyase, respectively. Because the term "photolyase" was used to refer to cyclobutane pyrimidine dimer photolyase long before the discovery of (6–4) photolyase, for historical reasons as well as a matter of convenience, we will use the terms photolyase and (6–4) photolyase to refer to the two enzymes that repair Pyr<>Pyr and (6–4) photoproducts, respectively. Several reviews on photolyase have been published in the past decade.^{6–16}

I. Introduction

Photoreactivation^{1,2} is the reversal of the harmful effects, such as growth delay, mutagenesis, and killing, of far UV (200–300 nm) on organisms by concurrent or subsequent exposure to blue light (350–450 nm). A striking example of photoreactivation is the resurrection of UV-killed *Escherichia coli* by subsequent exposure to a light flash of millisecond duration³ (Figure 1). Although more than a single molecular process contributes to both UV inactivation and blue-light reactivation phenomena,⁴ the main

† Phone: (919) 962-0115. Fax: (919) 843-8627. E-mail: Aziz_Sancar@med.unc.edu.

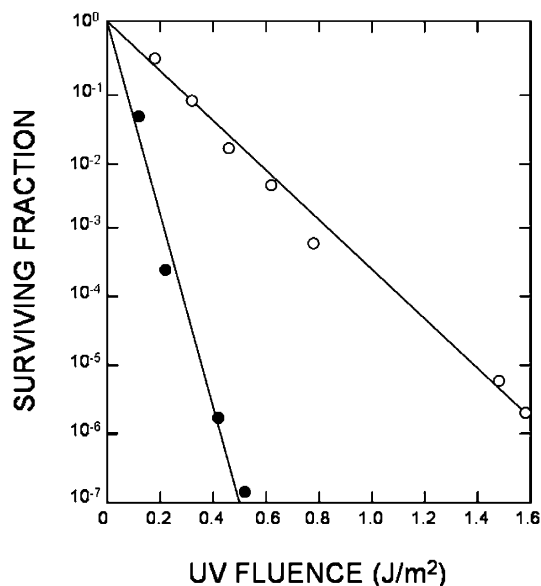


Figure 1. Photoreactivation. UV-killed *E. coli* were resurrected with a light flash of 1 ms. Key: closed circles, cells irradiated with UV and plated on growth medium; open circles, UV-irradiated cells exposed to a 1 ms camera flash before plating. Reprinted with permission from ref 3a. Copyright 1978 Elsevier.

A protein with high sequence homology to photolyases but with no photolyase activity has been found in plants, animals, and some bacteria and is referred to by the generic term cryptochrome.^{14,15,17} Cryptochromes regulate some of the blue-light responses in plants such as growth and development¹⁷ and synchronize the circadian rhythm with the daily light–dark cycles in animals.^{14,15} Circadian rhythm is the oscillation in the biochemical and behavioral functions of organisms with about 24 h periodicity (circa = about; dies = day). The rhythm is an innate property of many organisms ranging from cyanobacteria to humans, and it is maintained under constant conditions, that is, in the absence of environmental input to the system.^{18–22} However, in nature the rhythm is synchronized with the solar day by light, which affects different organisms differently, such that humans are active during the light phase (diurnal) and mice are active during the night phase (nocturnal) of the day. The cryptochrome blue-light photoreceptor appears to be the major photoreceptor for entraining (synchronizing) the circadian clock to the daily light–dark cycles in many organisms including humans and mice.

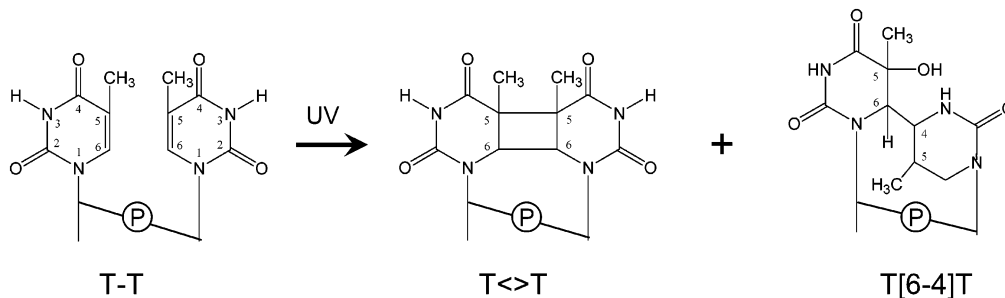


Figure 2. UV-induced DNA photoproducts. The two major lesions induced in DNA by ultraviolet irradiation are pyrimidine cyclobutane dimers and pyrimidine–pyrimidone (6–4) photoproducts. The figure shows the photoproducts that form between adjacent thymines. The same type of photoproducts may form between any type of adjacent pyrimidines T–T, T–C, C–T, and C–C except the (6–4) photoproduct does not form at C–T sites.

Photoreactivation and circadian photoentrainment may have had a common origin.²³ It is conceivable that, in the distant past when more UV reached the earth's surface, the same blue-light photoreceptor was used to repair the UV damage to DNA (photolyase) and to regulate the circadian behavior (cryptochrome) in a primitive organism such as to minimize the occurrence of DNA damage and to repair it with a readily available energy source (blue light) when damage occurred. Subsequently, this hypothesis suggests that the blue-light photoreceptor carrying out these functions diverged to give rise to present day photolyases and cryptochromes.

Despite the apparent selective advantage they give, neither photolyase nor cryptochrome is universally found in all species. In fact, there are some species from all three kingdoms of life that do not have these proteins. Of significance, photolyase and (6–4) photolyase are absent in placental mammals including humans,^{24,25} (6–4) photolyase has, as yet, not been found in prokaryotes, and the role of cryptochrome in certain bacteria such as *Vibrio cholerae*, which do not have a circadian rhythm, remains to be determined (Table 1). Finally, interestingly, certain animal viruses carry their own photolyase gene.^{12,26,27}

II. Photolyase

Photolyases are monomeric proteins of 450–550 amino acids and two noncovalently bound chromophore cofactors. One of the cofactors is always FAD, and the second is either methenyltetrahydrofolate (MTHF) or 8-hydroxy-7,8-didemethyl-5-deazariboflavin (8-HDF). Accordingly, the enzymes have been classified into folate class and deazaflavin class photolyases.^{28,29} Figure 3 shows near-UV/vis absorption spectra of two representatives of these two classes. The FAD is the essential cofactor both for specifically binding to damaged DNA and for catalysis.^{30–33} The “second chromophore” (MTHF or 8-HDF) is not necessary for catalysis and has no effect on specific enzyme–substrate binding. However, under limiting light the second chromophore may increase the rate of repair 10–100-fold depending on the wavelength used to effect catalysis. This is because the second chromophore has a higher extinction coefficient than FADH[–] and an absorption maximum at longer wavelength relative to that of the two-electron-reduced flavin that is the active form

Table 1. Distribution of Photolyase and Cryptochromes in Three Kingdoms^a

	enzyme/photoreceptor		
	photolyase	(6–4) photolyase	cryptochrome
Eubacteria			
<i>E. coli</i>	+	–	–
<i>B. subtilis</i>	–	–	–
<i>B. firmus</i>	+	–	–
<i>Synechocytis</i> sp.	+	–	+?
<i>V. cholerae</i>	+	–	+ (2)
Archaea			
<i>M. thermoautotrophicum</i>	+	–	–
<i>M. Jannaschii</i>	–	–	–
Eukarya			
<i>S. cerevisiae</i>	+	–	–
<i>S. pombe</i>	–	–	–
<i>C. elegans</i>	–	–	–
<i>D. melanogaster</i>	+	+	+
<i>X. laevis</i>	+	+	+ (3)
<i>H. sapiens</i>	–	–	+ (2)
<i>A. thaliana</i>	+	+	+ (2)

^a The presence or absence of photolyase/cryptochromes is based on data from direct analyses as well as genome sequences. The sequence of *V. cholerae* reveals three photolyase homologues. One encodes photolyase; the other two may function as blue-light photoreceptors (cryptochrome). *X. laevis*, *H. sapiens*, and *A. thaliana* contain three, two, and two cryptochrome genes, respectively.

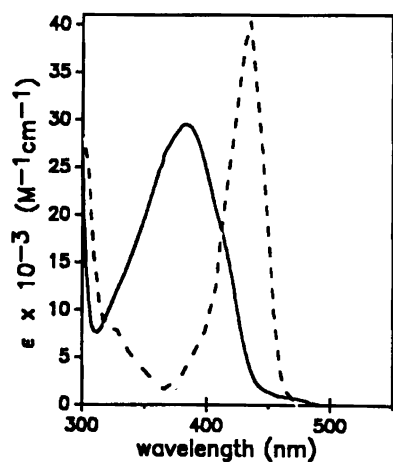
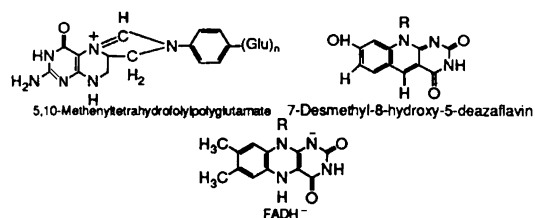


Figure 3. Absolute absorption spectra of folate and deazaflavin class photolyases in the near-UV/vis. These are the absorption spectra of *E. coli* photolyase (solid line, folate class) and *A. nidulans* photolyase (dashed line, deazaflavin class). The structures of the chromophore cofactors responsible for the UV/vis absorption are shown above the spectra. All deazaflavin class photolyases have essentially the same absorption spectrum with a peak at 440 nm, whereas the absorption maxima of folate class photolyases range from 370 to 420 nm. Adapted from ref 28.

of the flavin in the enzyme. In the following we will first summarize our current knowledge on the structure of the enzyme and then analyze the reaction mechanism of repair and repair-related phenomena.

A. Structure

1. Primary Structure

The amino acid sequences of about 50 photolyases are known. The sequences of these proteins reveal varying degrees of homology ranging from 15% to 70% or more sequence identity.¹² Several points of interest that emerge from sequence alignment are the following. (1) The C-terminal 150 amino acids exhibit the highest degree of homology among all photolyases belonging to both the folate and deazaflavin classes, and hence, this region was predicted to be the FAD binding domain.³⁴ This was later confirmed by both protein chemistry³⁵ and crystallography.^{36–38} (2) In general, plant and animal photolyases show a limited degree of homology (usually confined to the FAD binding site) to microbial photolyases,^{39,40} and hence, photolyases were divided into type I (microbial) and type II (animal) sequence groups. However, with the availability of more gene sequences in the photolyase/cryptochrome family,^{12,27} it appears that there are more sequence groups in the family that limit the utility of sequence type classification for the present. (3) Photolyases show no obvious sequence homology to flavoprotein oxidoreductases. This has been rationalized by suggesting that photolyases bind to both ground-state and excited-state flavin as opposed to oxidoreductases, which operate with a flavin from the ground state.¹⁰ Since the excited state of a molecule, to a certain degree, represents a different species, a protein that accommodates both ground- and excited-state flavin is not expected to have the same active site geometry as a protein operating from the ground-state cofactor only.¹⁰ However, a recent molecular phylogenetic analysis has found some distant relationship between photolyases and other nucleotide binding proteins including class I aminoacyl-tRNA synthetases and electron-transport flavoproteins.⁴¹ Sequence comparisons among some members of the photolyase/cryptochrome family highlighting the highly conserved C-terminal region are shown in Figure 4.

2. Chromophore Cofactors

All photolyases contain FAD and either MTHF or 8-HDF as the second chromophore (Figure 5). The properties of these are briefly summarized below.

a. Flavin. Flavin is perhaps the most commonly used cofactor in nature. At least 151 enzymes are known to use FAD and/or FMN as cofactors.⁴² FAD is the most common form of flavin found in enzymes. Flavin can be reduced and oxidized by one- and two-electron-transfer reactions, and as a consequence in electron-transfer reactions in nature it functions as a redox switch between NADH and heme, which can carry out only two- and only one-electron-transfer reactions, respectively.⁴³ The active form of flavin in photolyase is the two-electron-reduced form.⁴⁴ FAD is bound noncovalently but very tightly to *E. coli* and *A. nidulans* photolyases and can be released only after mild denaturation of the enzyme.^{45–47} Interestingly, even though an *E. coli* cell contains only about 10–20 free FAD molecules, when *E. coli* photolyase is amplified from the physiological level of 10–20

E.c. CPD	-----TTHLVVFRQDLRLHDNLALA-----AACRNS SARVLALYIATPRQWATHMMSPRQAEILINAQLNGLQIALAEK	68
D.m. 6-4	-----MDSQRS-----TLVHWFRKGLRLHDNPALSHIFTAANAAPGKYFVRPIFILD PGILDWMQVGANRWRFLQQTLEDLDNQLRKL	78
A.t. CRY1	-----MSGSVGGCGSGGCSLVMFRDLRFVEDNPAL-----AAAVRAGPVIALFVWAPEEFGHYHPGRVSRWUWLNKSLAQLDSSLRSL	77
H.s. CRY1	-----MGV-----NAVHWFRKGLRLHDNPAL-----KECIQGADTIRCVYILD PWFAGSSNVGINRWRFLQLCLEDLDANLRKL	69
H.s. CRY2	MAATVATAAAVAPAPAFGTDSA-----SSVHWFRKGLRLHDNPAL-----LAAVRGARCVRVCYILD PWFASSSSVGINRWRFLQLSLEDLDTSLRKL	88
<hr/>		
E.c. CPD	GIPLLFREVDDFVASVEIVKQVCAENSVTHLFYNYQYEVMERARDVEVERALRN--VYCEGFDDSVILPFGAVMTGNHE---MYKVFTPKNNAWLKRLR	162
D.m. 6-4	NSRLFVVRG---KPAEVFPRIKSWRVEMLTFETDIEPYSVTRDAAVQKLAKEAGVRVETHCSHTIYNPELVIAKRLGKAPITTYQKFLGIVEQLKVPKV	174
A.t. CRY1	GTCLITKRST--DSVASLLDVVKSTGASQIFFNHLYDPLSLVRDHRADVLTAQGIAVRSFNADLLYEP-WEVTDDELGRPFMSFAAFW-----ERC	165
H.s. CRY1	NSRLFVVRG---QPADVFPRLFKENWITKLSIEYDSEPPGKERDAAIKKLATEAGVEVIVRISHTLYDLDKIIEIENGGQPPLTYKRFOTLISKMEPLEI	165
H.s. CRY2	NSRLFVVRG---QPADVFPRLFKEWGVRITLTFEYDSEPPGKERDAAIMKMAKEAGVEVVTENSHTLYDLDRIIENGGQKPLTYKRFQAIISRMELPKK	184
<hr/>		
E.c. CPD	EGMPECVAAKVRSSGSIIEPSPSITLNYP-----RQSFDTAHPFVEEKAALIAQLRQFCQNG--AGEYEQRDFP--AVEGTSRLSASLATGGLSPR-	249
D.m. 6-4	LGVPEKLNKMPFPKDEVEQKDSAAAYDCPTMKQLVKRPEELGPNKFPGGETEALRMEESLKDEIUVARFEKPTAPNSLEPSTTVLSPYLKFGCLSR-	273
A.t. CRY1	LSMPLDPEPPLLPPKLIISGDVSKCVADP--LVFEDDSEKGSNALLARAWSPGWNGDKALTTIFNGPLLEYSKRRKADSAITTSFLSPHLHFGVSVRK	263
H.s. CRY1	P-VETITSEVIEKCTTPLSDDHDEKYGVPSLEELGFDTDGLSSAVVPGGETEALTRLERHLERKAWVANFERPRMNANSLASPTGLSPYLRFGCLSCR-	263
H.s. CRY2	P-VGLVTSQQMESCRAEIQENHDETYGVPSLEELGFPTEGLGPAVWQGGETEALARLDKHLERKAWVANFERPRMNANSLASPTGLSPYLRFGCLSCR-	282
<hr/>		
E.c. CPD	-----QCLHRLAEQFQALDGGAGSVWLNELINREFYRHLYTHPSLCKHRPFIAWDRVQWQSNPAHLQANQEGKTYPIVDAAMRQLNSTGUMHRL	343
D.m. 6-4	---LNFQKLEIKRQPKHSQP-PVSLIGQLM-WREFFYTVAAAEENFDRMLGNV-YCMQIPWQEHDPDHEAETHGRTGYPFIDAIMRQLRQEGWIHHLA	367
A.t. CRY1	VFHLVRIKQVAVANEGNEAGEE-SVNLFLKSTGLREYSRYISFNHPYSHERPLLG-HLKFFPWAVDENYFKAWRQGRTYGPIVDAAGMRELWATGWLHRI	361
H.s. CRY1	---LFYFKLTDLYKKVKNSSP-PLSLYGQLL-WREFFYTAATNPNRFDKMEGNP-ICVQIPMDKNPEALAKWAEGRTFGPWIDAIMTQLRQEGWIHHLA	357
H.s. CRY2	---LFYFRLWDLYKKVKNSTP-PLSLYGQLL-WREFFYTAATNPNRFRMEGNP-ICVQIPMDRNPEALAKWAEKGTGFPWIDAIMTQLRQEGWIHHLA	376
<hr/>		
E.c. CPD	RMITASFLVK-DLLIDWREGERYFMSQLIDGDLAANNGGWAASTGTDAAPIYRIFNPTTQGEKFDHEGEFTRQNLPELRDVPKGVVHEPWKMAQKAG-	441
D.m. 6-4	RHAVACFLTRGDLWISWEEGQRVFEQLLDQDQWALNAGNWMWLS-ASAFFHQYFRVYSVPAVFGKKTDPQGHYIRKYVPELSKYPAAGCIYE PWKASLVDQR	466
A.t. CRY1	RVVVSSFFVK-VLQLPWRWGMKYFDWTLDDADLESADALGQYITGTLDPDSREFDRIIDNPQFEGYKDPNGEYVRRULPELSRLPTDWIHPWNAPEVLQ	460
H.s. CRY1	RHAVACFLTRGDLWISWEEGKRVFEELLDADW SINAGSWMWLS-CSSFFQQFFHCYCPVGFGRRTDPNGDYIRRYLPVLRGFPKAYIYDPWNAPEGIQK	456
H.s. CRY2	RHAVACFLTRGDLWISWESGVRVFEELLDADFSVNAGSWMWLS-CSAFFQQFFHCYCPVGFGRRTDPNGDYIRRYLPKLLKAFP SRYIYEPWNAPESIQK	475
<hr/>		
E.c. CPD	-----VILDYFPQIVEHKEARVQTLAAYEAARKGK-----	471
D.m. 6-4	AYGCVLGTIDYPHRIKHEVVKENIKRMGAAYKVMREVR-----TGKEEE-----SSFEKSET	520
A.t. CRY1	AAGIELGSNYPLPIVGLDEAKARLHEALSQWQLEASRAAIENGSEELGDSAEVEEAPIEFPRDITMEETEPTRLNPNRRYEDQMVPSITSSLRPEE	560
H.s. CRY1	WAKLIGVNYPKPMVHAEASRLNIERMKQIYQQLSRYRGLGLLASVPSN-----PNGNGGFMGYSANI-----PGCSSSGSCS	531
H.s. CRY2	AAKCIIGVDYPRPIVNHAEATSRNLNIERMKQIYQQLSRYRGLGLLASVPSN-----VED---L SHPVAE-----PSSSQAGSM	545
<hr/>		
E.c. CPD	-----	
D.m. 6-4	STSGKRVRRATGSAP-----KPKK-----	540
A.t. CRY1	DEESSLNLENSVQDSRAEVPRNMVNTINQAQRRAEPASNQVTAMIEFNIRIIVAEATEDSTAESSSSGRRERSGGIVPEWSPGYEQFPSEENRIGGGST	660
H.s. CRY1	QSGSGLHYAHGDSQTHLLKQGRSSMGTGLSGGKRPSQEEDTQSIGPKVQRQSTN-----	586
H.s. CRY2	S-AGPRPLPSGPA SPKRKLEAAEPPGEELSKRVAELP-----TPELPSKDA-----	593
<hr/>		
E.c. CPD	-----	
D.m. 6-4	-----	
A.t. CRY1	TSSYLQNHHEILNWRRLSQTG	681
H.s. CRY1	-----	
H.s. CRY2	-----	

Figure 4. Sequence homology among members of the photolyase/cryptochrome family. In the alignment representatives of photolyase, (6-4) photolyase, and plant and animal cryptochromes are included. Key: yellow, identical; blue, most frequent; pink, strongly similar; green, weakly similar; Ec, *E. coli*; Dm, *D. melanogaster*; At, *A. thaliana*; Hs, *Homo sapiens*.

molecules per cell⁴⁸ to about 10⁵ molecules per cell by genetic engineering,⁴⁹ the enzyme still contains FAD at virtually 1:1 stoichiometry with respect to the apoenzyme.⁵⁰ However, many members of the photolyase/cryptochrome family do not contain stoichiometric FAD when expressed in heterologous systems. For example, when *M. thermoautotrophicum* photolyase is expressed in *E. coli*, it contains no FAD⁴⁰ and the *Drosophila melanogaster* (6-4) photolyase⁵¹ and cryptochrome,⁵² and human cryptochromes 1 and 2^{25,53} overproduced in *E. coli* contain only 1–5% FAD, whereas *Xenopus laevis* (6-4) photolyase⁵⁴ and *Arabidopsis thaliana* cryptochrome¹⁵⁵ overproduced in *E. coli* contain a stoichiometric amount of FAD. Regarding the flavin cofactor of photolyases, a final point of interest is the redox

status of the cofactor. FAD can be found in three redox states: oxidized, one-electron-reduced (neutral blue radical or anionic red radical), and two-electron-reduced (neutral or anionic) forms. The absorption and EPR spectra of purified *E. coli* photolyase, which contains MTHF and the FADH^o flavin neutral radical, is shown in Figure 6, and absorption spectra of *E. coli* photolyase containing the flavin in one- or two-electron-reduced forms and with and without the MTHF cofactor are shown in Figure 7. The active form contains the two-electron-reduced FADH⁻.^{32,44,55} Under physiological conditions FAD is synthesized in the FAD_{ox} form and is incorporated into appropriate apoenzymes in this form; it is converted into one- and two-electron-reduced forms as part of its catalytic cycle. However, we know of no light-independent

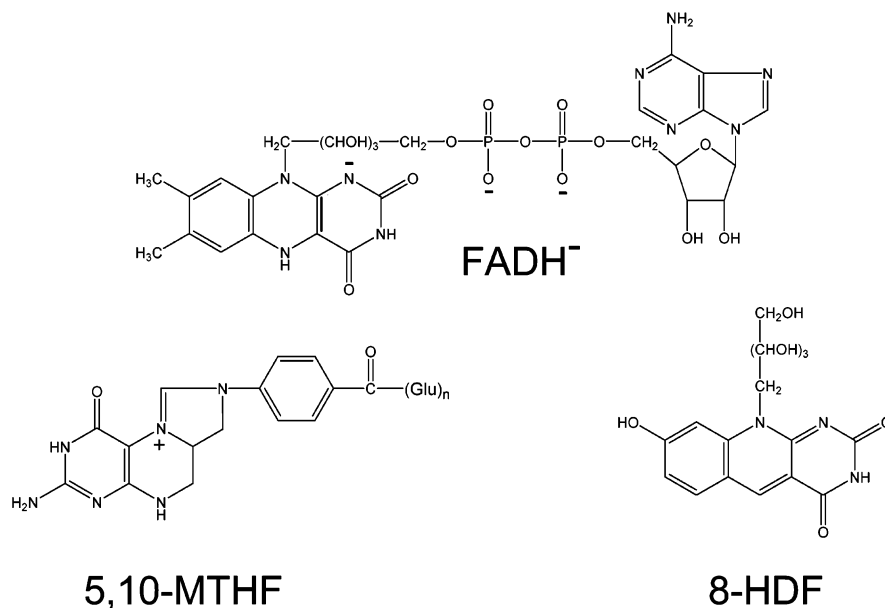


Figure 5. Cofactors of the photolyase/cryptochrome family. All family members contain FAD, which in all functionally characterized enzymes is in the form of two-electron-reduced anionic flavin. The FAD is the essential catalytic cofactor. In addition, the enzymes contain a second chromophore, which is either a pterin in the form of methenyltetrahydrofolate or a deazaflavin in the form of 8-hydroxydeazariboflavin. The second chromophores are not essential for activity, but because of their higher extinction coefficients than FADH⁻ in the near-UV/blue region, they are responsible for absorbing >90% of the photoreactivation photons in sunlight.

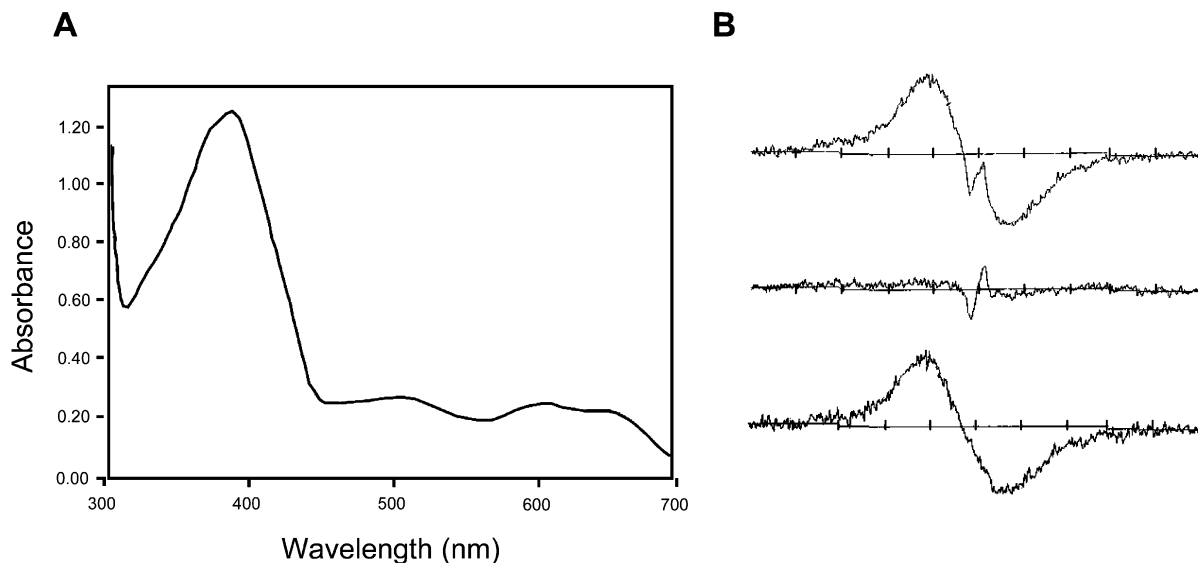


Figure 6. Detection of flavin neutral radical in *E. coli* photolyase by UV/vis and EPR spectroscopy. (A) Absorption spectrum. The peak at 380 nm is mostly due to MTHF. The peaks at 480 and 580 nm and the shoulder at 625 nm originate from the FADH[•] blue-neutral radical. (B) EPR spectra. Spectra were recorded at -90 °C at microwave power 0.5 mW, modulation amplitude 2.5 G, and microwave frequency 9.07 GHz. The prominent signal with a line width of 19 G is typical of flavin neutral radical. Key: top, enzyme; middle, buffer; bottom, enzyme-buffer. Each division on the x-axis is 10 G. Reprinted from ref 64. Copyright 1987 American Chemical Society.

redox reaction carried out by photolyase, and thus, at present the mechanism by which the photolyase flavin is converted into FADH⁻ is unknown. As will be discussed below, photolyase containing FADH[•] can be reduced photochemically,^{30,33} but even cells grown in the dark, or cells with nonphotoreducible mutants of photolyase, contain the flavin in the two-electron-reduced form. Thus, photoreduction does not appear to be the only mechanism of converting flavin to its active form in vivo. Interestingly, in *Chlamydomonas reinhardtii* the photolyase function is determined by two genes; *PHR2* encodes the photolyase apoenzyme

and requires the product of the *PHR1* gene for full activity.⁵⁷ However, in this case the endogenous and overproduced photolyase encoded by *PHR2* was largely inactive in both binding and catalysis. Since photolyase with FAD in all three oxidation states binds to DNA with essentially the same affinity,⁴⁴ it appears that *PHR1* of *C. reinhardtii* most likely plays a role in loading photolyase with FAD rather than reducing the cofactor.

With the exception of *Saccharomyces cerevisiae* photolyase,⁵⁸ the flavin cofactor of all photolyases characterized to date becomes oxidized to the FADH[•]

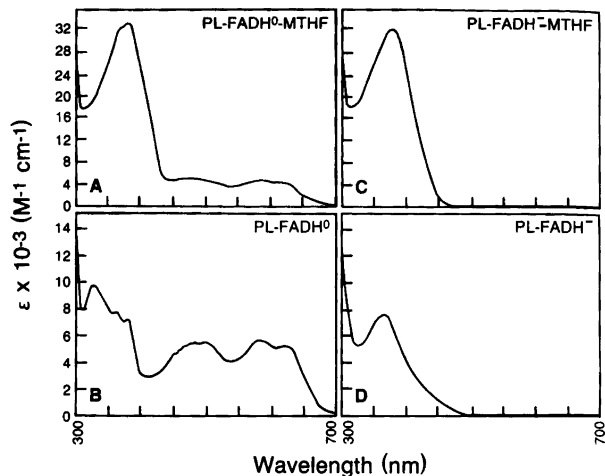


Figure 7. Absorption spectra of different States of *E. coli* photolyase. During purification the flavin cofactor of the enzyme is oxidized to the neutral radical form and the folate cofactor may be partially or completely lost. The folate absorption can be eliminated by exposure to strong light or treatment with sodium borohydride. Similarly, the flavin cofactor can be reduced photochemically or by treatment with dithionite. As a consequence, photolyase that contains flavin in either one-electron-reduced (panels A and B) or two-electron-reduced (panels C and D) form, and with (panels A and B) and without (panels B and D) MTHF may be obtained. The absorption spectra of these various forms which were crucial in understanding the reaction mechanism are shown.

blue-neutral radical or to FAD_{ox} during purification.^{59–61} This conversion is particularly striking in *E. coli* photolyase as shown by the following example: The *E. coli* cell pellet that contains photolyase at about 15% of the total cellular proteins is EPR silent; however, upon cell lysis a strong EPR signal ascribed to FADH^{\bullet} appears⁴⁴ along with the characteristic FADH^{\bullet} absorption bands at 480, 580, and 625 nm (Figure 8). This form of flavin is catalytically inert and must be either chemically or photochemically reduced to FADH^- to activate the enzyme.^{44,62–64}

b. Pterin. The majority of photolyases contain a pterin as the photoantenna. In *E. coli* photolyase⁶⁵ and other folate class photolyases expressed in *E. coli*,⁶⁶ the pterin is in the form of 5,10-methenyltetrahydropteroylpolyglutamate (methenyltetrahydrofolate, MTHF). The number of glutamates ranges from three to six, and the polyglutamate contains the novel $(\gamma_3)(\alpha_n)$ linkage.⁶⁵ The α -linkage of folate glutamates so far has been observed only in prokaryotes. In contrast to flavin, the folate cofactor dissociates from some of photolyases readily. Thus, *E. coli* photolyase purified through several columns contains substoichiometric (20–30%) folate, mainly because MTHFs with three to four Glu residues are lost during purification.^{67–69} Despite the importance of the polyglutamate tail, however, the enzyme can be made to contain stoichiometric amounts of the monoglutamate form of MTHF by incubating either the apoenzyme or the E-FAD form of the enzyme with the chromophore at high enzyme and cofactor concentrations.⁶⁵ The 5,10-methenyl bridge of the folate is responsible for the near-UV absorption at 360 nm. However, upon binding to the apoenzyme polar interactions with the positive charge on the methenyl

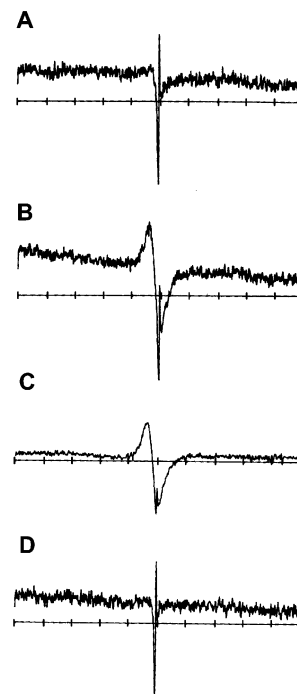


Figure 8. EPR spectra of *E. coli* photolyase in vivo and in vitro: (A) cell pellet; (B) concentrated cell-free extract; (C) Blue-Sepharose column peak fraction; (D) buffer. Note the 19G flavin blue radical signal in the concentrated cell extract (B) but not in the cell pellet (A). Each division on the x -axis represents 10 G. Reprinted from ref 44. Copyright 1987 American Chemical Society.

group combined with the hydrophobic interactions of the pterin ring within the binding pocket cause a red shift such that in all folate class photolyases studied to date the λ_{max} is at longer wavelength than 360 nm with absorption maxima ranging from 377 nm in *S. cerevisiae* photolyase⁵⁸ to 390 nm in *Neurospora crassa*⁷⁰ and 415 nm in *Bacillus firmus* photolyases.⁷¹

c. Deazaflavin. The second chromophore of the deazaflavin class enzymes is 8-hydroxy-7,8-didemethyl-5-deazariboflavin, which is also called F_0 .⁷² In fact, for many years F_0 was thought to be the only cofactor in deazaflavin class photolyases.^{73,74} Only after the discovery of the two-chromophore photoantenna–photocatalyst system in *E. coli* photolyase^{32,59,65} was it found that the deazaflavin class enzymes also contained FAD. This led to the realization that FADH^- is the universal photocatalyst in all photolyases.⁶⁰ 5-Deazaflavin was first discovered in anaerobic methanogenic bacteria and was named F420 for its absorption peak at 420 nm.⁴³ In fact F420 is a F_0 derivative containing four to eight γ -glutamates linked to the ribityl phosphate group of F_0 , reminiscent of the folate polyglutamate tail. F420 in the ground state is an obligatory two-electron redox cofactor and functions in this capacity in enzymes involved in methane and chlorotetracycline synthesis. Thus, despite its name and structural similarity to flavin 5-deazaflavin, it is in fact functionally more analogous to NAD, which also can only carry out a two-electron redox reaction. Hence, because of its relative abundance in archaea, and because of its redox properties, 5-deazaflavin has been called an “ancient molecule” and an “NAD in a flavin coat”.⁴³

Table 2. Biochemical Properties of Photolyases^a

enzyme	<i>E. coli</i>	<i>A. nidulans</i>
class	folate	deazaflavin
protein size (amino acids)	471	484
M_r	53994	54475
subunit	monomer	monomer
cofactors	FADH ⁻ + MTHF	FADH ⁻ + 8-HDF
absorption maxima (nm)		
E-FADH ^o -SC	384, 480, 580	438, 480, 588
E-FADH ⁻ -SC	384	438
E-SC	384	438
E-FADH ⁻	366	355
fluorescence emission maxima (nm)		
E-FADH ^o -SC (weak)	465, 505	505, 470
E-FADH ⁻ -SC	465	470, 505
E-SC	465	470
E-FADH ⁻	505	505
binding constant (K_D)	10^{-8} to 10^{-9} M	10^{-8} to 10^{-9} M
catalytic constant (k_{cat})	1.0 s^{-1}	1.0 s^{-1}
quantum yield of repair (Φ_r)		
E-FADH ^o -SC	0.7–0.75	0.9–1.0
E-FADH ⁻	0.8–0.9	0.9–1.0

^a Adapted from ref 10.

Despite the latter designation, however, 5-deazaflavin in its excited state is a strong one-electron reductant and is often used in this capacity to reduce flavoproteins.⁷⁵ Perhaps for this reason 5-deazaflavin was considered a candidate for Pyr <> Pyr photosplitting even after the two-chromophore system was discovered in deazaflavin class photolyases.⁶⁰ However, the E-8HDF form of *A. nidulans* photolyase neither specifically binds to nor repairs Pyr <> Pyr.⁴⁷ Thus, as in the case of MTHF, 8-HDF appears to function strictly as a photoantenna. Like MTHF the relatively strong interaction of 8-HDF with the apoenzyme causes a 20 nm red shift in the absorption maximum to 440 nm. In contrast to folate class enzymes, however, all of the deazaflavin class enzymes have the same absorption maximum at 440 nm.^{71–74,76} In addition, 8-HDF appears to be tightly bound to the apoenzyme and is present in stoichiometric amounts in all well-characterized deazaflavin class enzymes.^{72,76} Certain biochemical properties of *E. coli* (folate class) and *A. nidulans* (deazaflavin class) photolyases are summarized in Table 2.

3. Crystal Structure

Crystal structures of three photolyases have been determined: *E. coli*,³⁷ *A. nidulans*,³⁸ and *Thermus thermophilus*.⁷⁷ Although the first belongs to the folate class and the latter two belong to the deazaflavin class, and the level of overall homology among these enzymes is only about 25% sequence identity, the structures of all three are remarkably similar. The rms deviations for C α atoms common to photolyase pairs are 1.12 Å for *E. coli*–*A. nidulans* photolyases (413 C α atoms), 1.54 Å for *E. coli*–*T. thermophilus* photolyases (388 C α atoms), and 1.60 Å for *A. nidulans*–*T. thermophilus* photolyases (355 C α atoms).⁷⁷ Therefore, in the following discussion the crystal structure of the *E. coli* photolyase³⁷ will be summarized and where necessary the differences from the two other photolyases will be indicated.

E. coli photolyase is composed of two well-defined domains: an N-terminal α/β domain (residues 1–131)

and a C-terminal α -helical domain (residues 204–471), which are connected to one another with a long interdomain loop (residues 132–203) that wraps around the α/β domain (Figure 9).

a. Photoantenna. The MTHF photoantenna is located in a shallow cleft between the two domains and partially sticks out from the surface of the enzyme. Two important contacts are made with the apoenzyme. One is between the carbonyl side chain of Cys292 and the positive charge on the five-membered ring of MTHF. This interaction might be responsible for the red shift in the absorption of enzyme-bound MTHF relative to free MTHF. The other is between Lys293 and the single Glu moiety of MTHF (the enzyme was crystallized with the monoglulamate form of MTHF), which establishes a salt bridge that increases the affinity of the enzyme to the cofactor. Considering that MTHF with longer Glu tails bound the enzyme with higher affinity,^{67,69} it is very likely that there are additional salt bridges with the MTHF Glu residues of the natural cofactor.

The 8-HDF of *A. nidulans* and *T. thermophilus* photolyases (the latter was crystallized without 8-HDF) is or is presumed to be located in the analogous cleft between the two domains. However, in contrast to the above case with MTHF, in *A. nidulans* photolyase (and presumably in the *T. thermophilus* enzyme) the entire 8-HDF is buried inside the cleft.^{38,77} This offers an explanation of the tighter binding of 8-HDF to deazaflavin class photolyases compared to the relatively weaker association of the MTHF cofactor in most folate class enzymes. However, this distinction does not constitute a general rule because MTHF binds to *S. cerevisiae*⁵⁸ and *B. firmus*⁷¹ photolyases nearly as tightly as 8-HDF does to its cognate apoenzyme. Although the interdomain cleft harboring the light-harvesting cofactor is structurally conserved, in contrast to the FAD binding site (see below), the amino acids making contacts with the photoantenna are not conserved either between the folate and deazaflavin classes or among members of the same class.^{13,77} Thus, of the 12 residues

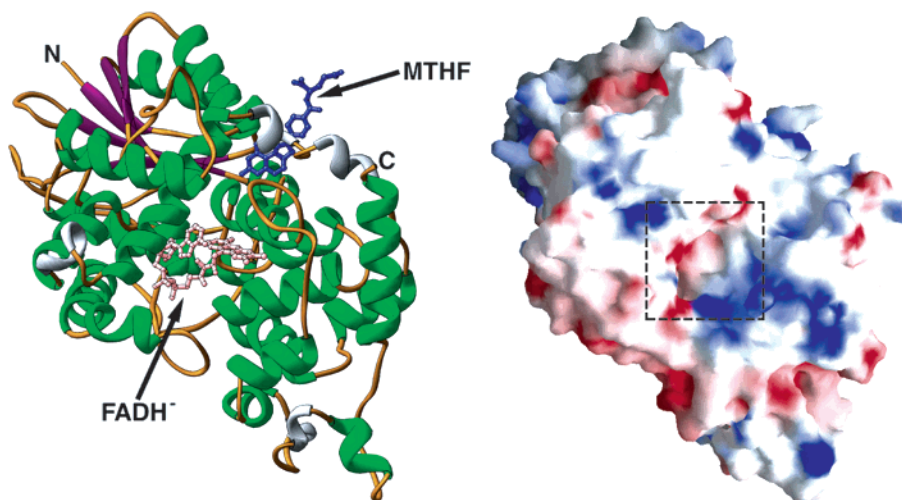


Figure 9. Crystal structure of *E. coli* photolyase: (A) Ribbon diagram representation showing the N-terminal α/β domain, the C-terminal α -helical domain, and the positions of the two cofactors; (B) surface potential representation showing the solvent-exposed residues. Key: blue, basic groups; red, acidic groups; white, hydrophobic groups. The square marks the hole leading to FAD in the core of the α -helical domain.³⁷

contacting 8-HDF in *A. nidulans* photolyase, 11 are different in the *E. coli* enzyme, and of the 6 residues contacting MTHF in *E. coli* photolyase, 5 are different in the *A. nidulans* enzyme. More strikingly, of the 12 residues contacting 8-HDF in *A. nidulans* photolyase, only 2 Arg residues are conserved in the *T. thermophilus* enzyme.⁷⁷

b. FAD Photocatalyst. The FAD cofactor is deeply buried within the α -helical domain and has an unusual U-shaped conformation with the isoalloxazine and adenine rings in close proximity. The FAD is held tightly in place by contact with 14 amino acids, most of which are conserved in the photolyase/cryptochrome family.^{37,77} Essentially all of the residues are located at the same positions relative to FAD in the three photolyase structures solved to date.⁷⁷ It should be noted that, even though the active form of flavin in photolyases is FADH^- , the crystal structures are those containing either the FADH° blue-neutral radical or the FAD_{ox} form, and therefore, some subtle changes in the structure around flavin are expected in the active form of the enzyme. A point related to this issue is the solvent accessibility of FAD. The flavin is accessible to the flat surface of the α -helical domain through a hole in the middle of this domain (Figure 9). The hole is too small to allow the diffusion of FAD in and out of the enzyme but allows easy accessibility to oxygen. This explains the relative ease with which FADH^- is converted to FADH° in most photolyases. Of special significance, this hole has the right dimensions and polarity to allow the entry of a thymine dimer to within van der Waals contact distance to the isoalloxazine ring of FAD. A surface potential representation of the enzyme reveals a positively charged groove running the length of the molecule and passing through the entrance of the hole. These structural features led to the current model³⁷ of binding to the DNA backbone through the positively charged groove and flipping out the thymine dimer into the active site cavity lined with FAD and aromatic residues (“dinucleotide-flipping model”).

In addition to shedding light on the specifics of the bindings of the chromophores to the apoenzyme, the crystal structure revealed another feature of functional significance. In *E. coli* photolyase, the center-to-center distance between MTHF and FAD is 16.8 Å and the planes of the chromophores are nearly perpendicular to one another. In *A. nidulans* photolyase, the two chromophores are 17.5 Å apart but as described below the cofactors are more favorably oriented. The rate and efficiency of energy transfer from the photoantenna to the photocatalyst depend on the distance and the relative orientation between the two. Because the efficiency of energy transfer is more favorable over a short distance and between transition dipole moments of the same direction and orientation,⁷⁸ the structures reveal why energy transfer is more efficient in *A. nidulans* photolyase (~100%) compared to *E. coli* photolyase (~70%). Finally, the crystal structure revealed potential pathways for intraprotein electron transfer that occurs during photoreduction of the FADH° cofactor;³⁰ this will be addressed below.

B. Reaction Mechanism

Photolyase carries out catalysis by Michaelis–Menten kinetics. It binds S to form ES, which performs catalysis to yield EP, and then P dissociates. It differs from classic Michaelis–Menten kinetics in one important aspect, however; the $\text{ES} \rightarrow \text{EP}$ transition is absolutely light dependent.^{79–83} This unique property of the enzyme has made it possible to carry out detailed pre-steady-state and steady-state kinetic experiments with photolyase in vivo, and to compare the reaction parameters obtained with those obtained with the purified enzyme/substrate system.^{32,34,48,82} The in vivo and in vitro values are remarkably similar.^{30–34}

The overall reaction may be summarized as follows (Figure 10). The enzyme binds a $\text{Pyr} \leftrightarrow \text{Pyr}$ in DNA independent of light, and flips the dimer out of the double helix into the active site cavity to make a stable ES complex. The folate (or 8-HDF) then

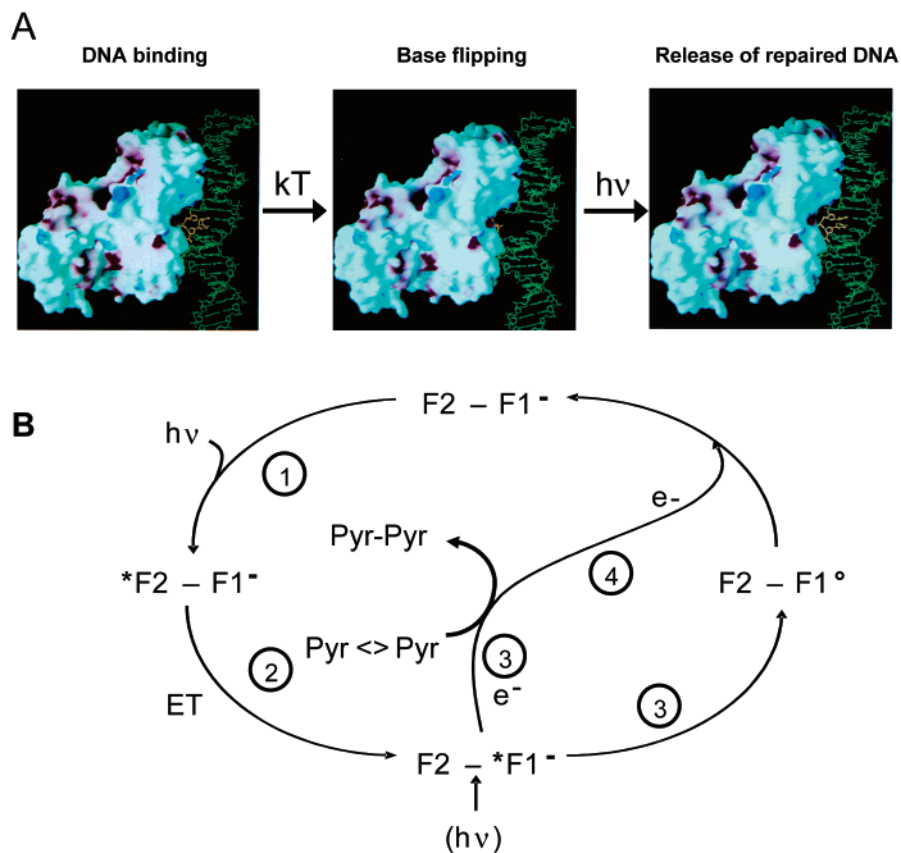


Figure 10. Reaction mechanism of photolyase. (A) Dark reactions. The enzyme binds to DNA and flips out the pyrimidine dimer from the double helix into the active site cavity by a thermal (kT) reaction; following photochemical ($h\nu$) repair, the dinucleotide moves out of the cavity and the enzyme and product dissociate. (B) Photocycle. The folate ($F2$) absorbs a photon and transfers energy to $FADH^-$ ($F1^-$) in the step indicated by ET. The excited reduced flavin ($*F1^-$) transfers an electron to $Pyr <> Pyr$. This causes the pyrimidine dimer to split into two pyrimidines in a concerted reaction with back electron transfer to the newly formed $FADH^\circ$ ($F1^\circ$) to restore it to the catalytically active form. An alternative pathway involves direct excitation ($h\nu$) of $FADH^-$ to initiate the photocycle.

absorbs a near-UV/blue-light photon and transfers the excitation energy (via dipole–dipole interaction) to flavin, which then transfers an electron to the $Pyr <> Pyr$; the 5–5 and 6–6 bonds of the cyclobutane ring are now in violation of Hückel rules, and therefore, the $Pyr <> Pyr$ is split to form two pyrimidines. Concomitantly, an electron is transferred back to the nascently formed $FADH^\circ$ to regenerate the $FADH^-$ form. To a first approximation, the reaction is a photon-powered cyclic electron transfer that does not result in a net gain or loss of an electron and hence, strictly speaking, is not a redox reaction.

1. Binding

Photolyase is a “structure-specific DNA binding protein”. Its specificity is determined by the backbone structure of the duplex at the binding site and by the chemical structure of the photolesion itself. This contrasts with “sequence-specific DNA binding proteins” whose specificity is governed mostly by the nature of the hydrogen bond donors and acceptors in the major and minor grooves of the duplex. As a general rule, the binding affinity of structure-specific DNA binding proteins is sequence independent. However, if such binding involves base flipping, as it presumably does in the case of photolyase,³⁷ it is expected to be affected by the neighboring sequences. For example, it is harder to flip out a $Pyr <> Pyr$ in

a G–C-rich sequence than in an A–T-rich sequence. Experimental tests of this prediction, however, have failed to reveal a major effect of neighboring sequences on the specific binding constant of *E. coli* photolyase to DNA,^{84,85} suggesting that either the effect of neighboring sequences was outside the detection limit of the assays used or there are compensatory mechanisms that nullify the sequence effects.

a. Kinetics and Thermodynamics. Photolyase binds to $Pyr <> Pyr$ with essentially the same affinity in single- and double-stranded DNA.^{86,87} The specific binding constant to a T<>T in DNA is $K_S = 10^{-9}$ M, and the nonspecific binding constant for undamaged DNA is $K_{NS} \approx 10^{-4}$ M. This means that the enzyme has a discrimination ratio (or selectivity factor) of $K_{NS}/K_S \approx 10^5$.⁸⁷ Because the enzyme binds to a T<>T dinucleotide with an equilibrium constant $K_D \approx 10^{-4}$ M, it appears that approximately half of the binding energy is contributed by enzyme–DNA backbone interactions and the other half by interactions of FAD and active site residues with the dimer itself.^{88–90} The *M. thermoautotrophicum* photolyase binds with higher affinity to the substrate, having $K_S = 10^{-11}$ M; however, it also has a comparably higher nonspecific binding constant, $K_{NS} \approx 10^{-6}$ M, such that the discrimination ratios of photolyases from *E. coli* and *Methanobacterium* are not that different.⁷⁶ The two

enzymes have similar association rate constants in the range of $k_{\text{on}} \approx 10^7 \text{ M}^{-1} \text{ s}^{-1}$. In contrast, the dissociation rate constants (k_{off}) are 5×10^{-2} and $2 \times 10^{-4} \text{ s}^{-1}$, respectively, which indicate that the different affinities of the two enzymes can be accounted for entirely by the difference in the dissociation rate constant.⁷⁶ The association rate constants of all photolyases investigated to date are well within the Smoluchovski limit for binding by three-dimensional diffusion, in contrast to many other DNA binding proteins such as the *lac* repressor which make 6–8 ionic bonds with the backbone phosphates and thus employ diffusion in reduced dimensionality to find their targets.³⁰

b. Binding Determinants on the Enzyme. The presence or absence of the light-harvesting factor does not affect the enzyme–substrate interaction.^{47,67,69} The three structural features that determine the affinity and specificity of the enzyme are the positively charged groove that runs across the surface of the helical domain, the hole in the center of this groove that has the dimensions to accommodate a Pyr<>Pyr, and the FAD that lines the bottom of this hole.³⁷ Site-specific mutagenesis studies show that the positively charged residues in the binding groove around the rim of the hole affect the specific binding affinity more drastically than they affect the non-specific binding. This indicates that the distorted DNA backbone is an important contributor to specificity.^{91–93} The hole has the right dimensions to fit Pyr<>Pyr, and the residues lining its sides are hydrophobic on one side and polar on the other. This asymmetry fits well with the asymmetric polarity of a Pyr<>Pyr in which the cyclobutane ring is hydrophobic and the opposite edges of the dimer have oxygens and nitrogens capable of forming H-bonds.

Mutations of either aromatic residues or polar residues lining the side walls of the hole drastically reduce the affinity of the enzyme for Pyr<>Pyr.⁹³ In particular, mutation of Trp277 in *E. coli* photolyase to a nonaromatic residue virtually eliminates specific binding, suggesting that Trp277 plays a crucial role in specific binding.⁹⁴ Further evidence of the proximity of Trp277 to the Pyr<>Pyr in the photolyase active site is that upon excitation with 280 nm rather than 380 nm this residue can directly split the cyclobutane ring by electron transfer with a relatively high quantum yield.⁹⁵ Finally, relatively direct evidence for the flipping of Pyr<>Pyr out of the DNA helix into the active site cavity has come from the cocrystal of *T. thermophilus* photolyase with a thymine.⁷⁷ In this structure a single thymine base is located within the hole, makes van der Waals contacts with the isoalloxazine ring, and is sandwiched between two Trp residues that correspond to Trp277 and Trp384 of *E. coli* photolyase. A fluorometric probe of the photolyase–DNA complex has also provided data consistent with the base-flipping model of binding.^{95a} Interestingly, in several computational studies published on photolyase–substrate interactions, only one⁹⁶ predicted van der Waals contacts between the isoalloxazine ring and the Thy<>Thy, while the others predicted a distance of about 10 Å.^{97–99} Clearly, the structure of the enzyme–sub-

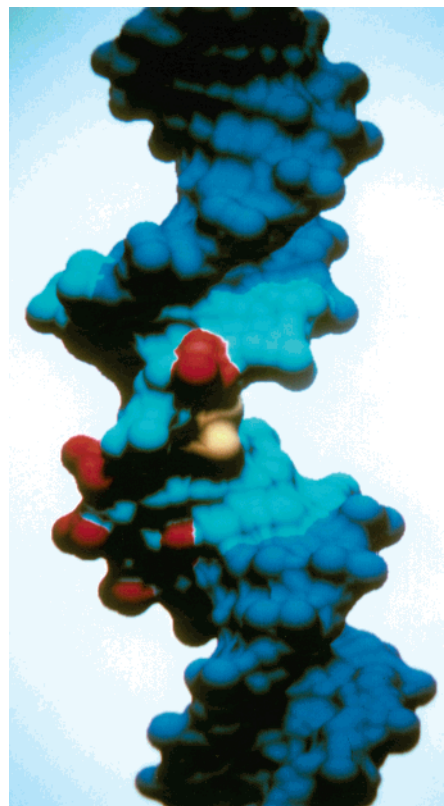


Figure 11. Photolyase contact sites on DNA. A space-filling (raster) display of the molecular surface of DNA accessible to water is shown. The photolyase contact sites are indicated by a color: cyan, methidium propyl-EDTA–Fe(II) footprint; red, phosphates and guanine N7 atoms implicated in binding; yellow, cyclobutane ring. In this model the DNA is kinked by 27° into the major groove at the dimer site. Reprinted with permission from ref 100. Copyright 1987 *Journal of Biological Chemistry*.

strate complex is needed to understand the fine details of binding; however, the available data overwhelmingly support the dinucleotide-flipping model of bringing the Pyr<>Pyr into the active site of the enzyme.

c. Binding Determinants on the Substrate. Chemical footprinting of DNA in the presence of *E. coli*, *S. cerevisiae*, and *M. thermoautotrophicum* photolyases revealed nearly identical contacts around a T<>T substrate^{76,91,100} (Figure 11): A six-bp region around the T<>T is protected from hydroxyl radicals. The enzyme contacts the phosphate that is 5' and the three phosphates that are 3' to the T<>T, as well as the phosphate that is opposite the dimer across the minor groove on the complementary strand. It also occludes the major groove for about half of a turn 3' to the dimer. Significantly, it does not contact the intradimer phosphate. Thus, nearly all of the contacts are with the damaged strand. Importantly, the intradimer phosphate can be ethylated (with ethylnitrosourea) without interfering with binding. This is consistent with the dimer-flipping model in which upon flipping of the thymine dimer into the photolyase hole the intradimer phosphate remains outside the cavity, exposed to the solvent. Indeed, for this reason the enzyme can even repair cyclobutane pyrimidine dimers that are formed between nonadjacent bases.¹⁰¹ The phosphate that is 5' and the

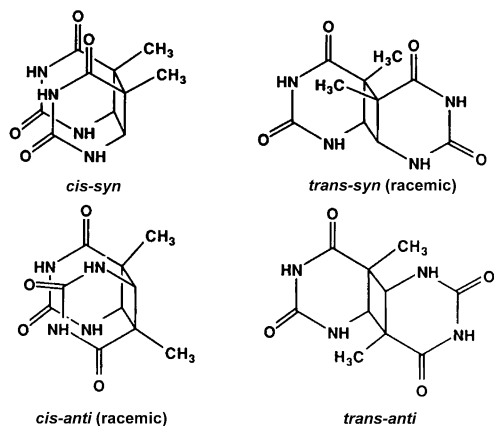


Figure 12. Stereochemical isomers of the cyclobutane pyrimidine dimer. Only the *cis,syn* isomer forms in double-stranded DNA; the *trans,syn* isomer forms at about a 1% frequency in single-stranded DNA. The other isomers are obtained by irradiating frozen solutions of pyrimidine bases.

three phosphates that are 3' to the T<>T help to anchor the substrate in place by making ionic bonds with positively charged residues in the binding groove of the enzyme.^{63,76,84} The fact that the enzyme binds with equal affinity to single- and to double-stranded DNA^{30,87,102} suggests that the single phosphate contact detected on the complementary strand by ethylation interference probes is in fact most likely due to steric hindrance of ethylation at that position to spatial complementarity of the enzyme–substrate rather than the presence of a salt bridge between that phosphate and a positively charged group on the enzyme. Indeed, photolyase repairs Pyr<>Pyr in the DNA strand of DNA–PNA (peptide nucleic acid) and DNA–RNA duplexes poorly.^{103,104} This indicates that within the context of the double helix the overall structure affects the accessibility to the substrate, but with single-stranded DNA there are less constraints. With these considerations, then, it is predicted that a substrate of the form NpT<>TpNpNp should contain all of the binding determinants for binding photolyase with high affinity. Indeed, it was found that such an oligomer bound photolyase with affinity comparable to that of a 40-bp duplex with a T<>T.^{87,88}

In addition to the phosphodiester backbone and the cyclobutane dipyrimidine structure, the nature of the pentose, the identity of the bases making up the dimer, and the stereochemistry of the cyclobutane pyrimidine dimer affect binding. First, the enzyme binds to a U<>U in RNA with 10^5-fold lower affinity than to a U<>U in DNA presumably because of the energy cost of fitting the 2'-OH into the binding cavity.⁹⁰ Second, perhaps for the same reason, the enzyme can only bind the *cis,syn* isomer of the cyclobutane dimer. Of the six isomers of the T<>T dimer (Figure 12) this is the only one that forms in double-stranded DNA. The *trans,syn* isomer forms at about 10% the level of T<*cis,syn*>T in single-stranded DNA, and hence, it is of some biological relevance. No binding of photolyase could be detected to T<*trans,syn*>T with relatively sensitive assays; however, it was found that photolyase does repair this photoproduct, albeit with extremely low efficiency.¹⁰⁵ With respect to the effect of base composi-

tion on the binding of photolyase to Pyr<>Pyr, the following hierarchy of affinities was found: T<>T > T<>U > U<>U > C<>C, with T<>T having 10-fold higher affinity than C<>C. However, a follow-up study suggests that U<>U may be the more efficient substrate (see ref 129). This order of affinity suggests that the enzyme contacts the bases through H-bond donors to C2=O (common to all pyrimidines) and C4=O (replaced by NH₂ in C), and that the lower affinity of the enzyme to C-containing dimers might be due to the loss of H-bonds because of a replacement of a H-bond acceptor at that position by a H-bond donor.

Finally, the structure of DNA in a photolyase–DNA complex deserves some comment. The structure of DNA with a T<>T is a matter of some controversy, with some studies indicating ~30° kinking^{106,107} while others suggest minimal perturbation of the duplex.^{108–113} It is of significance, however, that all DNA glycosylases and methyltransferases that are known to function by base flipping have been found to severely kink the DNA (35–60°) in DNA–protein cocrystals.^{114–118} Indeed, using atomic force microscopy, it was reported that photolyase from *A. nidulans* bends DNA by 35° at the Pyr<>Pyr site.¹¹⁹ However, it is unclear from this study whether photolyase kinked the DNA or bound to DNA already kinked by the T<>T.

In fact, a recent crystallographic study^{107b} has put an end to all the controversy surrounding this issue. The crystal structure of a decamer duplex containing a *cis,syn* thymine dimer was solved at 2.0 Å resolution. This structure showed that the overall helix axis bends ~30° toward the major groove and unwinds the duplex by ~9° (Figure 13) in remarkable agreement with the 30° bending obtained from a DNA circularization assay^{107a} and close to the 27° predicted from a theoretical calculation¹⁰⁶ but significantly different from the ~10° or less reported for the NMR structures^{109–113} and from a gel mobility retardation assay.¹⁰⁸

2. Catalysis

Photolyase catalyzes light-initiated ($\pi_s^2 + \pi_s^2$) cycloreversion of the cyclobutane ring joining the two pyrimidines. The photoreactivating light (300–500 nm), however, is of insufficient energy to populate the excited states (single or triplet) of Pyr<>Pyr, which does not absorb appreciably at $\lambda > 250$ nm. There is also no evidence for formation of a charge-transfer complex between the enzyme and substrate that can be populated by direct excitation by photoreactivating light.^{33,45,90,120} Rather, all available evidence suggests that photoexcited photolyase transfers an electron to the Pyr<>Pyr and the resulting radical anion splits into two pyrimidines (Figure 10). Below, the photophysical and photochemical/thermodynamic evidence for this model will be summarized, followed by a mechanistic model for splitting the cyclobutane ring by single-electron transfer (SET).

a. Photophysics. Three lines of investigation have been pursued to define the roles of the chromophores and describe the elementary photophysical processes

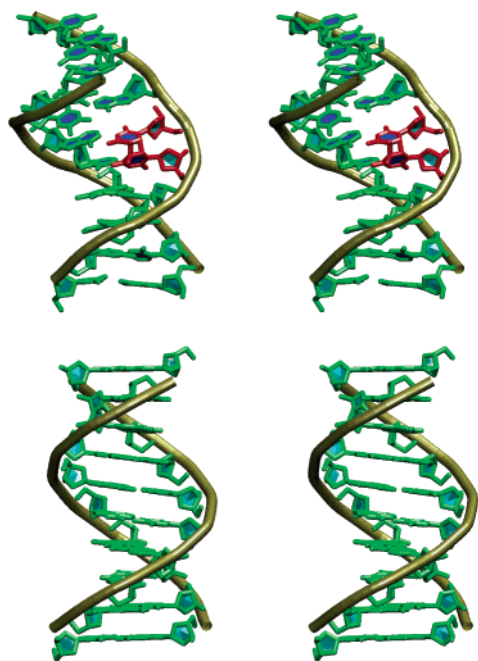


Figure 13. Stereoview representations of the crystal structures of (A) a decamer containing a T<->T and (B) the corresponding B-DNA. The thymidines making up the dimer are drawn in red. The view shows part of the major groove of the molecule. In T<->T-containing DNA, the phosphodeoxyribose backbone shows a sharply kinked (30°) structure. Reprinted with permission from ref 107b. Copyright 2002 National Academy of Sciences (courtesy of Dr. ChulHee Kang).

during photoreactivation: action spectra for repair, picosecond flash photolysis, and time-resolved fluorescence spectroscopy.

i. Action Spectrum. Absolute action spectra of both folate and deazaflavin class photolyases containing either or both chromophores have been determined with enzyme preparations in which the flavin was chemically or photochemically reduced to the biologically relevant FADH⁻ form.^{33,47} Qualitatively, these analyses showed that while the E-FADH⁻ forms (enzyme containing reduced flavin but no second chromophore) of the *E. coli* and *A. nidulans* photolyases were active, the E-MTHF and E-8-HDF forms (enzyme containing folate or deazaflavin but no FAD) were not. This unambiguously demonstrated that FADH⁻ was the catalytic factor and the second chromophore was not. Quantitatively, the photolytic cross-sections ($\epsilon \times \varphi$) in vitro of reduced enzyme closely matched the values obtained in vivo as shown in Figure 14 for *E. coli* photolyase, thus validating the use of reduced enzymes for photochemical characterization.³³ The absolute action spectra of the E-FADH⁻ and E-MTHF-FADH⁻ and E-8HDF-FADH⁻ forms of *E. coli* and *A. nidulans* photolyases, respectively, are shown in Figure 15. In both cases the absolute action spectra of the E-FADH⁻ forms match well the absorption spectra of the corresponding enzymes, and quantum yields of 0.85 for the *E. coli* and 0.90 for the *A. nidulans* photolyases could be calculated.

These values set a lower limit on the quantum yield of electron transfer from ¹(FADH⁻)* to the Pyr<->Pyr as the quantum yield of electron transfer must be

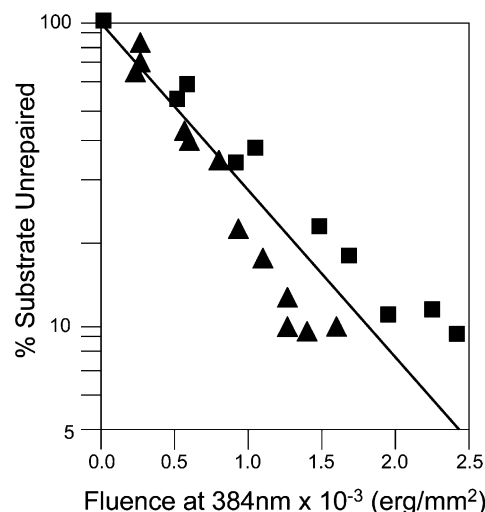


Figure 14. Comparison of in vivo and in vitro repair efficiencies of *E. coli* photolyase under single-turnover conditions. The fraction of dimers remaining as a function of 384 nm light dose are plotted for a photolyase (E-FADH⁻-MTHF form)-substrate mixture (squares) or for photolyase-overproducing *E. coli* cells (triangles). The slope of the line (k_p) is related to the photolytic cross-section by $\epsilon\Phi$ ($M^{-1} cm^{-1}$) = $k_p(5.2 \times 10^9)$ ($mm^2 erg^{-1}$) λ^{-1} (nm). The divergence between in vivo and in vitro repair efficiencies in the range of 70–90% repair may be due to the presence of some heterogeneity in the chromophore status in a fraction of the purified enzyme. Reprinted from ref 33. Copyright 1990 American Chemical Society.

equal to or higher than the quantum yield of repair. The absolute action spectrum of the E-8-HDF-FADH⁻ form of *A. nidulans* photolyase matches well to the absorption spectrum^{47,72} and, moreover, reveals a quantum yield of 1.0 for repair. Because 8-HDF can repair Pyr<->Pyr only through FADH⁻, the theoretical maximum quantum yield for the holoenzyme is 0.90. The discrepancy arises from the errors in obtaining accurate values for the molar extinction coefficients and absolute action spectra of the two forms of the enzyme. Disregarding this minor discrepancy, it can be concluded that 8-HDF transfers energy to FADH⁻ with a quantum yield near unity.

In contrast, the action spectrum of the *E. coli* holoenzyme shows about a 5 nm blue shift relative to the absorption spectrum of the enzyme and reveals an overall quantum yield of about 0.7.^{33,34} From the overall quantum yield it is calculated that the quantum yield for energy transfer from MTHF to FADH is in the range of 0.7–0.8. The minor change of the quantum yield of repair with wavelength is due to the fact that at shorter wavelengths the contribution of FADH⁻ to overall absorption becomes more significant. This is because a photon absorbed by FADH⁻ is about 25% more efficient than a photon absorbed by MTHF in splitting the cyclobutane ring as the latter transfers energy to FADH⁻ with 70–80% efficiency.^{33,34} The quantum yield for energy and electron transfer calculated from the action spectra and the rate of these processes were determined independently from time-resolved absorbance and fluorescence measurements and are in reasonable agreement with the values obtained by these methods (Table 3).

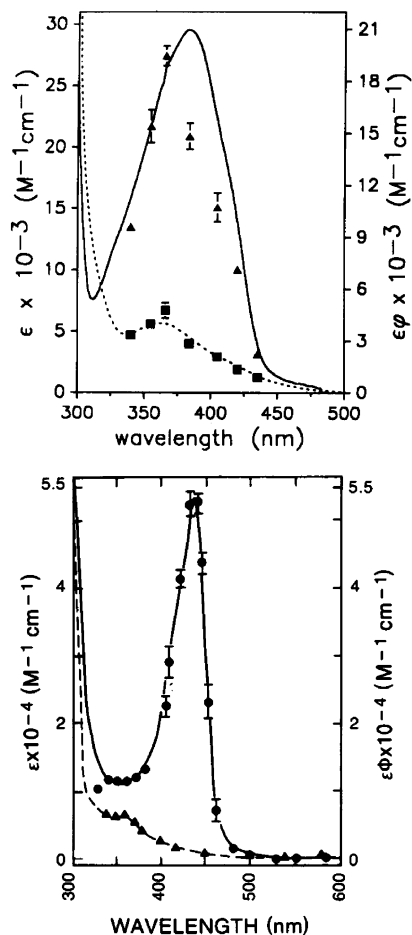


Figure 15. Absolute absorption and action spectra of folate and deazaflavin class photolyases. (Top) *E. coli* photolyase. Solid and dashed lines are the absorption spectra of the E-FADH⁻-MTHF and E-FADH⁻ forms of the enzyme. The triangles and squares are the values for the quantum yield (Φ) times the molar extinction coefficient (ϵ) of the two forms. (Bottom) *A. nidulans* photolyase. Absorption spectra of the E-FADH⁻-8-HDF (solid line) and E-FADH⁻ (dashed line) forms of the enzyme are superimposed onto the photolytic cross-section ($\epsilon \times \phi$) of these two forms. Adapted from refs 10, 33, and 71.

ii. Energy Transfer. Steady-state fluorescence analysis revealed that in *E. coli* photolyase all three oxidation states of the FAD quenched the MTHF

fluorescence,¹²¹ indicating singlet-singlet energy transfer. The kinetics of this energy transfer was analyzed by time-resolved spectroscopy.¹²² Figure 16 (top) shows the fluorescence decay curves of E-MTHF and E-MTFH-FADH⁻ forms of the enzyme. The ¹MTHF* singlet state decays with $\tau_1 = 350$ ps, which decreases to $\tau_2 = 140$ ps in the presence of flavin. From eq 1

$$\Phi_{\text{ET}} = 1 - \tau_2/\tau_1 \quad (1)$$

a quantum yield for energy transfer of 0.62 is calculated. The quantum yield for energy transfer can be used to calculate the distance (R) between donor and acceptor using the Förster equation⁷⁸

$$\Phi_{\text{ET}} = R_0^6/(R_0^6 + R^6) \quad (2)$$

In this equation, R_0 is the “critical distance” at which the energy-transfer rate (K_{ET}) is equal to the decay rate of the donor in the absence of acceptor ($\Phi_{\text{ET}} = 0.5$). The value of R_0 in angstroms is calculated from eq 3,

$$R_0 = (9.79 \times 10^3)^{1/6} JK^2 \Phi_F n^{-4} \quad (3)$$

where J is the overlap integral between donor emission and acceptor absorption envelopes, Φ_F is the quantum yield for fluorescence of the donor, and n is the refractive index of the medium, all of which can be experimentally measured. K^2 is the orientation factor for the transition dipoles of the donor emission and acceptor absorbance. K^2 is usually assumed to be 2/3 for systems of isotropic motion. Using this value, a distance of 21.7 Å was calculated as the interchromophore distance in *E. coli* photolyase. However, when the crystal structure was solved, it became apparent that the two chromophores were in a rather unfavorable orientation for energy transfer. Thus, from the crystal structure and using certain assumptions about the dipole moment orientation relative to the chromophore framework, $K^2 = 0.2$ was estimated.¹²³ Using this value in the Förster equation, $R = 17.7$ Å was calculated for the MTHF-FADH⁻ distance, which is in reasonably good agreement with the crystallographic value of 16.8 Å.³⁷

Table 3. Photophysical Properties of Photolyases

enzyme	<i>E. coli</i>	<i>A. nidulans</i>
class	folate	deazaflavin
excited-singlet-state lifetime (ns) ^a		
E-SC*	0.35(F)–0.48(A)	2.0(F)
E-FADH ⁻ -SC*	0.14(F)–0.18(A)	0.05(F)
E-FADH ^o -SC*	<0.03	<0.03
energy transfer (SC*-FADH ⁻)		
rate (s ⁻¹)	4.6 × 10 ⁹	>1.9 × 10 ¹⁰
efficiency (%)	62	98
interchromophore distance (Å)	16.8	17.5
excited singlet state lifetime (ns)		
E-FADH ⁻ *	1.5(F)–1.7(A)	1.8(F)
E-FADH ⁻ * + T<>T (U<>U)	0.16(F)–0.2(0.05)(A)	0.16(F)–0.2(0.05)(A)
electron transfer (FADH ⁻ *-T<>T) ^b		
rate (s ⁻¹)	~(1–2) × 10 ¹⁰	~(1–2) × 10 ¹⁰
efficiency (%)	89	92

^a (F), from time-resolved fluorescence; (A), from time-resolved absorbance. Adapted and updated^{129,132} from ref 10. ^b Electron transfer to U<>U is about 2-fold faster than to T<>T.

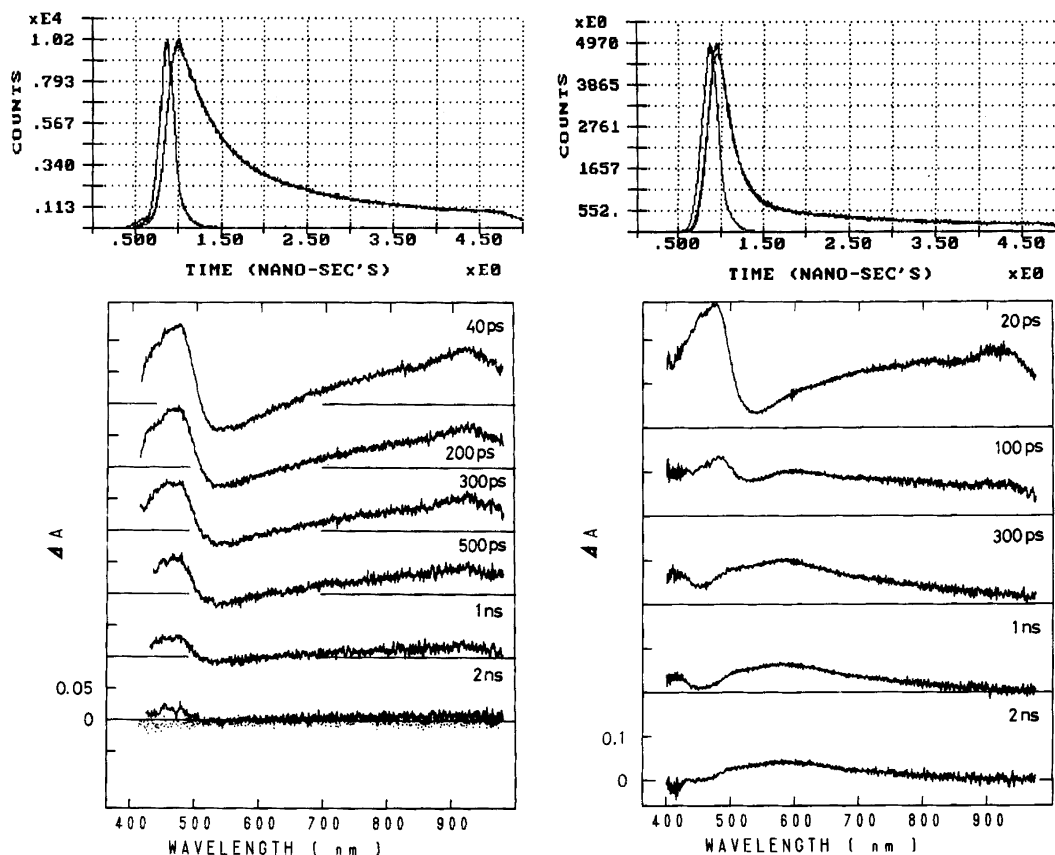


Figure 16. Detection of energy transfer from folate to flavin in *E. coli* photolyase by time-resolved fluorescence and absorption spectroscopy. (Top) Fluorescence decay curve of MTHF in the absence (left) and presence (right) of FADH^- . The excitation wavelength was 355 nm (Nd:YAG laser), and emission was monitored at 470 nm. The short-lifetime peaks are from the laser without sample. (Bottom) Transient changes in absorption spectra of photolyase containing either folate alone or folate and flavin: left, E-MTHF; right, E-MTHF-FADH $^-$. Delay times after excitation are indicated in the figure. The samples were excited with either a 366 nm laser pulse with a width of 8 ps (left) or a 340 nm pulse with a width of 12 ps (right). Note the rapid decay of the 480 nm $^1(\text{MTHF})^*$ band and the subsequent buildup of the 500–600 nm $^1(\text{FADH}^-)^*$ band in the 100 ps to 1 ns range in the right panel. Reprinted from ref 122. Copyright 1991 American Chemical Society.

The results obtained from time-resolved fluorescence studies were complemented and augmented with picosecond flash photolysis.¹²² Figure 16 (bottom) shows the transient difference spectra of E-MTHF and E-MTHF-FADH $^-$ forms of *E. coli* photolyase after an 8 ps pulse of 366 nm (left panel) or a 12 ps pulse of 340 nm (right panel). The E-MTHF spectra show two major bands at ca. 480 and 600–900 nm, which decay with $\tau = 480$ ps. These are in good agreement with the fluorescence lifetime of $\tau = 354$ ps. The transient absorption spectrum of the E-MTHF-FADH $^-$ immediately after the pulse ($\tau = 20$ ps) is nearly identical to the absorption spectrum of E-MTHF, and is therefore consistent with the species being the MTHF singlet. However, in this case the singlet absorption decays more rapidly ($\tau_2 = 180$ ps), again in reasonable agreement with the fluorescence lifetime ($\tau_2 = 140$ ps). More importantly, the decay of the MTHF* singlet is followed by the appearance of a new absorption band at 500–600 nm, which decays with a $\tau \approx 2$ ns and is nearly identical to the absorption of $^1(\text{FADH}^-)^*$ observed upon excitation of the E-FADH $^-$ form of the enzyme.¹²⁴ Therefore, Figure 16 constitutes direct evidence for high-efficiency singlet-singlet energy transfer from MTHF to FADH $^-$ in *E. coli* photolyase.^{122,125}

Similar analyses were performed on *A. nidulans* photolyase.¹²⁵ Figure 17 (top) shows the fluorescence decay curves for the E-8HDF and E-8HDF-FADH $^-$ forms of the enzyme. From these decay curves $\tau_1 = 2.0$ ns and $\tau_2 = 0.05$ ns were determined. These values permit calculation of a quantum yield of energy transfer $\Phi_{\text{ET}} = 0.98$. Using this value and $K^2 = 2/3$ in the Förster equation (eq 3), an interchromophore distance of $R = 15$ Å was estimated.¹⁰⁷ In fact, the crystal structure reveals that the distance between the centers of 8-HDF and FADH $^-$ is 17.5 Å, the angle between the transition dipole moments of the two cofactors is 35.6°, and the angles between the dipole moments and the vectors connecting the two chromophores are 41.3° and 22.4° for FAD and 8-HDF, respectively.³⁸ From this orientation $K^2 = 1.6$ is calculated, which when substituted into the Förster equation gives $\Phi_{\text{ET}} = 0.97$. This is in excellent agreement with the $\Phi_{\text{ET}} = 0.98$ calculated from fluorescence lifetimes.^{38,125} Evidence for singlet energy transfer from $\Phi(8\text{-HDF})^*$ to FADH $^-$ in *A. nidulans* photolyase was obtained by flash photolysis. However, because of the nearly 10-fold faster rate of energy transfer, even at the earliest scan time (100 ps) after a 10 ps pulse of 355 nm, only the $\Phi(\text{FADH}^-)^*$ could be detected (Figure 17, bottom).¹²⁵

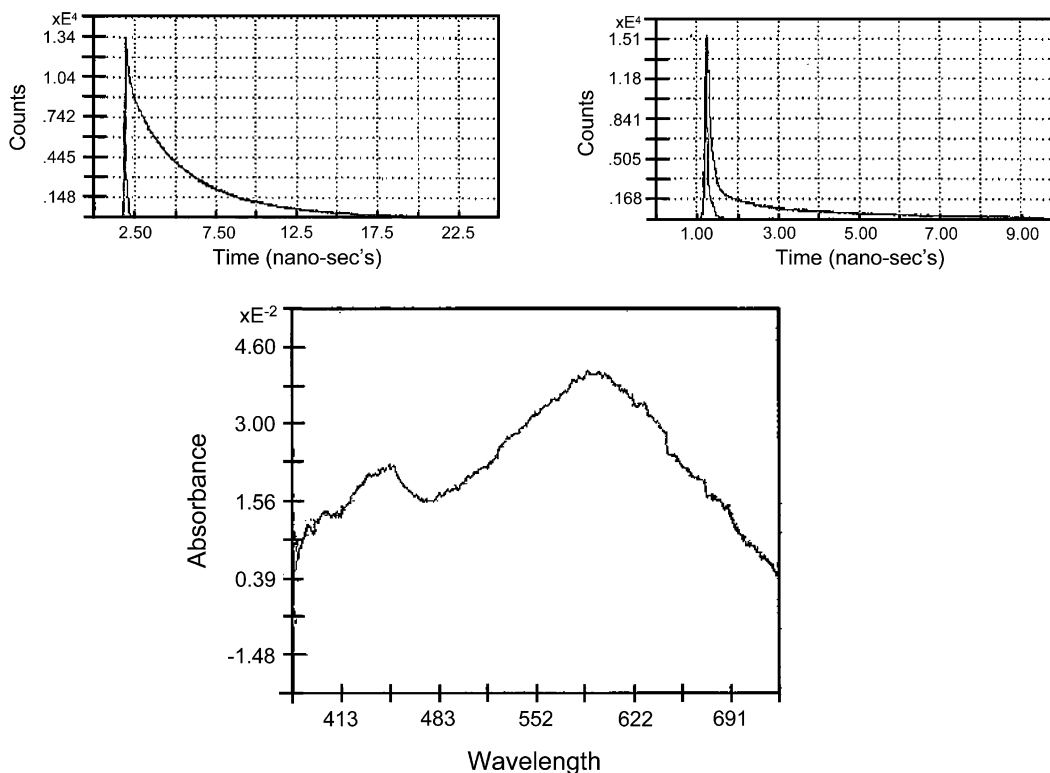


Figure 17. Energy transfer in *A. nidulans* photolyase detected by ultrafast spectroscopy. (Top) Fluorescence decay curves of E-8HDF (left) and E-8HDF-FADH⁻ (right) forms of the enzyme. Excitation was with 30 ps laser pulses of 355 nm. Emission was monitored at $\lambda > 435$ nm. (Bottom) Transient absorption spectrum of E-8HDF-FADH⁻ recorded 100 ps after excitation with a 10 ps pulse of 355 nm averaged over 200 laser pulses. Note the 500–600 nm band typical of ¹(FADH⁻)* and no evidence of ¹(8-HDF)*, which is consistent with an energy-transfer rate that is faster than the resolution limit of the instrumentation system. Reprinted from ref 125. Copyright 1992 American Chemical Society.

iii. Electron Transfer. The $\Phi(\text{FADH}^-)^*$ formed directly by absorption of a photon by flavin, or more often by energy transfer from the light-harvesting cofactor, splits the cyclobutane ring of Pyr \leftrightarrow Pyr. Even though it is generally accepted that catalysis is initiated by electron transfer, there is no direct experimental evidence for electron transfer from or to the flavin during catalysis. Moreover, because the excited-state flavin is an efficient redox cofactor in all three oxidation states, and because Pyr \leftrightarrow Pyr radical anions and cations are equally prone to cycloreversion,^{126,127} the question arises as to why only the FADH⁻ form of the enzyme is catalytically active. This question has been addressed by calculating the free energy for SET in either direction by the relevant excited states of flavin and Pyr \leftrightarrow Pyr.¹²⁸ The results of these calculations, which are based, in part, on certain assumptions lacking direct experimental support, indicate that, on thermodynamic grounds, SET from ¹(FADH⁻)* to Pyr \leftrightarrow Pyr is the only possible mechanism for photolyase ($\Delta G^\circ = -30$ kcal mol⁻¹). With this as a starting point, then, the experimental approaches that were used to determine the direction, rate, and efficiency of electron transfer and to capture the reaction intermediates are summarized below.

iii.a. Time-Resolved Fluorescence. The lifetimes of flavin fluorescence of the E-FADH⁻ form of *E. coli* photolyase was reduced from $\tau_1 = 1.4$ ns to $\tau_2 = 0.16$ ns by the presence of saturating amounts of T \leftrightarrow T substrate (Figure 18, top).¹⁰⁴ The corresponding values for the *A. nidulans* photolyase were $\tau_1 = 1.8$

ns and $\tau_2 = 0.14$ ns.¹²⁵ These values correspond to a rate of electron transfer of 5.5×10^9 s⁻¹ at a quantum yield of 0.88 for the *E. coli* enzyme and a rate of 6.5×10^9 s⁻¹ and a quantum yield of 0.92 for the *A. nidulans* photolyase.

iii.b. Picosecond Laser Flash Photolysis. Excitation of the E-FADH⁻ form of photolyase with a 12 ps pulse of 340 nm gives rise to a broad absorption band in the 500–600 nm region with a lifetime of 1.7 ns.¹²⁴ This species was assigned to $\Phi(\text{FADH}^-)^*$. In the presence of U \leftrightarrow U the transient decayed faster ($\tau = 0.2$ ns) and corresponded to an electron-transfer rate of 5.5×10^9 s⁻¹, which is in agreement with the value obtained by fluorescence lifetime measurements. The decay of the flavin singlet was followed by the appearance of a 400–420 nm species with a lifetime of 0.5–2 ns.^{124,129} (Figure 18, bottom). This species was also observed with a U \leftrightarrow T substrate, but not with a T \leftrightarrow T substrate, which is equally effective in quenching the ¹(FADH⁻)* absorbance.¹²⁹ Hence, the 410 nm species can be ascribed to a substrate radical. In fact, pulse radiolysis studies with radical anions of C5–C6 saturated dihydropyrimidines show a 410 nm absorption maximum for uracil dihydrate and a 380 nm maximum for the dihydrothymine radical, suggesting that the 410 nm transient observed in flash photolysis is either the uracil cyclobutane dimer anion or the uracil radical.¹³⁰

To confirm that the 410 nm transient originated from a radical, a magnetic field (700 G) was applied to the sample. In spatially separated radical pair systems an external magnetic field can affect sin-

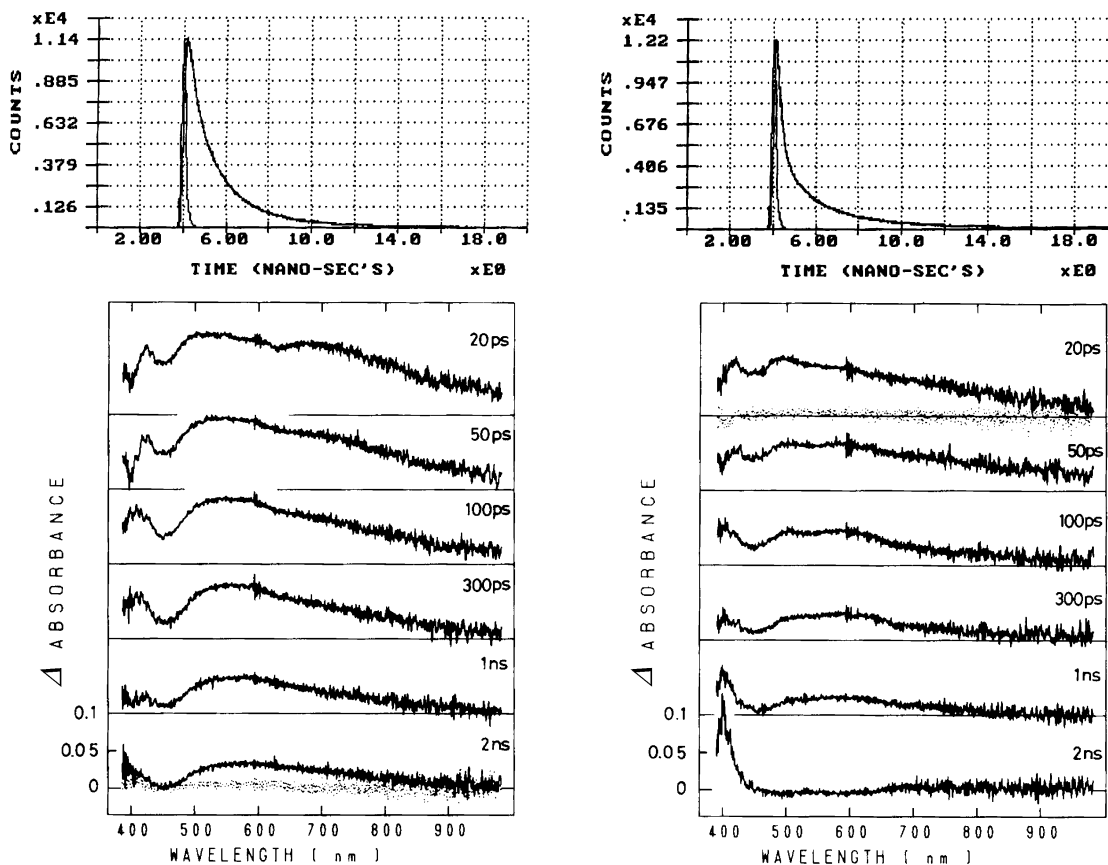


Figure 18. Detection of electron transfer from flavin to Pyr \leftrightarrow Pyr in *E. coli* photolyase by ultrafast fluorescence and absorption spectroscopy. (Top) Fluorescence decay of FADH $^-$ in the absence (left) and presence (right) of T \leftrightarrow T substrate. Delay times after excitation with a 30 ps laser pulse of 355 nm are indicated. (Bottom) Transient absorption spectra of the E-FADH $^-$ form of *E. coli* photolyase in the absence (left) and presence (right) of U \leftrightarrow U substrate. The samples were excited with a 12 ps pulse of 340 nm, and the difference spectra were recorded after the indicated delay times. Note the rapid decay of the 500–600 nm flavin singlet band and the buildup of a 410–420 nm species in the left panel. This species was not observed when T \leftrightarrow T was used as substrate in a follow-up study.¹⁶² Adapted from refs 122 and 124.

glet–triplet mixing via the Zeeman effect on the unpaired electrons, and thus, it increases the lifetime of the radical.¹³¹ In the case of the photolyase–substrate system the external magnetic field did not affect the lifetime of the 410 nm species.¹²⁹ Even though this could be due to a variety of reasons unique to the particular system, the failure to identify this species as a radical makes the assignment of the 410 nm species to a substrate/product radical provisional. Finally, it should be noted that if the reaction proceeds by electron transfer to generate a charge-separated radical pair (E-FADH $^{\circ-}\cdots$ U \leftrightarrow U $^{\circ-}$), the transient spectrum should reveal the characteristic flavin neutral radical absorption (peaks at 480, 580, and 526 nm) concomitant with the 410 nm species. Although the spectrum occurring between 50 ps and 1 ns in the presence of U \leftrightarrow U in Figure 18 is suggestive of a neutral flavin semiquinone, no definitive assignment could be made and there is no temporal complementarity between this broad band and the 410 nm species. A variety of reasons can be advanced for this lack of complementarity. However, it is clear that flash photolysis studies have failed to identify the predicted reaction intermediates unambiguously.

In a follow-up picosecond photolysis study¹³² on (FADH $^-$) * absorption quenching by substrate using T \leftrightarrow T, T \leftrightarrow U, U \leftrightarrow T, and U \leftrightarrow U dimers (Figure 19)

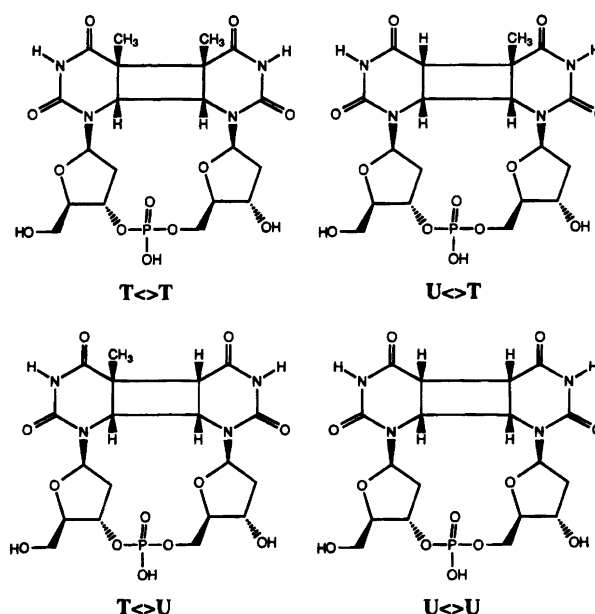


Figure 19. *cis, syn* cyclobutane pyrimidine dimers used to study substrate effects on the electron-transfer rate from $^1(\text{FADH}^-)^*$ to substrate.

in the temperature range 275–90 K, it was found that (a) the lifetime of $^1(\text{FADH}^-)^*$ in the presence of substrate was dependent on the nature of the sub-

Table 4. Quenching of E-(FADH⁻)* Excited-State Absorbance by Different Substrates at Different Temperatures^a

substrate	temp, K	short time constant from fit, ps	short time constant from amplitude, ps	long time constant (fixed in fit), ns
U<>U	275	<100	~50	1.8
	90	170 ± 80		7.5
U<>T	275	<100		1.8
	90	130 ± 30		7.5
T<>T	275	110 (+70, -50)	~100	1.8
	170	310 ± 40		7.5
T<>U	90	350 ± 60		7.5
	275	80 (+30, -20)		1.8
	170	460 ± 120		7.5
	90	510 ± 90		7.5

^a The long time constant was assumed to be the decay time of the free FADH⁻* and was fixed during the fit. Two estimates of the short time constant are given, based upon fitting the decay curve and the decrease of the amplitude. Adapted from ref 132.

strate (Table 4), suggesting that the rate of electron transfer to U<>U and U<>T was 2–3-fold faster than the rate of electron transfer to T<>U and T<>T and (b) the lifetimes of ¹(FADH⁻)* were found to be 1800 ps in the absence of substrate, 50 ps in the presence of U<>U and U<>T dinucleotide dimers, and 100 ps in the presence of T<>T or T<>U dinucleotide dimers. Thus, the revised rates of electron transfer are in the range of $= 2 \times 10^{10} \text{ s}^{-1}$ for U<>U and 10^{10} s^{-1} for T<>T dinucleotide substrates, respectively. The quantum yield of dimer splitting was temperature dependent, and from the quantum yield as a function of temperature (Figure 12), an overall activation energy of splitting ($E_A = 0.45 \pm 0.2 \text{ eV}$) was calculated. No splitting was detected below 200 K. Importantly, this study revealed that, upon cooling of the system from 275 to -90 K, the lifetime of ¹(FADH⁻)* in the absence and presence of substrate increased by approximately the same factor as the decrease of the rate of forward electron transfer under these conditions. Therefore, the reduced efficiency of electron transfer at low temperature cannot be responsible for the decrease of the yield of repair with decreasing temperature (Figure 20). This finding, in turn, leads to the important conclusion that the polypeptide chain provides some of the necessary activation energy for splitting of Pyr<>Pyr; hence, photolyase is not simply a “photon-powered DNA repair” factory.^{11,132,133}

The temperature dependence of the quantum yield of dimer splitting is consistent with the notion that the actual bond breaking that follows the photoreaction is the rate-determining step of the reaction. This step needs energy supplied from an external source; otherwise the reaction would be trapped in the equilibrium between forward and back electron transfer without leading to dimer splitting. This external energy is supplied by the strain imposed by the polypeptide chain on the Pyr<>Pyr upon binding of photolyase to the DNA substrate. This might explain why in a model system a T<>T anion radical generated by electron transfer from dimethylaniline

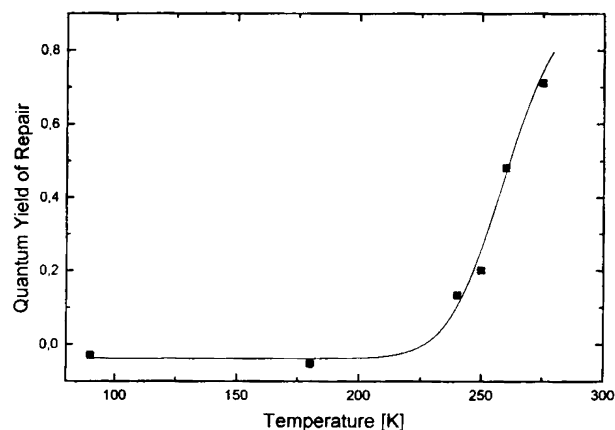


Figure 20. Quantum yield of repair of U<>T by the E-FADH⁻ form of *E. coli* photolyase as a function of temperature. No dimer splitting occurs below 200 K. Reprinted from ref 129. Copyright 1994 American Chemical Society.

is split at a rate of $\sim 1 \mu\text{s}$, or about 1000-fold slower than the rate of enzymatic splitting.^{133–135}

iii.c. Time-Resolved EPR. Direct evidence for a radical intermediate during catalysis by *E. coli* photolyase was obtained by time-resolved EPR.¹³⁶ When the E-FADH⁻ + T<>T mixture was exposed to a 17 μs flash of light, an EPR signal, separate from that of FADH⁰, was detected that decayed with the instrument time constant (Figure 21). This species ($\tau > 10 \mu\text{s}$) is clearly different from the transient detected in flash photolysis ($\tau = 0.5\text{--}2 \text{ ns}$)^{124,132} and may arise from the final state (E-FADH⁰...T-T⁰⁻) rather than the initial state (E-FADH⁰...T<>T⁰⁻) of catalysis, or it may even be a side product of the electron-transfer reaction. It must have arisen from electron transfer from the enzyme-bound flavin to substrate, however, because repeated light flashes, which consumed the substrate, led to eventual disappearance of the EPR signal.

iii.d. Isotope Effects. The direction of electron transfer in photolyase was investigated by determining the secondary deuterium isotope effects on the enzyme¹³⁷ and comparing the results with those of model compounds known to split the cyclobutane ring by either electron donation or electron abstraction. As shown in Figure 22 cleavage of a uracil dimer radical cation (using anthraquinone as an electron acceptor) exhibits a substantial secondary deuterium isotope effect at the 6,6 position and a negligible effect at the 5,5 position,¹³⁸ while both cleavage of a dimer anion radical¹³⁸ (using indole as an electron donor) and cleavage of U<>U by photolyase¹³⁷ exhibit a relatively large isotope effect for both 5–5 and 6–6 bond cleavage. These results are more consistent with generation of a photodimer radical anion by photo-induced electron transfer by photolyase rather than with the radical cation path.

iii.e. Substrate Analogues. A number of substrate analogues have been synthesized to investigate the cleavage pathway of the cyclobutane ring with both model photosensitizers¹³⁹ and with photolyase by trapping reaction intermediates in model systems.¹⁴⁰ Attempts with trapping experiments with photolyases and substrate analogues have been unsuccessful

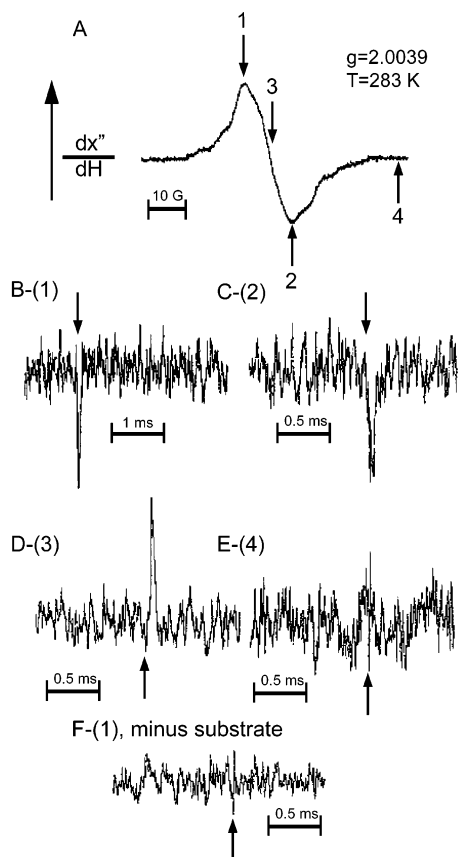


Figure 21. Time-resolved EPR spectra of Pyr<>Pyr splitting by *E. coli* DNA photolyase: (A) dark-stable EPR spectrum of E-FADH[•]; (B–E) kinetic transients of E-FADH[•] + T<>T at field positions 1–4, respectively. (F) is the kinetic transient of E-FADH[•] at field position 1 in the absence of substrate. The arrows in (B)–(F) indicate the position of 17 μ s light flashes. At each field position 1200 flashes were averaged. Reprinted from ref 136. Copyright 1992 American Chemical Society.

because the analogues either gave ambiguous results or were not substrates for photolyase.⁹

b. Photochemistry. Cyclobutane pyrimidine dimers are formed by the [2 + 2] cycloaddition reaction. This is the classic example of a photochemical reaction allowed by the rules of conservation of orbital symmetry (Woodward–Hoffmann rules). The same rules apply to the splitting of the photodimer by [2 + 2] cycloreversion with far ultraviolet light (240 nm), which occurs with a quantum yield of near unity. However, photolyase splits dimers with near-UV/blue photons (300–500 nm), which have energies of 250–300 kJ mol⁻¹, far less than the 500 kJ mol⁻¹ needed to excite Pyr<>Pyr to ¹(Pyr<>Pyr)*.¹¹ Therefore, photolyase-mediated splitting of cyclobutane dimers cannot occur by orbital symmetry-allowed concerted [2 + 2] cycloreversion. Instead, photolyase initiates splitting by electron transfer to Pyr<>Pyr, and because Pyr<>Pyr⁻ is not a photochemically excited species, strictly speaking, splitting of the cyclobutane ring is not a photochemical but is a thermal reaction. Hence, it must follow the rules of the conservation of orbital symmetry for thermal reactions.¹¹ In fact, it can be shown¹¹ that conversion of a cyclobutane radical anion into ethene + ethene radical anions is also forbidden by the rules of

conservation of orbital symmetry for thermal reactions.¹¹ Thus, it appears that photolyase does not mediate photocycloreversion of the cyclobutane ring by converting a symmetry-forbidden reaction into a symmetry-allowed reaction; rather, it lowers the splitting activation energy barrier to about 0.45 eV (~10 kcal mol⁻¹),¹³² so as to allow a “symmetry-forbidden” reaction to proceed very efficiently at ambient temperatures.

i. Orbital Energy Diagram for Photorepair. With the assumption that splitting of the cyclobutane ring occurs by electron transfer between flavin and the Pyr<>Pyr, orbital energy diagrams for the reaction may be drawn as shown in Figure 23.¹¹ Absorption of a photon by FADH⁻ promotes an electron from the highest occupied molecular orbital (HOMO) to the lowest unoccupied molecular orbital (LUMO), which corresponds to the $\pi \rightarrow \pi^*$ transition ($E = 240$ kJ mol⁻¹ on the basis of the well-resolved vibronic structure of the FADH⁻ fluorescence emission spectrum at low temperatures). This ¹(FADH⁻)* state is a more efficient electron donor than FADH⁻ because of the now-occupied LUMO and is also a more efficient electron acceptor because the HOMO is now a singly occupied molecular orbital (SOMO). Therefore, the incoming electron will fall into this low-energy SOMO rather than the much higher energy LUMO. However, even the low-lying SOMO of ¹(FADH⁻)* is at a higher energy level than the HOMO of Pyr<>Pyr, which makes electron transfer from the photodimer to ¹(FADH⁻)* unlikely. Instead, electron transfer must occur from the high-energy SOMO of ¹(FADH⁻)* to the LUMO orbital of Pyr<>Pyr.

ii. Thermodynamic Cycle. By combining the energetics of the excited states of flavin within the enzyme with the redox potentials of Pyr<>Pyr and of known or presumed intermediates on the photo-splitting reaction pathway, a thermodynamic cycle for photolyase-mediated splitting of a Pyr<>Pyr has been generated and is shown in Figure 24.¹¹ First, absorption of a photon generates the high-energy FADH⁻ excited state ($\Delta G = 240$ kJ mol⁻¹). Electron transfer from ¹(FADH⁻)* to Pyr<>Pyr is exergonic with $\Delta G = -125$ kJ mol⁻¹. There is considerable uncertainty about the free energy of splitting of the dimer anion radical, but $\Delta G = -88$ kJ mol⁻¹ is estimated to be a likely value. Finally, the return of the electron to FADH[•] to complete the catalytic cycle calculated from the redox potentials of the reactants is estimated to be $\Delta G = -120$ kJ mol⁻¹. In this scheme, the free energy difference between reactants and products, in apparent violation of Hess’s law, appears to depend on the reaction pathway (290 kJ mol⁻¹ vs 333 kJ mol⁻¹).¹¹ This is due to some uncertainties in the energetics of some of the reactions along the presumed catalytic pathway. In fact, a significantly different thermodynamic cycle for the overall reaction has also been proposed.¹⁴¹ This difference is, in part, due to uncertainties in the exact values in the reduction potential of ¹(FADH⁻)* and the oxidation potential of Pyr<>Pyr. However, these uncertainties are unlikely to be of sufficient magni-

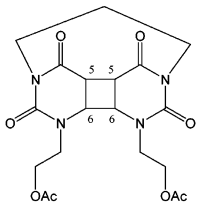
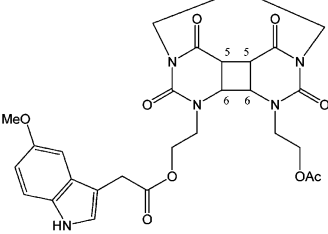
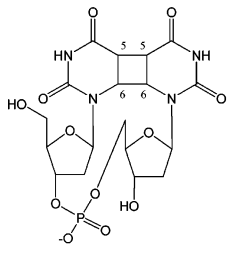
Sensitizer		
Anthraquinone (electron acceptor)	Indole (electron donor)	Photolyase
		
Isotope Effects		
5,5-D ₂ 1.03 ± 0.02	5,5-D ₂ 1.17 ± 0.01	5,5-D ₂ 1.08 ± 0.01
6,6-D ₂ 1.19 ± 0.02	6,6-D ₂ 1.08 ± 0.01	6,6-D ₂ 1.07 ± 0.01

Figure 22. Secondary isotope effects on splitting the pyrimidine dimer radical cation on an anion compared with splitting by photolyase. Splitting of the dimer radical cation exhibits a negligible secondary deuterium isotope effect at the 5,5 position. In contrast, the isotope effect on cleavage in a model anion reaction or by photolyase shows a substantial isotope effect on 5–5 cleavage; these are consistent with a dimer radical anion as an intermediate in catalysis by photolyase. Modified from refs 137 and 138.

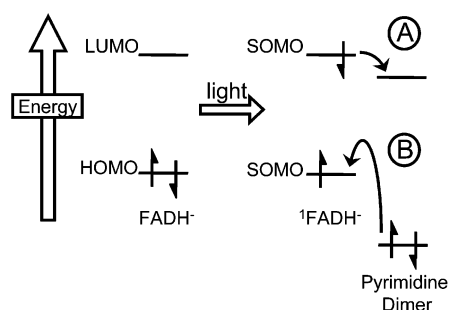


Figure 23. Orbital energy diagram for electron transfer between $^1(\text{FADH}^-)^*$ and $\text{Pyr} \leftrightarrow \text{Pyr}^-$ in the ground and excited states: (A) electron transfer from $(\text{FADH}^-)^*$ to $\text{Pyr} \leftrightarrow \text{Pyr}^-$; (B) electron transfer from $\text{Pyr} \leftrightarrow \text{Pyr}^-$ to $^1(\text{FADH}^-)^*$. Adapted from ref 11.

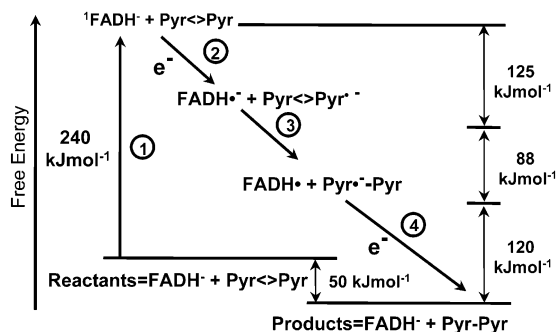


Figure 24. Thermodynamic cycle for catalysis by photolyase: (1) electronic excitation; (2) electron transfer from $^1(\text{FADH}^-)^*$ to $\text{Pyr} \leftrightarrow \text{Pyr}^-$; (3) splitting of the dimer to a Pyr and Pyr anion radical ($\text{Pyr}^{\circ-}$); (4) back electron transfer from $\text{Pyr}^{\circ-}$ to FADH° . The energetics were estimated from the vibronic structure of FADH^- fluorescence at low temperature, photothermal beam deflection calorimetry, and fluorescence quenching by $\text{Pyr} \leftrightarrow \text{Pyr}^-$ of a series of excited-state electron donors of known excited-state redox potential. Reprinted with permission from ref 11. Copyright 1995 Royal Society of Chemistry.

tude to change the general shape of the thermodynamic cycle.

c. Reaction Mechanism. On the basis of current knowledge from studies with photolyases as well as with model systems, a mechanistic model for *E. coli*

photolyase is shown in Figure 25. Step 1: a blue-light photon (350–450 nm) is absorbed by MTHF, or by FADH^- , but at much lower efficiency due to the lower extinction coefficient of FADH^- . Step 2: $^1(\text{MTHF})^*$ transfers energy to FADH^- over a distance of 16.8 Å at a rate of $5 \times 10^9 \text{ s}^{-1}$ via dipole–dipole coupling between the donor and acceptor. Step 3: $^1(\text{FADH}^-)^*$ transfers an electron to $\text{Pyr} \leftrightarrow \text{Pyr}^-$ at a rate of 7×10^9 to $2 \times 10^{10} \text{ s}^{-1}$ over a distance of 5–10 Å.^{96,98,142} It has been proposed that the U-shape of FAD (the adenine is stacked on top of the flavin ring) facilitates electron transfer from the 7,8-dimethylalloxazine through the adenine ring by a superexchange mechanism, and that the superexchange mechanism has the advantage over the direct transfer pathway of minimizing the rate of back electron transfer in competition with splitting of the cyclobutane ring.^{143,144} It has also been argued that the back electron transfer from the $\text{Pyr} \leftrightarrow \text{Pyr}^{\circ-}$ to FADH° is highly exergonic. Thus, in the nonpolar active site this exergonic reaction would fall into the Marcus inverted region¹⁴⁵ because of the high reorganization energy caused by back electron transfer. The net outcome is a slow rate of back electron transfer and very efficient splitting.^{11,146–148} However, this suggestion has been contested on the grounds that the immediate product of electron transfer is the $[\text{FADH}^\circ \cdot \text{Pyr} \leftrightarrow \text{Pyr}^{\circ-}]$ charge-transfer complex and not the zwitterionic $[\text{FADH}_2^{\circ+} \cdot \text{Pyr} \leftrightarrow \text{Pyr}^{\circ-}]$ form with high exergonic energy for back electron transfer.¹³³ The faster rate of electron transfer to the $\text{U} \leftrightarrow \text{T}$ dinucleotide dimer ($\geq 2 \times 10^{10} \text{ s}^{-1}$) relative to the $\text{T} \leftrightarrow \text{U}$ dinucleotide dimer ($\sim 10^{10} \text{ s}^{-1}$) has led to the suggestion that there is better electronic coupling between the donor and acceptor when the uracil residue is the 5' base, and hence after being abstracted from $^1(\text{FADH}^-)^*$, the electron may be located on the 5' moiety of the dimer.¹³² Studies with a model system in which *N*α-acetyltryptophan was the electron donor support this model.¹⁴⁹ It must be noted that the rates of electron transfer from $^1(\text{FADH}^-)^*$ to $\text{Pyr} \leftrightarrow \text{Pyr}^-$ were obtained with dinucleotide dimers. It is likely that when photolyase binds to a $\text{Pyr} \leftrightarrow \text{Pyr}^-$

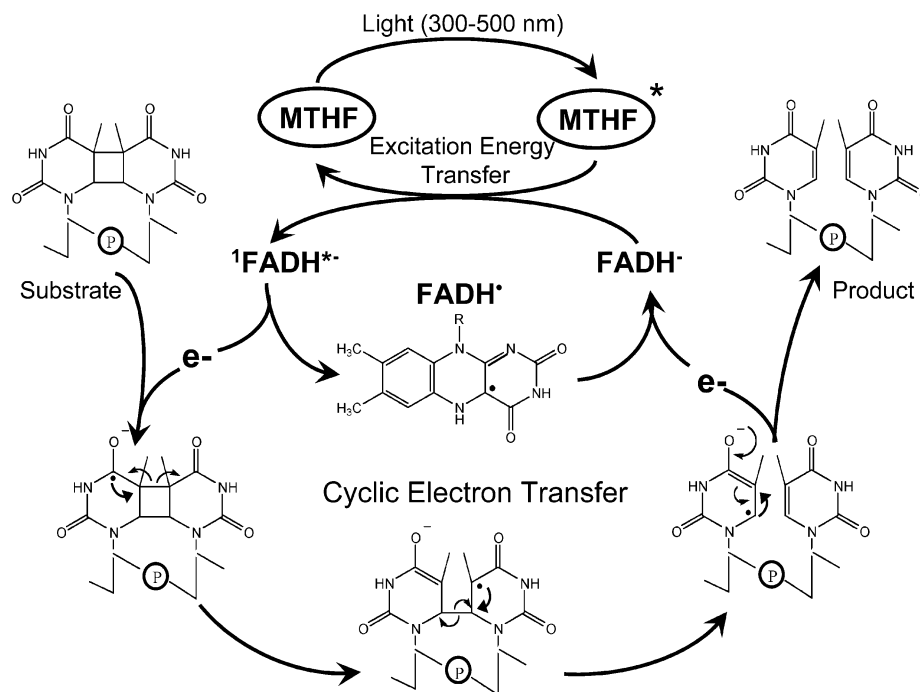


Figure 25. Reaction mechanism of DNA photolyase. MTHF absorbs a 300–500 nm photon and transfers the excitation energy to FADH[•] by FRET. The ¹(FADH[•])^{*} transfers an electron to Pyr<>Pyr, which undergoes [2 + 2] cycloreversion to generate a Pyr and a Pyr^{•-}; back electron transfer to FADH[•] restores the catalytic cofactor to the active reduced form, and the dimer is converted to canonical bases.

in DNA there is better electronic coupling between the flavin and the dimer (relative to that in complexes formed with dinucleotide dimers) due to stabilization of the enzyme–substrate complex with additional interactions with the DNA backbone, and as a consequence the rates of electron transfer to cyclobutane pyrimidine dimers in DNA might be faster than those for dimers in the form of dinucleotides. Step 4: The 5–5 and 6–6 bonds are cleaved by an asynchronous concerted mechanism. The fact that the secondary isotope effects on C5–C5 cleavage are more pronounced when the electron donor is a 5-methoxyindole excited singlet (Figure 22)¹³⁸ compared to when photolyase ¹(FADH[•])^{*} is the donor¹³⁷ suggests that enzymatic cleavage might be mechanistically significantly different than cleavage in model systems, perhaps due to changes in the conformation of the substrate or to secondary effects of Trp277 and Trp384, which are expected to stack with the dimer with partial π -orbital overlap.^{77,95} Step 5: Back electron transfer from either the 5–5 cleaved dimer radical anion¹¹ or from the pyrimidine anion radical resulting from 5–5 and 6–6 cleavage¹⁰ restores FADH[•] to FADH⁻. Although the splitting is exergonic by 38 kJ mol⁻¹ relative to the neutral dimer, the active site residues of the enzyme make substantial contributions to the free energy and hence to the rate of splitting in competition with back electron transfer before repair.¹³²

Studies with model systems have provided important clues for the significance of the deprotonated two-electron-reduced flavin FADH⁻ rather than FADH₂ as the electron donor. (It must be noted that in most flavoproteins the two-electron-reduced state is stabilized in the form of FADH⁻.^{149a}) Using covalently linked flavin–cyclobutane dimer model com-

pounds, it was found that at neutral pH the dihydroflavin form of the cofactor was a poor photosensitizer as a splitting agent, but its efficiency dramatically increased at high pH where the N1 (pK_a = 6.5) of flavin is deprotonated.^{133,150,151} It has been argued that electron transfer from FADH₂ would generate the zwitterionic FADH₂^{•+}–Pyr<>Pyr^{•-} charge-shift intermediate, which favors back electron transfer, compared with the FADH[•]–Pyr<>Pyr^{•-} charge-transfer intermediate, which favors splitting of the cyclobutane ring.¹⁶ The entire splitting and back electron transfer are expected to be complete within 0.5–2 ns¹²⁹ to close the photocycle.

While it is generally assumed that back electron transfer from the repaired pyrimidine to FADH[•] restores the cofactor, the evidence for this is indirect. First, the restoration of FADH[•] to FADH⁻ cannot be by an amino acid of the apoenzyme. Even though Trp306 can reduce FADH[•], this photoreduction occurs only when FADH[•] is in an excited state [²(FADH[•])^{*} or ⁴(FADH[•])^{*}]. The FADH[•] generated by the ^{*}FADH⁻ $\xrightarrow{e^-}$ Pyr<>Pyr reaction is in the ground state and is not reduced by either Trp306 or external reducing agents such as DTT. Second, there is no accumulation of significant quantities of FADH[•] after multiple rounds of catalysis by photolyase under conditions where there was negligible photoreduction.^{33,34,89} Third, splitting of the dimer is a monophotonic reaction;⁸² hence, FADH[•] is not converted to FADH⁻ by a second photon after each cycle. In fact, the strongest evidence for a cyclic electron transfer during catalysis is the finding that the quantum yields for repair obtained under pre-steady-state (single-turnover) and steady-state (multiple-turnover) conditions are, within experimental error,

identical.^{33,34,47,74} The quantum yield for repair by the enzyme containing FADH⁻ is 0.7–1.0,^{32–34,47,74} whereas the quantum yield of photoreduction of FADH[°] to FADH⁻ is 0.05–0.1,^{32,62,63,82b} and hence, if photoactivation of the enzyme were necessary after each round of repair, the overall quantum yield under multiple-turnover conditions would be expected to be that of photoreduction, that is, 0.05–0.1.³² In reality, the quantum yield under steady-state conditions is essentially the same as that obtained with single turnover for both folate class^{33,34} and deazaflavin class^{47,74} photolyases, indicating that FADH[°] is restored to FADH⁻ after each catalytic cycle by back electron transfer from the product. However, the back electron transfer to FADH[°] at the end of the catalytic cycle still remains poorly defined and is in need of analyses by new methodologies. Finally, it must be noted that the reaction scheme given here is for *E. coli* photolyase. In some other folate class photolyases⁷¹ and in all deazaflavin photolyases studied to date, the rate and efficiency of energy transfer from the photoantenna to FADH⁻ are greater than those for *E. coli* photolyase, but all indications are that the basic catalytic steps are identical in all photolyases.

3. Model Systems

Studies with model systems using simple organic compounds capable of photoexcited redox chemistry to mimic the kinetic, thermodynamic, and mechanistic aspects of dimer splitting by photolysis^{9,11,16,126,134,135,141,154–160} have been instrumental in designing and analyzing experiments conducted with photolyase and in developing a mechanistic model for the enzyme. Some of these studies have been mentioned in the appropriate sections dealing with the structure and function of the enzyme. In general, studies with model systems have shown that Pyr^{<>}Pyr can be split by either electron donors or electron acceptors and that the dielectric properties and the pH of the medium can have profound effects on the efficiency of splitting. However, a detailed analysis of the studies with the model systems is outside the scope of this review.

C. Photoreduction of Photolyase (Preillumination Effect)

In the seminal work on photolyase^{79–83} that established the basic mechanism of the enzyme using partially purified yeast extract as the enzyme source, it was found that, if the extract (enzyme) was exposed to light prior to mixing with substrate, no repair occurred, but if the enzyme was first mixed with UV-irradiated DNA and then illuminated either with a white-light source or with a single light flash, the DNA was repaired (sequential reaction-ordered mechanism). This classic experiment, which revealed that formation of the Michaelis complex by photolyase was light independent, but that catalysis was initiated by light (second substrate), also uncovered a curious phenomenon:⁸³ even though light exposure after mixing with substrate was essential for catalysis, it was found that extracts, particularly old extracts, that were exposed to light before mixing with substrate were more active than control extracts in the

subsequent photorepair experiments. This phenomenon was called the “preillumination effect”⁸³ and remained unexplained until photolyase was purified in large quantities from *E. coli*⁵⁰ and subsequently from yeast and many other species.

Work with purified enzymes showed that in the majority of photolyases the flavin cofactor is converted to the catalytically inert form upon cell lysis under aerobic conditions.^{32,44} It must be noted that, even after 10000-fold overproduction, *E. coli* photolyase is maintained in the two-electron-reduced form in vivo and that conversion to the FADH[°] form occurs rather rapidly after cell lysis.⁴⁴ In contrast, yeast photolyase, either from its native host or when purified as a recombinant protein produced in *E. coli*, retains its flavin in the FADH⁻ form, even after purification through several columns to homogeneity. It is converted to the FADH[°] form only upon prolonged storage under aerobic conditions.⁵⁸ Thus, it should be noted that, while exposure of the FADH[°] form of photolyase to light elicits an interesting set of photochemical reactions (as discussed below),^{161–163} in all likelihood these are of only marginal physiological significance, because this form of the enzyme either does not exist in vivo or is present at a rather low level⁴⁴ and is not generated during the photolyase photocycle in vivo.

Exposure of the E-FADH[°] form of *E. coli* photolyase to light in the presence of a reducing agent converts it to the E-FADH⁻ form⁶² and increases its quantum yield for repair drastically.³² This is because the quantum yield of repair of the FADH[°] form of the enzyme is simply the quantum yield for photoreduction of FADH[°] to FADH⁻, which then repairs DNA by a second round of excitation (Figure 26). Hence, the preillumination effect is due to photoreduction of the catalytic cofactor to its active FADH⁻ form.³²

1. Electron Donor

Transient absorption spectroscopy on the E-FADH[°] form of photolyase suggests that the excited doublet state (D₁) is converted to the lowest excited quartet state by intersystem crossing^{161,162} (Figure 27). This excited state then is quenched by abstracting an electron from the apoenzyme. The proximate donor in photoreduction is intrinsic to the enzyme, but in the absence of external reducing agents such as DTT, there is rapid back electron transfer, resulting in reoxidation of flavin to FADH[°].⁶² Even in the presence of DTT under aerobic conditions, photochemically reduced enzyme gradually (over a period of minutes) reoxidizes to the neutral radical form. Thus, difference spectra taken at $t > 1 \text{ ms} < 1 \text{ min}$ are simple reflections of FADH[°] → FADH⁻ conversion, and because FADH⁻ does not absorb strongly in the visible range, they look like mirror images of the FADH[°] spectrum (Figure 28). However, difference spectra taken on the microsecond time scale reveal a distinctive feature consistent with the appearance of a UV/vis-absorbing species superimposed onto the FADH[°] depletion spectrum.^{63,164} Thus, by taking the second differential, that is, by subtracting difference spectra recorded in the minute range from the

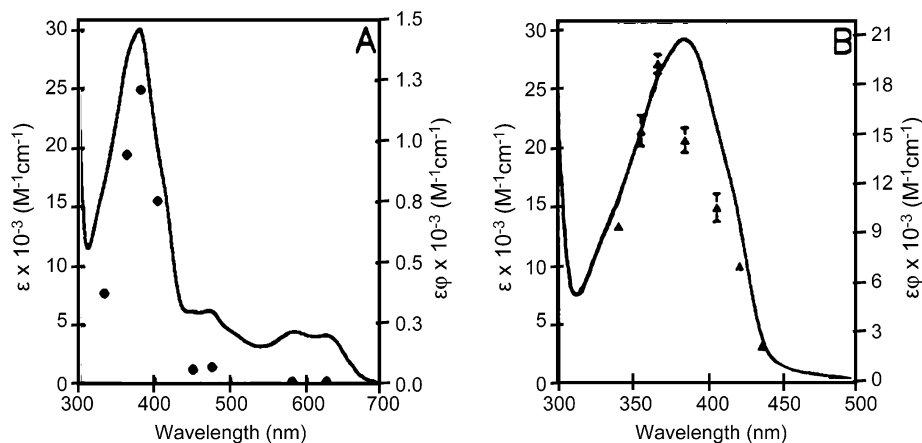


Figure 26. Absolute action spectra of E-MTHF-FADH° and E-MTHF-FADH⁻ forms of photolyase. (A) Enzyme with a neutral radical. The action spectrum does not match the absorption spectrum, and the quantum yield is variable with wavelength. Even at its highest value (at about 390 nm) the quantum yield is only about 10% of the in vivo quantum yield. (B) Enzyme with reduced flavin. The absorption and action spectra match, and the in vivo and in vitro photolytic cross-sections are nearly identical. Adapted from refs 33 and 168.

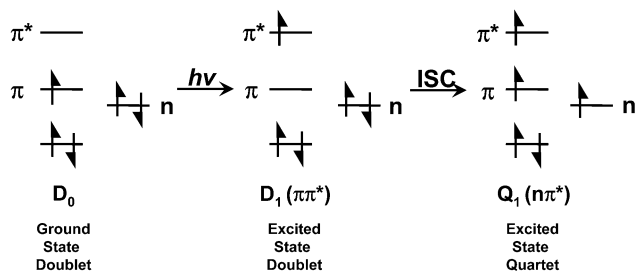


Figure 27. Possible electronic configurations of π - π^* doublet and $n\pi^*$ quartet States of FADH°. Nanosecond flash photolysis of E-FADH° indicates that the excited-state FADH° may have a lifetime of about 1 μ s. This long-lived species has been assigned to the lowest excited quartet state that is generated by a doublet-quartet intersystem crossing. Reprinted with permission from ref 165. Copyright 1995 Academic Press.

difference spectra recorded in the microsecond range, the identity of the electron donor can be determined.^{164,165} Figure 28 (left) shows difference spectra taken at 1 min and 4 μ s after a 532 nm laser flash and the differential $\Delta\Delta A = \Delta A(4 \mu\text{s}) - \Delta A(1 \text{ min})$. Theoretically, $\Delta\Delta A$ should correspond to the radical absorption (D° or $DH^{\circ+}$) of the donor, assuming that the radical did not undergo secondary reactions on the microsecond time scale. The result, seen in Figure 28 (left) shows an absorption spectrum that matches reasonably well with a Trp neutral radical (Trp°), suggesting photoreduction by H-atom transfer. However, the match is not perfect, and a mixture of $\text{Trp}^\circ + \text{TrpH}^{\circ+}$ spectra could not be eliminated as a possibility. Thus, even though fast absorption spectroscopy identified the electron donor as a Trp residue, it did not conclusively discriminate between a Trp cationic radical ($\text{TrpH}^{\circ+}$) and a Trp neutral radical (Trp°), which would arise from electron and H-atom transfer, respectively.¹⁶⁴ The issue was resolved by conducting time-resolved EPR experiments with photolyase containing isotopically labeled tryptophans.

Using gated integration (48 μ s integration window and a 4 μ s delay following the light flash) and ac coupling ($\nu = 10$ Hz) to discriminate against the time-independent FADH° signal, a spectrum of the tran-

sient EPR signal induced by the light flash was obtained.^{56,166} Figure 28 (right) shows EPR spectra typical of a Trp radical. MO calculations show that the electron density of a Trp radical cation ($\text{TrpH}^{\circ+}$) is primarily localized at the C2 and C3 positions whereas the spin density in Trp neutral radical (Trp°) is localized at C3 and N1. Thus, it was possible to differentiate between electron transfer ($\text{TrpH}^{\circ+}$) and H-atom transfer (Trp°) by examining the transient spectra of photolyase containing indole-*d*₅ (spectrum B), indole-2,5-*d*₂ (spectrum C), and indole-¹⁵N (spectrum D) tryptophans. Spectra B and C are nearly identical and reveal the disappearance of fine structure on the low-field edge of the spectrum, consistent with a $\text{TrpH}^{\circ+}$ spectrum. This is further supported by the EPR spectrum of indole-¹⁵N enzyme (spectrum D), which shows that the contribution of the ¹⁴N nucleus to the hyperfine splitting (which would have been the main cause of splitting in the neutral radical) is in fact nonexistent. Thus, isotopic labeling experiments clearly identify the light-induced transient as $\text{TrpH}^{\circ+}$, leading to the conclusion that photoreduction of FADH° occurs by electron transfer from a Trp residue in the apoenzyme. A subsequent picosecond flash photolysis study¹⁶⁷ has confirmed this conclusion and furthermore has led to the suggestion that the $\text{TrpH}^{\circ+}$ radical is subsequently deprotonated rapidly (300 ns) by ejecting a proton into the solvent.

The Trp residue that acts as the electron donor in photoreduction was identified by site-specific mutagenesis. Photolyase is extremely rich in tryptophans. The 471 amino acid long *E. coli* apoenzyme contains 15 Trp residues, which is about 10 times more frequently than for an average *E. coli* protein.¹⁶⁸ To identify the Trp residue responsible for photoreduction, each of the 15 Trp residues was replaced individually by Phe, and the mutant enzymes were tested in vivo and in vitro.¹⁶⁸ With the exception of the W6F mutant enzyme (which was apparently not expressed), all mutant enzymes exhibited normal photoreactivation activity in vivo (Table 5). Nine of the mutant proteins were purified and tested for their capacity to photoreduce; only the W306F mutant

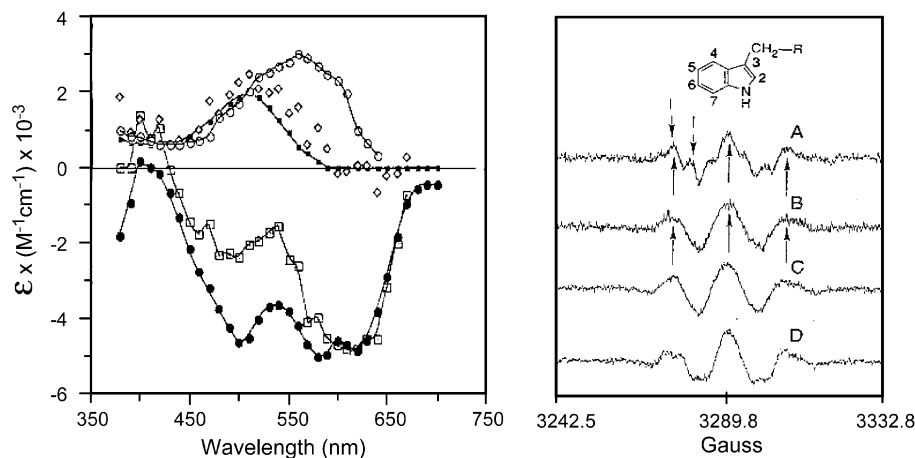


Figure 28. Identification of tryptophan as the intrinsic electron donor in photoreduction. Left: transient absorption spectroscopy of E-FADH[•]. Flash-induced difference spectra are plotted on an absolute extinction coefficient scale. Key: closed circles, 1 min after a single camera flash; open squares, 4 μs after a laser flash; diamonds, ΔΔA = ΔA(4 μs) - ΔA(1 min); closed squares, absorption spectrum of tryptophan neutral radical (Trp[•]); open circles, absorption spectrum of tryptophan cation radical (TrpH^{•+}). Right: Transient EPR spectroscopy using isotopically labeled tryptophans. All spectra are in the first-derivative mode. The spectrum of E-FADH[•] containing labeled tryptophans was obtained following a 17 μs flash and using a 48 μs integration window and a 4 μs delay after the flash. (A) native enzyme, (B) indole-d₅, (C) indole-2,5-d₂, and (D) indole-¹⁵NTrp containing enzyme spectra. The Trp structure and numbering system of the indole ring are shown at the top. Adapted from refs 56, 63, and 165.

Table 5. Properties of W → F Mutants of *E. coli* Photolyase^e

amino acid position	over-production	in vivo relative εΦ ^a	in vitro relative photo-reduction rate ^b	MTHF photodecomposition ^d
PL-WT	+	1.0	1 (0.7–1.4)	+
W6F	-	0	ND ^c	ND
W41F	+	0.98	1.1	+
W157F	+	0.98	0.7	+
W271F	-	1.10	ND	ND
W277F	+	0.96	1.0	+
W300F	-	1.00	ND	ND
W306F	+	1.00	0.0	-
W316F	-	1.05	ND	ND
W338F	-	1.03	ND	ND
W359F	-	0.89	ND	ND
W382F	+	1.14	2.2	+
W384F	+	1.10	1.3	+
W418F	+	1.00	1.1	+
W434F	+	1.00	1.4	+
W436F	+	1.00	0.9	+

^a The εΦ measurements at 384 nm were conducted in parallel with a strain containing the wild-type enzyme. ^b Photoreduction was conducted in the presence of 25 mM dithiothreitol. The two values given for the wild type are the rates obtained in two separate experiments. The rates of the mutants are relative to the average value for the wild type. ^c Not determined. ^d The mutants with a + sign were not distinguishable from the WT; the maximum photodecomposition observed with the W306F mutant was 5% of the wild type. ^e Adapted from ref 169.

failed to photoreduce, as evidenced by transient EPR spectroscopy (Figure 29) and by absorption spectroscopy (see Figure 31). Because of the reasonably high quantum yield of photoreduction (Φ ≈ 0.1), Trp306 was therefore presumed to be in the active site close to FAD to effect such high-efficiency electron transfer.¹⁶⁹

2. Electron-Transfer Path

It was, therefore, rather surprising when the crystal structure revealed that Trp306 is in fact 13

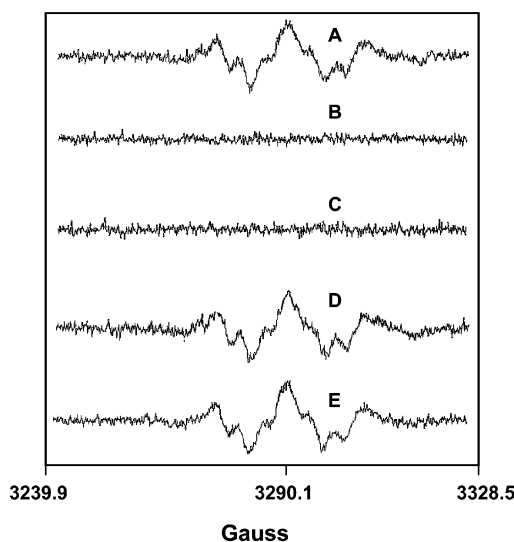


Figure 29. Identification of Trp306 as the electron donor in photoreduction. Time-resolved EPR on wild-type *E. coli* photolyase and various W → F mutants were obtained as in Figure 28. Only W306F fails to produce the transient Trp radical signal. Key: (A) WT; (B) W306F; (C) W306Y; (D) W157F; (E) W418F. Note the lack of transient in (B) and (C). Reprinted with permission from ref 56. Copyright 1993 National Academy of Science.

Å away from FAD and is located near the protein surface where it can exchange electrons with external reductants.³⁷ Inspection of the crystal structure revealed two potential pathways for electron transfer³⁷ (Figure 30): One pathway passed through Trp306 → Trp358 → Trp382 and involved three electron hops, and the other consisted of the α-helix (α-15) between residues 358 and 366 and the side chain of Phe366. At the time the crystal structure was solved the W358F and W382F mutant proteins necessary to test the Trp-hopping pathway were not available,¹⁶⁹ and hence, no definitive statement could be made regarding the path and the mechanism of electron transfer from W306 to FADH[•]. Subse-

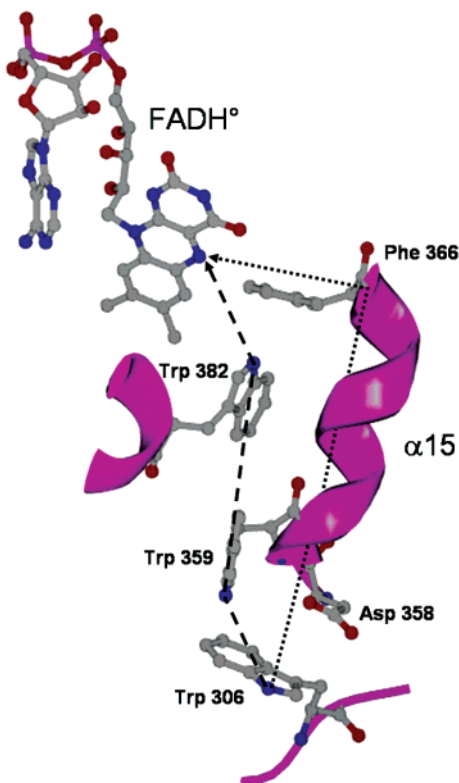


Figure 30. Potential pathways for electron transfer from Trp306 to FADH[•]. In one pathway the electron makes three hops through W306 → W359 → W382 → FADH[•]. In the second pathway the electron goes through α -helix 15. Experimental data support a superexchange mechanism between Trp306 and FADH[•] rather than electron abstraction from W382 followed by hopping from W359 and then W306.

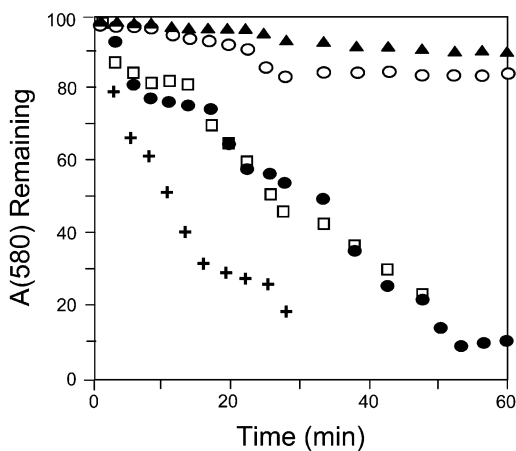


Figure 31. Effect of Trp → Phe mutations on electron transfer from Trp306 to FADH[•]. Replacement of W306 by F or Y blocks electron transfer, whereas replacement of W382 by Y does not affect the efficiency. The W382F mutation increases the quantum yield of photoreduction by a factor of 2, while the W382A or the W82N (not shown) mutation abolishes photoreduction. Symbols: closed circle, WT; triangle, W306F; open circle, W382A; square, W382Y; plus sign, W382F. The E-FADH[•] form of the enzyme preparations was exposed to 366 nm radiation for the indicated times, and the FADH[•] photoreduction was quantified by the decrease in absorbance at 580 nm.

quently, the W382F mutant was purified and analyzed to understand the electron-transfer mechanism in photoreduction.

3. Electron-Transfer Mechanism

Using time-resolved absorption spectroscopy in the picosecond range, it was reported that electron transfer from W382 to FADH[•] occurred in 30 ps and was followed by two subsequent transfers from W358 and W306 in less than 10 ns each. These findings clearly favor the pathway of electron hopping through the tryptophans¹⁶⁷ and exclude electron-tunneling or superexchange-mediated electron-transfer mechanisms.¹⁶⁷ To test the “electron-hopping” model, the W382F mutant was tested for photoreduction. As shown in Figure 31, photoreduction of W382F occurs with 2-fold higher quantum yield than that of the wild-type (WT) enzyme, which excludes W382 as the immediate electron donor in photoreduction. Other mutants, W382A and W382K, like W306F, were not photoreducible. However, W382Y was photoreduced with the same quantum yield as the WT protein. These data, which clearly disagree with the prediction of the electron-hopping model based on time-resolved absorption spectroscopy,¹⁶⁷ favor a superexchange or electron-tunneling mechanism of electron transfer from W306 to FADH[•] and have been supported by quantum chemical computations.¹⁷⁰

4. Physiological Relevance

Photoreduction by electron transfer from aromatic residues has also been demonstrated in *A. nidulans* photolyase (Trp and Tyr)¹⁷¹ and in *X. laevis* (6–4) photolyase (tyr).¹⁷² However, photoinduced redox reactions between flavin and aromatic residues in the protein are common to most flavoproteins, including xanthine oxidase¹⁷³ and glucose oxidase,¹⁷⁴ and are not germane to the reaction mechanisms of either those flavoproteins or photolyases, as explained above, and therefore will not be analyzed any further.

D. Radical Reactions in Photolyase

Light induces four types of electron-transfer reactions in photolyase. (1) $\text{FADH}^- \xrightarrow{e^-} \text{Pyr} \leftrightarrow \text{Pyr}^{\bullet 30}$ cyclic electron-transfer reaction from FADH⁻ to the substrate, which causes [2 + 2] cycloreversion followed by back electron transfer and hence repair of DNA, is perhaps the only physiologically relevant photoinduced electron transfer carried out by the enzyme. (2) $\text{FADH}^- \xrightarrow{e^-} \text{MTHF}$. This side reaction results in breakdown (photodecomposition) of MTHF.^{45,63} The transfer occurs from the excited-state FADH⁻, but not from excited states of FADH[•] or FAD_{ox}. The W306F mutation blocks the reduction of FADH[•] to FADH⁻ and, hence, blocks photodecomposition (Table 5).¹⁶⁹ The quantum yield of photodecomposition is very low (~0.01),⁶³ so that even though this pathway theoretically competes with the repair reaction, because of the vastly different quantum yields for the two processes, the decay of ¹(FADH⁻)^{*} by this pathway is insignificant. It is noteworthy, however, that, in the absence of substrate and with high doses of violet-blue light, this pathway may result in elimination of the folate photoantenna and drastic decreases in repair efficiency, which is defined as the number of photodimers repaired per incident photon. This phenomenon may explain the observa-

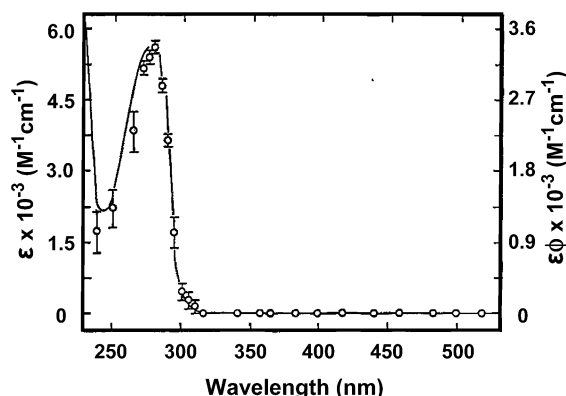


Figure 32. Repair of Pyr<->Pyr by a Trp residue in photolyase. The absolute action spectrum of the nonphotoreducible photolyase mutant W306F (circles) is superimposed on the absorption spectrum of tryptophan (absolute scale). In this mutant as well as in WT enzyme 7% of Trp fluorescence is quenched by the substrate, whereas in the W277F mutation there is no fluorescence quenching, identifying W277 as the electron donor. Reprinted with permission from ref 95. Copyright 1992 National Academy of Science.

tion that *E. coli* photolyase is inactivated by high doses of 366 nm irradiation of the bacterial culture.¹⁷⁵ A study with a series of model compounds in which the cyclobutane pyrimidine dimer was connected both to a flavin and to a deazaflavin revealed that at too close a photoantenna–photocatalyst distance this reaction (electron transfer from photocatalyst to photoantenna) becomes significant, and results in inhibition of repair by competitive electron transfer to the photoantenna.¹⁷⁶ (3) Trp306 $\xrightarrow{e^-}$ $^4(\text{FADH}^-)^*$. This transfer occurs over a 13 Å distance and has been investigated in some detail,^{161–166,168–172} as discussed above. It is of significance for in vitro studies of the enzyme, because in most photolyases purification results in conversion of FADH⁻ to the FADH^o neutral radical. In addition, this photo-reduction reaction is a good tool for studying the mechanisms of intraprotein electron transfer. However, there is no evidence that this reaction occurs in vivo, and hence, this transfer is probably of marginal or no physiological relevance. (4) $^1\text{Trp277}^* \xrightarrow{e^-} \text{Pyr} \leftrightarrow \text{Pyr}$.⁹⁵ In WT photolyase FADH⁻ $\xrightarrow{e^-}$ Pyr<->Pyr is the main photorepair reaction, and obscures any effect on repair at short wavelengths by aromatic amino acid residues. In the W306F mutant the enzyme contains FADH^o in vitro, and this form is inactive at photoreactivation wavelengths (350–500 nm) because it cannot be photoreduced. However, photorepair experiments with shorter wavelengths revealed an action spectrum peak at 280 nm with a quantum yield of 0.5⁹⁵ (Figure 32). This peak was absent in the W277F mutant, so it appears that Trp277 is in close contact with Pyr<->Pyr in the active site and can mediate repair with a high quantum yield. This reaction may contribute to photoreactivation of DNA with short-wavelength irradiation.

E. “Dark Function” of Photolyase

Photolyase is present in many bacteria such as *E. coli*, which are rarely exposed to DNA-damaging UV

light. Furthermore, nearly all species tested have a potent and general repair system called “excision repair”. This system eliminates Pyr<->Pyr and other photoproducts from DNA rapidly and thus ensures survival, even after relatively high doses of UV.^{29,177,178} In animals that express photolyase, the enzyme appears to be uniformly expressed in all tissues whether the tissues are exposed to light or not. It has been noted, for example, that, of all opossum tissues tested, the brain appears to contain the highest photolyase activity. What is photolyase doing in the opossum brain, which sees neither UV nor blue light? There is no satisfactory answer to this and similar observations.

A partial answer to what photolyase might do in the dark comes from studies of UV survival of *E. coli* and yeast mutant strains lacking photolyase.^{179–181} The mutant strains are more sensitive to killing by UV than the wild type, even when UV irradiation is not followed by photoreactivating light treatment. This effect is apparently due to stimulation of excision repair by photolyase.^{34,181,182} Excision repair is an ATP-dependent multi-subunit general repair system that eliminates virtually all types of DNA lesions by making single-stranded DNA scissions bracketing the lesion and thus excising the damage in 12-nucleotide-long oligomers in prokaryotes and 27-nucleotide-long oligomers in eukaryotes¹⁸³ (Figure 33). In general, lesions that grossly distort the duplex structure are more efficiently recognized and removed by the excision nuclease system.^{177,178} Cyclobutane pyrimidine dimers, in contrast to (6–4) photoproducts, cause relatively modest perturbations in the duplex structure¹⁰⁷ and, as a consequence, are removed relatively slowly by the excision nuclease. Photolyase, presumably by flipping out the Pyr<->Pyr, increases the helical deformity and accelerates the rate-limiting damage recognition step of the excision nuclease and hence the overall rate of excision.¹⁸²

Interestingly, photolyase recognizes, in addition to Pyr<->Pyr, DNA lesions that are caused by chemical agents and which cannot be repaired by photoreactivation. Among such lesions, of particular interest are caffeine intercalated into DNA¹⁸⁴ and the cisplatin–dGpG diadduct formed by the anticancer drug diamminedichloroplatinum.^{185,186} In yeast, binding of photolyase to cisplatin–dGpG inhibits its repair by excision nuclease and sensitizes the cell to killing by the drug,¹⁸⁵ whereas in *E. coli* photolyase binds to the cisplatin–dGpG diadduct, stimulates excision of the adduct, and increases cell survival.¹⁸⁶ Thus, it is conceivable that photolyase expressed in internal organs participates in recognition and removal of certain lesions produced by internal and external chemical genotoxicants. This light-independent function of photolyase remains to be fully characterized; however, it has provided a significant paradigm to understanding a related protein, cryptochrome, which also has dual functions: it is a photoreceptor in the light and a cog in the molecular clockwork of the circadian rhythm in the dark.^{14,15}

F. Regulation of Photolyase

About 30 *E. coli* genes involved in cellular defense to DNA damage are induced by a coordinated damage

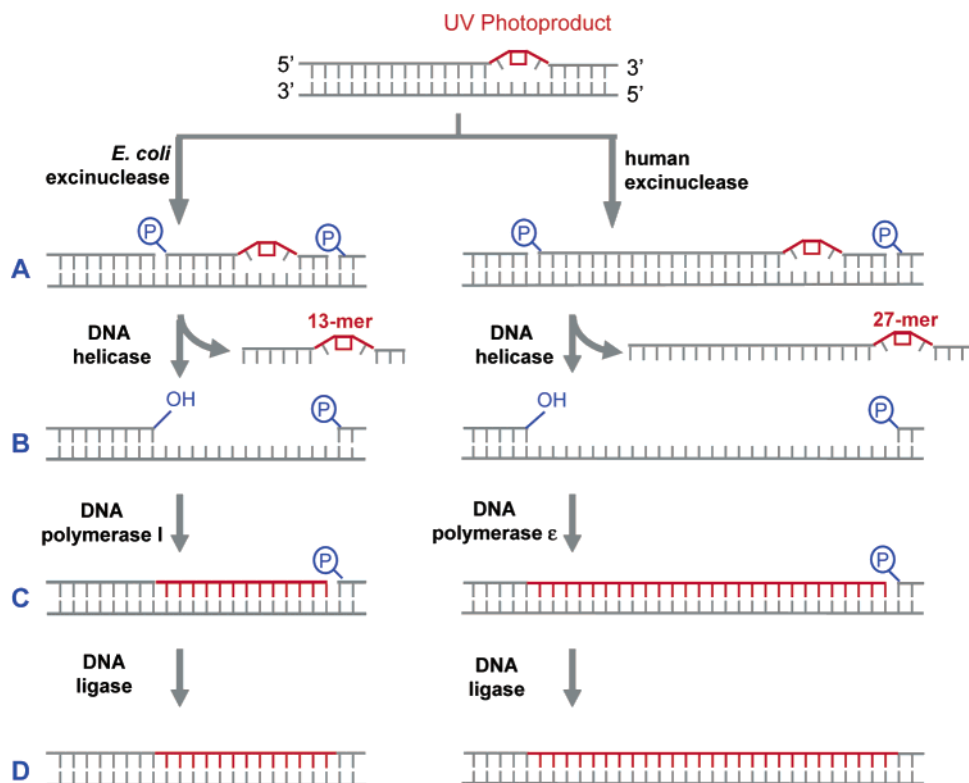


Figure 33. Repair of UV photoproducts by excision repair. Both Pyr\leftrightarrowPyr and (6–4) photoproducts can be removed from DNA in all free living organisms by nucleotide excision repair. In this repair system a multisubunit ATP-dependent enzyme called excision nuclease (excinuclease) cuts out a fragment of either 13 nucleotides (prokaryotes) or 27 nucleotides (eukaryotes) that carry the photoproduct and removes it from the duplex. The resulting single-stranded DNA gap is filled in by DNA polymerase and ligated. Adapted from ref 183.

response reaction called the SOS response.¹⁸⁷ The *phr* gene encoding the apoenzyme of photolyase is not induced by the SOS response, and as a consequence, the number of photolyase proteins in the cell does not increase after UV damage.¹⁸⁸ Curiously, mutations in the purine biosynthetic pathway cause a 10-fold increase in the number of photolyase molecules by an unknown mechanism.¹⁸⁹ Surprisingly, even though an *E. coli* cell contains only 10–20 free FAD molecules per cell, a 10000-fold overproduction of photolyase results in virtually a stoichiometric ratio of FAD to apoenzyme,⁵⁰ suggesting that overproduction of this flavoprotein (and some other flavoproteins as well) induces FAD biosynthesis by a feedback mechanism. Recently, an interesting regulatory mechanism was discovered that explains this apparent paradox. In *Bacillus subtilis* free FMN binds to the attenuator hairpin of mRNA of the first enzyme in the flavin biosynthetic pathway and interrupts transcription prematurely.^{189a} When the flavin is sequestered by an overproduced flavoprotein, the transcriptional inhibition is abolished, resulting in a high level of expression of the flavin biosynthetic enzymes. Presumably, this feedback regulatory mechanism operates in *E. coli* as well.

In *S. cerevisiae*, the photolyase gene is induced by DNA-damaging agents as well as other general stressors,^{190–192} but it is not clear at present whether this induction aids in cellular survival to UV damage in a significant way.¹⁹³ Similarly, in goldfish *Carassius auratus*^{194,195} and in the fungus *Trichoderma harzianum*,¹⁹⁶ blue light induces the transcription of

the photolyase gene. However, light induction appears to be through the generation of reactive oxygen species by photoexcited quinones and other blue-light-absorbing chromophores because the same effect can be mimicked by treatment with H₂O₂ and suppressed by radical scavengers.¹⁹⁷ The same appears to be true for *A. thaliana* photolyase¹⁹⁸ as well as goldfish (6–4) photolyase.¹⁹⁹ Clearly, there is no evidence of a specific regulatory mechanism for the photolyase gene in any organism studied to date. Finally, as noted elsewhere in this review, in multicellular organisms photolyase appears to be uniformly expressed in all organs regardless of whether those organs are exposed to light (skin, eyes) or not (liver, brain). In addition to these gene regulatory mechanisms in eukaryotes, the activity of photolyase is significantly influenced by the chromatin structure and transcription, which adversely affects the enzyme activity by limiting access to damage.²⁰⁰

III. (6–4) Photolyase

The pyrimidine (6–4) pyrimidone adduct or (6–4) photoproduct is the second major lesion induced in DNA by UV radiation. It constitutes 10–20% of the total photoproducts, compared to cyclobutane pyrimidine dimers, which make up 80–90% of the photolesions. In contrast to cyclobutane dimers, which are formed from the excited triplet state of pyrimidines following singlet–triplet intersystem crossing, the (6–4) photoproducts are formed from the pyrimidine excited singlet state.²⁰¹ Hence, using a triplet sensi-

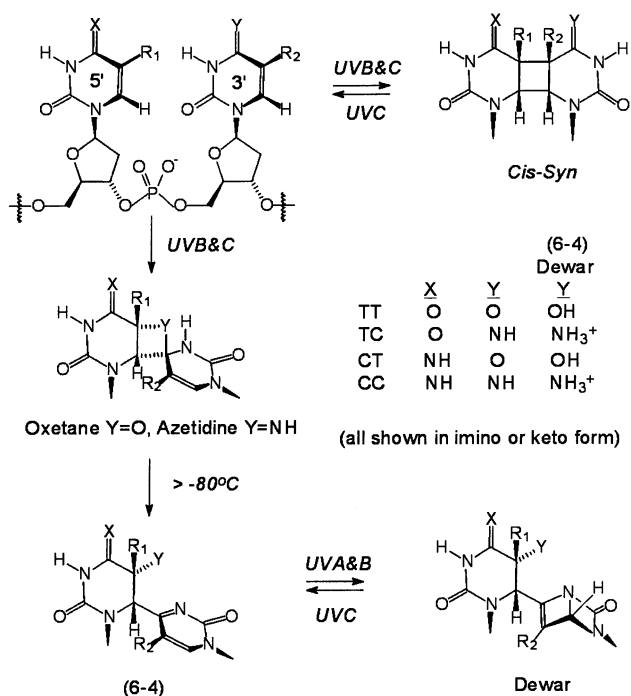


Figure 34. Formation of (6–4) photoproducts. The (6–4) photoproduct forms by a Paterno–Büchi reaction between two adjacent pyrimidines, which generates an oxetane or azetidone four-membered ring intermediate. This intermediate is not stable above -80°C , and undergoes rearrangement to produce the open form of the photoproduct, the (6–4) photoproduct. Irradiation of the (6–4) photoproduct by near UV ($\lambda_{\text{max}} \approx 310\text{--}330\text{ nm}$) converts the (6–4) photoproduct to the Dewar valence isomer, which can be reverted back to the open form by far-UV (254 nm) irradiation. Reprinted from ref 8. Copyright 1994 American Chemical Society.

tizer such as acetophenone, which populates the thymine π, π^* triplet exclusively, it is possible to form cyclobutane thymine dimers in DNA to the exclusion of (6–4) photoproducts.¹⁵⁸ The (6–4) photoproduct is thought to form in DNA as follows (Figure 34): a [2 + 2] cycloaddition of the C4 carbonyl (or amino) of the 3' thymine (cytosine) across the 5–6 double bond of the 5' thymine generates an oxetane (or azetidone) ring, which at temperatures above -80°C undergoes ring opening by C4–O bond cleavage accompanied by a proton shift from N5 to generate the “open form” of the (6–4) photoproduct.²⁰²

In contrast to cyclobutane dimers that, because of loss of aromaticity, lose the 260 nm absorption band typical of nucleobases and do not absorb significantly at $\lambda > 300\text{ nm}$, the (6–4) photoproducts exhibit a near-UV absorption maxima in the 310–330 nm region that depends on base composition. These properties of the two major photoproducts lead to an interesting photochemical phenomenon: irradiation of DNA with moderate doses of UV (254 nm) produces a Pyr<>Pyr to (6–4) photoproduct ratio of about 9:1. With increasing doses of UV radiation, however, the minor absorbance tail of Pyr<>Pyr permits its excitation to the excited singlet state, which splits the cyclobutane ring by the classical [2 + 2] symmetry-allowed cycloreversion with a quantum yield of nearly 1.0. Thus, after a certain UV dose, a steady state of Pyr<>Pyr formation and reversal is established and there is no further increase in the fraction

of pyrimidines in Pyr<>Pyr. By contrast, the (6–4) photoproduct is not reversible by UV so that its formation keeps increasing with increasing UV dose. As a consequence, the relative fractions of Pyr<>Pyr and (6–4) photoproducts in DNA are dose-dependent. Thus, at low doses the photolesions are almost exclusively Pyr<>Pyr. With higher UV doses the fraction of (6–4) photoproduct increases, reaching a maximum of about 40% of the total photoproducts at very high doses.²⁰² Although there is no 254 nm photoreversion effect on the (6–4) photoproduct, irradiation at longer wavelengths, where the photoproduct absorbs (310–360 nm), converts it to the Dewar valence isomer,^{203,204} which can then be reversed to the (6–4) photoproduct by 254 nm of radiation (Figure 34).

Cyclobutane dimers can be restored to their canonical forms by simply breaking the C5–C5 and C6–C6 σ bonds, either by direct excitation or by photolyase. However, the breaking of the C5–OH and C6–C4 bonds of (6–4) photoproducts by any means would not result in repair. Instead, it would generate two damaged bases. For this reason the repair of (6–4) photoproducts by photolyase seemed unlikely, and in fact classical photolyase does not repair the (6–4) photoproduct.²⁰⁵ Moreover, the (6–4) photoproduct and even its Dewar isomer are removed very efficiently by the excision repair system,^{85,206} and this system was considered the sole repair mechanism for removing (6–4) photoproducts in all organisms. Against this background, then, it came as a major surprise when a photolyase that repairs the (6–4) photoproduct was discovered in *Drosophila*²⁰⁷ and later on in *Xenopus*, rattlesnake, and *Arabidopsis*.^{208,210} However, *E. coli* and none of the other bacteria tested to date have a photolyase capable of repairing the (6–4) photoproduct. Similarly, mammalian organisms (including humans) lack (6–4) photolyase as well as classical photolyase.²⁵ An equally surprising finding was that, when the (6–4) photolyase from *Drosophila*, and later (6–4) photolyases from other organisms, were sequenced, they revealed sequences with high sequence identity to classical photolyase.^{12,211} The discovery of (6–4) photolyase and the subsequent identification of structural and cofactor similarities to the classical photolyase led to a proposal of a reaction scheme very similar to that of the cyclobutane photolyase.^{51,208,211,212} The (6–4) photolyase binds specifically to the damaged sites and causes “base flipping”⁵¹ to position the photoproduct in the active site where the photochemical reaction takes place. The model for catalysis is shown in Figure 35.

In the model for (6–4) photolyase, interchromophore energy transfer is presumed to be the same as for the classical photolyase, although at present direct experimental evidence for this step is lacking. A critical step, in which (6–4) photolyase differs from classical photolyase, is that upon binding to substrate the enzyme converts the open form of the (6–4) photoproduct to the oxetane intermediate by a thermal reaction. Although semiempirical MO calculations indicate that this step is energetically rather unfavorable,²¹³ the identification of two His residues

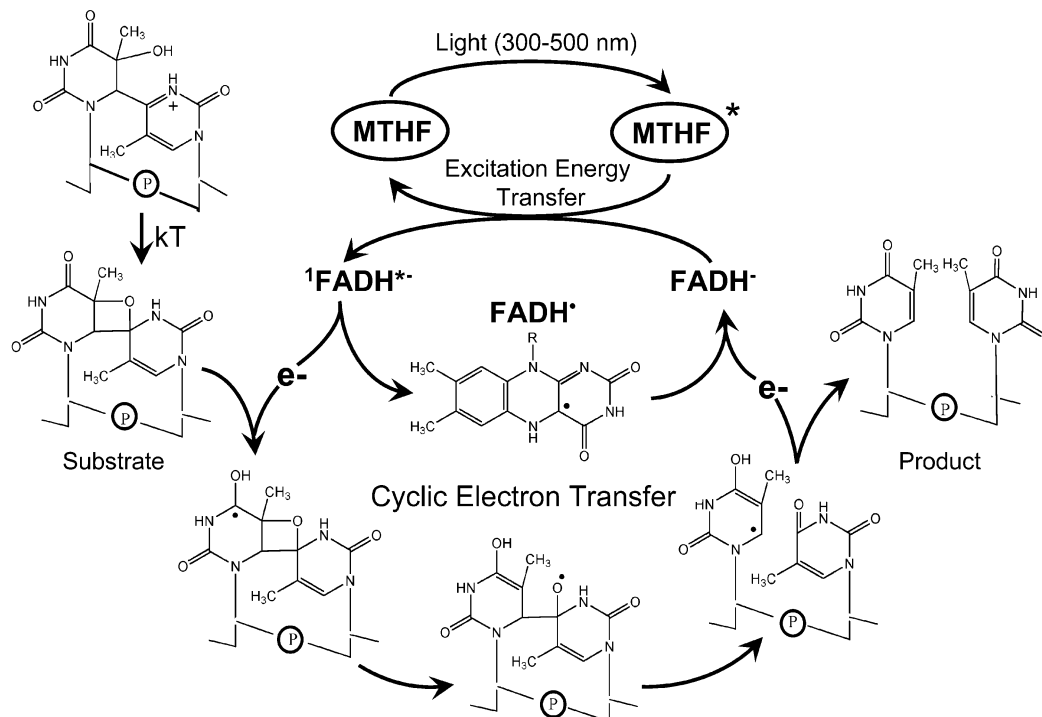


Figure 35. Reaction mechanism of (6-4) photolyase. The enzyme flips out the photoproduct into the active site cavity lined by flavin where the photochemistry takes place. The reaction mechanism is similar to that of classical photolyase, except that in (6-4) photolyase, upon binding, the 3' residue may be protonated by a histidine. This facilitates thermal conversion (kT) of the (6-4) photoproduct to the oxetane (azetidone) intermediate substrate, which undergoes the photochemical steps that include energy and electron transfer followed by back electron transfer to restore the catalytic cofactor, $FADH^-$.

in the active site that are necessary for catalysis suggests that charge interactions with these residues would provide sufficient energy to close the oxetane ring.²¹⁴ The histidine may protonate the (6-4) photoproduct, or at least form a strong H-bond with the N3 of the 3' residue. This allows the OH group to attack the pyrimidine ring to form the oxetane. The protonated intermediate is an acyliminium ion, which is known to react easily with even weak nucleophiles. The next step is photoinduced electron transfer to the oxetane form of the (6-4) photoproduct to initiate back rearrangement of the photoproduct to two pyrimidines.

Quantum chemical calculations²¹⁵ and laser flash photolysis studies with model systems provided additional support for the facile cleavage of the oxetane anionic radical.^{216,217} Perhaps the strongest support for the model, however, came from the investigation of photoinduced cleavage of an oxetane ring covalently linked to flavin. In this model system it was found that only two-electron-reduced and deprotonated flavin induced photosplitting of the oxetane ring with a high quantum yield.²¹⁸ This finding underscored the close mechanistic similarities between cyclobutane pyrimidine dimer and (6-4) photolyases, which at first glance appear to catalyze dissimilar reactions.

In summary, it appears that classical and (6-4) photolyases have similar structures, the same chromophores, and the same basic reaction mechanism. Despite these similarities, however, certain important differences exist between the two classes of enzymes. The most significant difference is that,

while cyclobutane photolyases repair the photodimers with a uniformly high quantum yield (0.7–0.98), the quantum yield of (6-4) photolyases is in the range of 0.05–0.10.^{54,208} Cocystal structures of photolyase–DNA complexes and ultrafast spectroscopic studies on (6-4) photolyase would aid in understanding the mechanistic details of reactions catalyzed by both enzymes, and might shed some light on the reason for this major difference in the quantum yields of the two types of photolyases, which in every other aspect appear very similar.

IV. Cryptochrome

Plant biologists have used for some time the generic term cryptochrome for hypothetical plant blue-light photoreceptors that imparted blue-light-specific photoresponses (photomorphogenesis, phototropism), but whose identity remained cryptic for nearly a century.²¹⁹ In fact, at least two blue-light-specific flavin-containing photoreceptors have now been identified in plants²²⁰ and would therefore qualify for the name cryptochrome as originally defined. However, the name was appropriated to a photoactive pigment that was first discovered in *A. thaliana*²²¹ and *Sinapis alba*²²² and which has high sequence homology to photolyase.^{221,223} Subsequently, when two photolyase homologues were discovered in the human genome database^{25,211,224,225} and shown to have no photolyase activity,²⁵ they were proposed to function as blue-light photoreceptors for synchronizing the circadian clock and were named cryptochromes 1 and 2.^{25,53,226} Thus, the term “cryptochrome” has currently assumed a precise meaning:

a photolyase sequence homologue with no DNA repair activity but with blue-light-activated enzymatic functions.^{14,15} Cryptochromes are widespread in nature and have been found in many plants, animals, and bacteria.

A. Structure of Cryptochromes

Cryptochromes exhibit 25–40% sequence identity to photolyase with higher degrees of homology to (6–4) photolyase than to classical photolyase.^{12,17,211} Cryptochromes contain both folate and FAD as cofactors.⁵⁵ A significant structural feature of cryptochromes is that many of them, especially those of plant origin, have a 50–250 amino acid C-terminal extension with no homology to photolyase.²²¹ It is thought that this extension mediates the effector function of cryptochrome, and indeed, overexpression of this extension in *Arabidopsis* conferred a phenotype of continuous blue-light exposure, even when the plant was kept under red light.^{227,228}

B. Function of Cryptochromes

The photochemical mechanism of action of cryptochromes is not known. Indeed, even though it is known that cryptochromes are essential for certain blue-light responses in both plants and animals, currently there is no known photochemical reaction mediated by cryptochromes. As a consequence, on the basis of biochemical (or rather lack of) data, it could actually be argued that cryptochromes are not photoreceptors, but in fact are phototransducers, molecules that transmit the photosignal from the photoreceptor to the effector molecules in the signaling pathway. Currently, the strongest evidence for a photoreceptive function of cryptochromes, aside from their high homology to photolyase, is genetic. In addition, an action spectrum for circadian gene induction in zebrafish is similar to the cryptochrome/photolyase absorption spectrum.²²⁹ In *Drosophila*^{230,231} and in mice^{232,233} total elimination of opsins does not appreciably affect circadian photoreception, but elimination of cryptochromes drastically reduces circadian photoresponse,^{232,234,235} and the elimination of both opsins and cryptochromes abolishes circadian photoresponse,^{231,232} indicating that both cryptochromes and opsins participate in circadian photoreception. Below, the role of cryptochrome in the circadian clock will be addressed after a brief overview of the circadian rhythms.

1. Circadian Rhythm

Circadian rhythm is the oscillation of the physiologic and behavioral functions of organisms with a periodicity of about a day. Many, but not all, organisms ranging from cyanobacteria to humans exhibit circadian rhythms.^{18–22} The rhythm is an innate property of the organism, and the amplitude (e.g., body temperature) and period length (which is variable among species, usually in the range of 22–26 h, but rather constant among members of the same species) are maintained under constant environmental conditions. For example, human volunteers, who lived in isolation in cold dark caves for months,

maintained circadian rhythms of body temperature and sleep–wake cycles of about 25 h periodicity.^{235a}

At the chemical level the rhythm is generated by a negative feedback mechanism, which differs from ordinary chemical feedback reactions (equilibrium or steady-state nonequilibrium) reactions by the presence of a delay phase between the product formation and the inhibitory action of the product on the chemical steps leading up to its formation. The result is an oscillatory chemical process. The core components of a molecular circadian clock are a transcriptional activator and a transcriptional repressor. The activator stimulates the synthesis of the repressor, which is separated from the activator gene by the nuclear membrane and which must be covalently modified (e.g., phosphorylated) for full activity.^{18–22} Because of these requirements, the repressor can fully repress the activator gene only after a delay of about 24 h, resulting in oscillation in the levels of the activator and repressor with circadian periodicity. The core circadian feedback machinery is interfaced with other biochemical pathways so that oscillation in the core “molecular clock” results in oscillation in the rates of the organism’s many biochemical reactions as well as in the physiology and behavior of the organism.

A cardinal property of circadian rhythms is their ability to be synchronized with the environment by light.^{18,20,236} Even though heat and other environmental inputs can affect the phase, the amplitude, and the period of the rhythm, by far the most predominant and perhaps the only physiologically relevant environmental cue (or *zeitgeber*, from the German *zeit* = time and *geber* = giver) is light. In many animals, for example, birds, there are multiple light-sensitive organs (eye, pineal gland, deep brain photoreceptors) that transmit the photosignal to the circadian center in the brain. In mammals such as man and mice, light input to the circadian system appears to be only through the eye.²³⁶

2. Mammalian Circadian System

The mammalian circadian system consists of three components: a photoreceptor/phototransducer, the master circadian clock, and the output system. The photoreceptor is located in the eye, the master circadian clock is in the hypothalamus in the mid-brain, and the output system consists of neuropeptides released from the master circadian clock and perhaps neural outputs to the other regions of the brain from the hypothalamus.^{21,22} Of relevance to this topic is the duality of the photosensory systems in mammals (Figure 36). It appears that mammals have two photosensory systems that are divergent at the molecular, histological, and anatomical levels: the visual system for 3-D vision and the circadian photosensory system for sensing the fourth dimension, time. Opsins that contain retinal (vitamin A) as the chromophore are responsible for vision. Opsins are expressed in rods and cones in the back (outer) part of the retina, they initiate phototransduction by *cis–trans* isomerization of retinal by light, and the signal is transmitted by the optic nerve to the visual cortex, which occupies about 30% of the cerebral cortex.

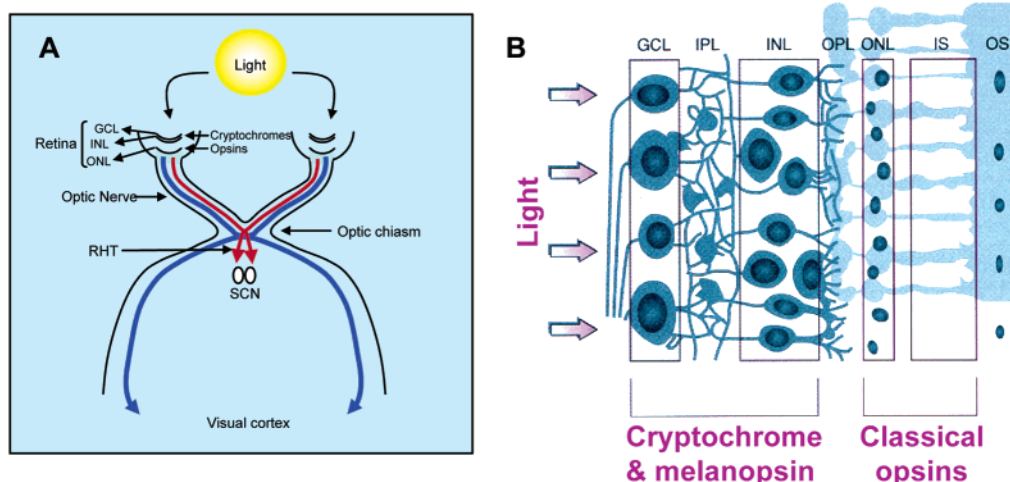


Figure 36. Duality in the molecular, histological, and anatomical properties of visual and circadian photosensory systems. (A) The visual photopigments are opsins that are located in the outer retina and transmit the photosensory signal to the visual center in the cortex. The circadian photopigments, the cryptochromes, are located in the inner retina and transmit the light signal through the retinohypothalamic tract (RHT) to the master circadian clock, the SCN in the midbrain. (B) Schematic histological cross-section of the mammalian retina showing locations of the photosensory pigments for vision and entrainment of the circadian clock. Cryptochromes are located in the front part of the retina in the ganglion cell layer (GCL) and inner nuclear layer (INL). Opsins are located in the rods (rhodopsin) and cones (color opsins) in the outer retina. Key: IPL, inner plexiform layer; OPL, outer plexiform layer; ONL, outer nuclear layer; IS, inner segment; OS, outer segment. Adapted from refs 14 and 18.

Cryptochromes are circadian photoreceptors with folate and flavin chromophores, they are expressed in the front (inner) part of the retina,²²⁶ they initiate phototransduction by an unknown mechanism (presumably by photoinduced electron transfer), and the signal is transmitted to the master circadian clock in the midbrain (hypothalamus) to a cluster of neurons called the suprachiasmatic nucleus (SCN) (Figure 36). The two photosensory systems function more or less independently. Thus, certain retinal degeneration diseases in humans and mice that destroy the outer retina and cause total visual blindness leave the circadian phototransduction system intact,^{236,237} and conversely, mutations in the circadian photosensory pathway that seriously compromise entrainment (synchronization) of the circadian clock do not affect the animal's vision.^{197–200}

3. Cryptochromes and the Circadian Clock

At present the reaction mechanisms of cryptochromes as photoreceptors in plants and animals is not known.^{15,17,18,238} However, a great deal is known about the dark function of cryptochrome in mammals. In addition to being expressed at high levels in the inner retina, where they are thought to perform their photoreceptive functions, human and mouse cryptochromes CRY1 and CRY2 are expressed in virtually all other tissues. This is reminiscent of the expression pattern of photolyase in certain animals that possess the enzyme. In the case of photolyase, the dark function consists of modulating the activity of other DNA repair systems.^{185,186} In the case of cryptochromes, the dark function is to help run the molecular clock. It appears that CRY1 and CRY2 perform light-independent negative regulatory functions in the transcriptional feedback loop, which constitutes the molecular clock,^{235,239,240} the autoregulatory transcriptional loop which engenders the macroscopic

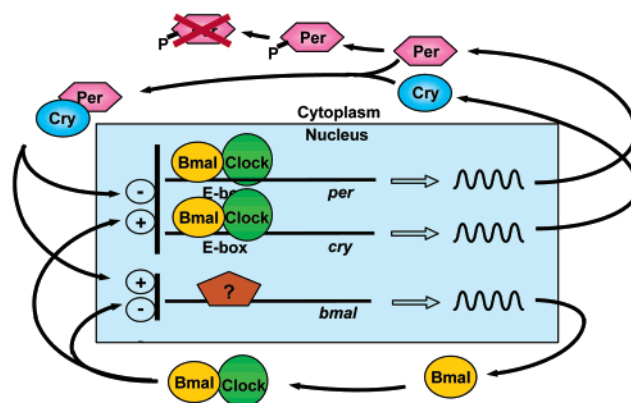


Figure 37. Model for the autoregulatory transcriptional loop that generates molecular oscillation. The loop consists of alternating transcriptional activators and repressors delayed from reaching their target by the nucleocytoplasmic division and the necessity for activation by posttranslational modifications. Bmal1 and Clock are positive transcriptional activators; cryptochromes (Cry) and Period (Per) proteins are negative transcriptional regulators of their own genes but positive regulators of the *BMal1* gene. In addition, the times of transcriptional activation and repression are modulated by posttranslational events such as phosphorylation and time of entry into the nucleus. The sinusoidal lines indicate circadian oscillation in the RNA levels of the various genes, which results in similar oscillation in the levels of corresponding proteins, indicated by colored boxes of different shapes.

rhythm of the organism (Figure 37). Consistent with this function, CRY1 is expressed at a high level in the SCN (Figure 38) where its level oscillates with a 24 h periodicity.^{236,241} As a consequence of this intimate involvement in the clock function, animals lacking CRY1 have short periods, those lacking CRY2 have long periods, and animals lacking both cryptochromes are arrhythmic under constant darkness^{234,235,239} (Figure 39). In fact, animals lacking both cryptochromes do have circadian photoresponse, as

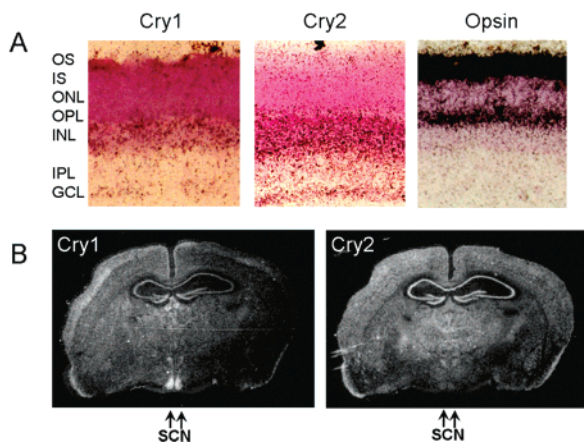


Figure 38. Expression of cryptochromes in the mouse retina and brain. Expression was measured by in situ hybridization with radiolabeled *Cry1* and *Cry2* probes followed by autoradiography. (A) Expression in the retina. The dark speckles in the GCL and INL layers (front of the retina) are *Cry* mRNAs. In the third panel the probe was for rhodopsin to show the contrast in the location of expressions of the two types of photopigments. (B) Expression in the brain. Coronal sections of the brain of a mouse were hybridized with either a *Cry1* or a *Cry2* probe and subjected to autoradiography. The light spots indicate mRNA expression. Note the high level of expression of *Cry1* in the SCN in the midbrain. This section was made at midday; at midnight *Cry1* expression in the SCN is virtually nondetectable. Reprinted with permission from ref 226. Copyright 1998 National Academy of Science.

evidenced by behavioral response to light–dark cycles of doubly mutant animals and by light-induced gene expression in the SCN of mice lacking both cryptochromes.^{235,239} This is because of some functional redundancy of cryptochromes and opsins. When, in addition to CRYs, opsins are eliminated, either by retinal degenerations^{232a,b} or by vitamin A deprivation,²³³ there is no longer either molecular (Figure 40) or circadian (Figure 41) photoreception.^{232,233} In these animals pupillary constriction in response to light is also severely blunted, providing further evidence for a photoreceptive function of cryptochromes in the mammalian eye.^{241a} In summary, all these data taken in their entirety indicate that CRYs are dedicated nonvisual photoreceptors in animals but that opsins, in addition to their roles in vision, play a redundant function in circadian photoreception.

It must be noted, however, that the photoreceptor function of cryptochromes in animals and particularly in mammals is not universally accepted. Even though there is a consensus that the vitamin A (retinal)-based rhodopsin and color opsins located in rods and cones (outer retina) are not required for circadian photoreception, many investigators believe that another opsin that is expressed in the inner retina, and not cryptochrome, is responsible for circadian photoreception. Indeed, a novel opsin called melanopsin has been discovered in all vertebrates tested,²⁴² and it has been found that in man and mouse melanopsin is exclusively expressed in the inner retina.²⁴³

Several features of melanopsin made it a strong candidate for being the mammalian circadian photoreceptor. First, it is expressed almost exclusively in ganglion cells with direct connections to the SCN

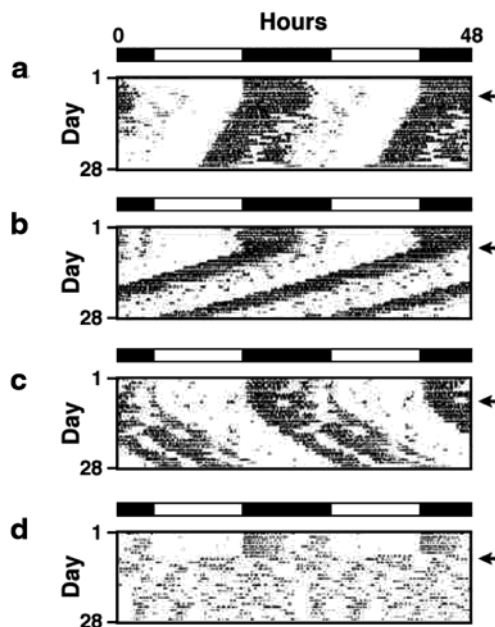


Figure 39. Effect of cryptochrome mutation on the circadian behavior of mice. These graphs (actograms) show the wheel running activity of individual mice. The bar on top indicates dark (closed rectangle) and light (open rectangle) phases of a day. On the *y*-axis the activity (rpm of the running wheel) is plotted, and the *x*-axis indicates the time of day. The activity profile of each day is plotted twice to make comparison of successive days easier. These graphs show activity profiles for a 28-day period (28 graphs in which *y* represents the rpm of the running wheel and *x* represents the time of day) were combined to create the activity function of the subject mouse). At the day indicated by arrows the animals were switched from a light–dark (LD) cycle to an all dark (DD) environment where the circadian rhythm is controlled by the innate clock without external input. Note that under DD, the “free-running” period lengths of singly mutant animals are different from those of the wild type: (a) WT mouse, 23.7 h; (b) *Cry1*^{-/-} mouse, 22.7 h; (c) *Cry2*^{-/-} mouse, 24.7 h. (d) The *Cry1*^{-/-}*Cry2*^{-/-} double mutant mouse shows rhythm under LD but is arrhythmic under DD conditions. Reprinted with permission from ref 235. Copyright 1999 National Academy of Science.

and to other brain regions involved in nonvisual irradiance detection.^{244–248} Second, these cells are directly sensitive to light as determined by patch-clamp analysis.^{246,247} Finally, it was reported that the action spectrum for action potential in these photosensitive ganglion cells matched the absorption spectrum of an opsin and not that of cryptochrome.²⁴⁶ Thus, despite the report showing that circadian photoreception was essentially intact in mice depleted of all functional opsins (presumably including melanopsin) by vitamin A starvation,²³³ it was claimed that melanopsin was the long-sought-after circadian photoreceptor.²⁴⁹ However, genetic experiments did not support this claim. Melanopsin knockout mice have basically normal circadian photoreception^{250,251} under ordinary lighting in agreement with the results obtained by total opsin depletion by vitamin A deprivation.²³³ Nevertheless, under dim light melanopsin appears to make some contribution to circadian photoreception.²⁵⁰ Thus, currently all available evidence is consistent with cryptochrome being the primary circadian photoreceptor in mammals with redundant or complementary photoreception pro-

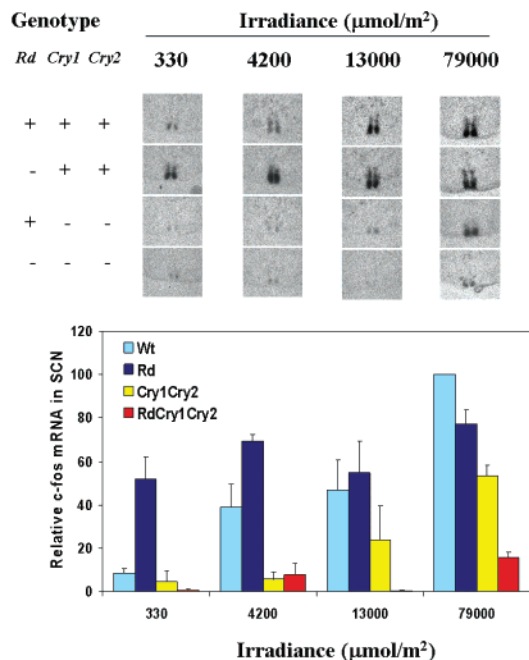


Figure 40. Roles of cryptochromes and opsins in phototransduction to the master clock in the SCN. Wild-type or mutant animals were exposed to a light pulse at midnight when the *c-fos* gene expression in the SCN is at its minimum. One hour after the light pulse, brain sections were made and the light induction of the *c-fos* gene in the SCN was probed by in situ hybridization. The top panel shows the SCN of nine animals of various genotypes and exposed to different light doses. The bottom panel shows quantitative analysis of *c-fos* induction from several experiments, including the one shown in the top panel. The + and - signs indicate that the animal had wild-type or mutant forms, respectively, of the relevant genes. Note the drastic reduction in light induction of *c-fos* in the cryptochromeless mice and virtual elimination of *c-fos* induction in triply blind mice. The residual induction seen in the triple mutant is due to a few surviving photoreceptor cells that express opsins and are not completely destroyed by the *Rd* mutation and possibly to melanopsin in the inner retina, which is not affected by the *Rd* mutation. Adapted from ref 232.

vided by classical opsins in rods and cones and melanopsin and perhaps other yet-to-be-discovered minor opsins in the inner retina.

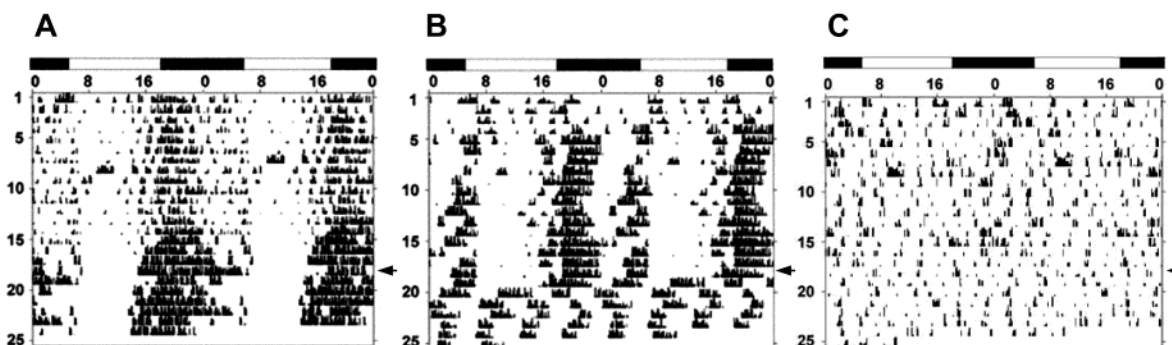


Figure 41. Elimination of cryptochromes and opsins abolishes circadian photoresponse. The actogram is a plot of physical activity (in this case the rpm of the running wheel in the mouse cage) as a function of the time of day. Actograms of (A) an *Rd* mouse that lacks rods and cones and of (B) a *Cry1^{-/-}Cry2^{-/-}* double mutant mouse that lacks both cryptochromes show behavioral photoresponse. However, (C) elimination of cryptochromes and rods and cones in *Rd Cry1^{-/-}Cry2^{-/-}* triply blind mouse abolishes behavioral circadian light response. At the day indicated by arrows the animals were shifted from an LD to a DD environment. Note that the *Cry1^{-/-}Cry2^{-/-}* is rhythmic under LD but the triple mutant is arrhythmic under all conditions. Adapted from ref 232.

V. Perspectives

Currently, our understanding of the structure and function of photolyase and cryptochromes is at considerably different levels. The atomic structure of photolyase is available, and its reaction mechanism has been studied in some detail. Two important areas of future research on photolyase are the determination of the enzyme–substrate cocrystal structure and the capture and identification of reaction intermediates by fast spectroscopic methods. Although these studies are expected to confirm the base-flipping mechanism for binding and the “photoinduced electron transfer” for catalysis, until the appropriate static and dynamic intermediates are experimentally captured, the proposed mechanisms will remain hypothetical models.

Compared to photolyase, our understanding of the photochemical function of cryptochrome is rudimentary. The only photochemical function associated with cryptochrome is the light-dependent binding of *Drosophila* cryptochrome to the clock proteins Per and Tim in vivo.^{252,253} This reaction is the opposite of the light effect on the enzyme–substrate complex of photolyase, where light repairs DNA and dissociates the complex. Furthermore, no such light effects have been observed on the interaction of mammalian cryptochromes with the clock proteins. Moreover, if cryptochrome is indeed an ocular photoreceptor, it is expected to generate an action potential that transmits the light signal to the brain through the optic nerve. There are some preliminary data that cryptochromes regulate a chloride channel in *Arabidopsis*²⁵⁴ and are phosphorylated after light exposure.²²⁸ However, the mechanistic details of cryptochrome function remain to be established. It is fair to state that at present the substrate of the cryptochrome has not been identified, and until this is accomplished, it will not be possible to find out whether cryptochrome functions by photoinduced electron transfer in a manner analogous to photolyase or utilizes the same molecular framework and the same two chromophores to perform an entirely different photochemical reaction.

VI. Acknowledgment

I thank my students Carol Thompson and Carrie Stentz for their help with organizing the review, Eddie Bondo for the cover art, Katherine Shields for obtaining the absorption spectrum in Figure 6A, Dr. Zahide Özer for generating the data shown in Figure 31, Professor ChullHee Kang for contributing Figure 13, Professor John-Stephen Taylor for providing Figure 34, and Professors Rowena Matthews and Thomas Carell for critical comments on the manuscript. This work was supported by NIH Grant GM31082.

VII. References

- (1) Kelner, A. *Proc. Natl. Acad. Sci. U.S.A.* **1949**, *35*, 73.
- (2) Dulbecco, R. *Nature* **1949**, *163*, 949.
- (3) (a) Sancar, A.; Rupert, C. S. *Gene* **1978**, *4*, 294. (b) Sancar, A. A study on photoreactivating enzyme (DNA photolyase) of *Escherichia coli*. Ph.D. Dissertation, 1977, University of Texas at Dallas.
- (4) Husain, I.; Carrier, W. L.; Reagan, J. D.; Sancar, A. *Photochem. Photobiol.* **1988**, *48*, 233.
- (5) Rupert, C. S.; Goodgal, S. H.; Herriott, R. M. *J. Gen. Physiol.* **1958**, *41*, 451.
- (6) (a) Sancar, G. B. *Mutat. Res.* **1990**, *236*, 147. (b) Heelis, P. F.; Kim, S. T.; Okamura, T. Sancar, A. *J. Photochem. Photobiol.* **1993**, *17*, 219.
- (7) Kim, S. T.; Sancar, A. *Photochem. Photobiol.* **1993**, *57*, 895.
- (8) Taylor, J.-S. *Acc. Chem. Res.* **1994**, *27*, 76.
- (9) Begley, T. P. *Acc. Chem. Res.* **1994**, *27*, 394.
- (10) Sancar, A. *Biochemistry* **1994**, *33*, 2.
- (11) Heelis, P. F.; Hartman, R. F.; Rose, S. D. *Chem. Soc. Rev.* **1995**, *24*, 289.
- (12) (a) Todo, T. *Mutat. Res.* **1999**, *434*, 89. (b) Sancar, G. B. *Mutat. Res.* **2000**, *451*, 25.
- (13) Deisenhofer, J. *Mutat. Res.* **2000**, *460*, 143.
- (14) Sancar, A.; Thompson, C.; Thresher, R. J.; Araujo, F.; Mo, J.; Özgür, S.; Vagas, E.; Dawut, L.; Selby, C. P. *Cold Spring Harbor Symp. Quant. Biol.* **2000**, *65*, 157.
- (15) (a) Sancar, A. *Annu. Rev. Biochem.* **2000**, *69*, 31. (b) Kavakli, I. H.; Sancar, A. *Mol. Interventions* **2002**, *2*, 484. (c) Thompson, C. L.; Sancar, A. *Oncogene* **2002**, 9043.
- (16) Carell, T.; Burgdorf, L. T.; Kundu, L. M.; Cichon, M. *Curr. Opin. Chem. Biol.* **2001**, *5*, 491.
- (17) Cashmore, A. R.; Jarillo, J. A.; Wu, Y. J.; Liu, D. *Science* **1999**, *284*, 760.
- (18) Hall, J. C. *Curr. Opin. Neurobiol.* **2000**, *10*, 456.
- (19) Young, M. W. *Trends Biochem. Sci.* **2000**, *25*, 601.
- (20) Devlin, P. F.; Kay, S. A. *Annu. Rev. Physiol.* **2000**, *63*, 729.
- (21) Reppert, S. M.; Weaver, D. R. *Annu. Rev. Physiol.* **2001**, *63*, 647.
- (22) (a) Cermakian, N.; Sassone-Corsi, P. *Nat. Rev.* **2000**, *1*, 59. (b) Van Gelder, R. N. *J. Biol. Rhythms* **2002**, 110.
- (23) Aschoff, J. *Cold Spring Harbor Symp. Quant. Biol.* **1960**, *25*, 11.
- (24) Li, Y. I.; Kim, S. T.; Sancar, A. *Proc. Natl. Acad. Sci. U.S.A.* **1993**, *90*, 4389.
- (25) Hsu, D. S.; Zhao, X.; Zhao, S.; Kazantsev, A.; Wang, R. P.; Todo, T.; Wei, Y. F.; Sancar, A. *Biochemistry* **1996**, *35*, 13871.
- (26) Afonso, C. L.; Tulman, E. R.; Lu, Z.; Oma, E.; Kutish, G. F.; Rock, D. L. *J. Virol.* **1999**, *73*, 533.
- (27) Srinivasan, V.; Schnitzlein, W. M.; Tripathy, D. N. *J. Virol.* **2001**, *75*, 1681.
- (28) Sancar, G. B.; Sancar, A. *Trends Biochem. Sci.* **1987**, *12*, 259.
- (29) Sancar, A.; Sancar, G. B. *Annu. Rev. Biochem.* **1987**, *57*, 29.
- (30) Sancar, G. B.; Smith, F. W.; Reid, R.; Payne, G.; Levy, M.; Sancar, A. *J. Biol. Chem.* **1987**, *262*, 478.
- (31) Jorns, M. S.; Baldwin, E. T.; Sancar, G. B.; Sancar, A. *J. Biol. Chem.* **1987**, *262*, 486.
- (32) Sancar, G. B.; Jorns, M. S.; Payne, G.; Fluke, D. J.; Rupert, C. S.; Sancar, A. *J. Biol. Chem.* **1984**, *262*, 492.
- (33) Payne, G.; Sancar, A. *Biochemistry* **1990**, *29*, 7715.
- (34) Ramsey, A. J.; Alderfer, J. L.; Jorns, M. S. *Biochemistry* **1992**, *31*, 4.
- (35) Malhotra, K.; Baer, M.; Li, Y. I.; Sancar, G. B.; Sancar, A. *J. Biol. Chem.* **1992**, *267*, 2909.
- (36) Park, H. W.; Sancar, A.; Deisenhofer, J. *J. Mol. Biol.* **1993**, *231*, 1122.
- (37) Park, H. W.; Kim, S. T.; Sancar, A.; Deisenhofer, J. *Science* **1995**, 1866.
- (38) Tamada, T.; Kitadokoro, K.; Higuchi, Y.; Inaka, K.; Yasui, A.; deRuiter, P. E.; Eker, A. P. M.; Miki, K. *Nat. Struct. Biol.* **1997**, *11*, 887.
- (39) Kato, T.; Todo, T.; Ayoki, H.; Ishizaki, K.; Morita, T.; Mitra, S.; Ikenaga, M. *Nucleic Acids Res.* **1994**, *22*, 4119.
- (40) Yasui, A.; Eker, A. P. M.; Yasuhira, S.; Yajima, H.; Kobayashi, T.; Takao, M.; Oikawa, A. *EMBO J.* **1994**, *13*, 6143.
- (41) Aravind, L.; Anantharaman, V.; Koonin, E. V. *Proteins* **2002**, *48*, 1.
- (42) Ames, B. N.; Elson-Schwab, I.; Silver, E. A. *Am. J. Clin. Nutr.* **2002**, *75*, 1.
- (43) Walsh, C. T. *Acc. Chem. Res.* **1986**, *19*, 216.
- (44) Payne, G.; Heelis, P. F.; Rohrs, B. R.; Sancar, A. *Biochemistry* **1987**, *26*, 7121.
- (45) Jorns, M. S.; Wang, B.; Jordan, S. P.; Chanderkar, L. P. *Biochemistry* **1990**, *29*, 552.
- (46) Payne, G.; Wills, M.; Walsh, C. T.; Sancar, A. *Biochemistry* **1990**, *29*, 5706.
- (47) Malhotra, K.; Kim, S. T.; Walsh, C. T.; Sancar, A. *J. Biol. Chem.* **1992**, *267*, 15406.
- (48) Harm, W.; Harm, H.; Rupert, C. S. *Mutat. Res.* **1968**, *6*, 371.
- (49) Sancar, G. B.; Smith, F. W.; Sancar, A. *Nucleic Acids Res.* **1983**, *11*, 6667.
- (50) Sancar, A.; Sancar, G. B. *J. Mol. Biol.* **1984**, *172*, 223.
- (51) Zhao, X.; Liu, J.; Hsu, D. S.; Zhao, S.; Taylor, J. S.; Sancar, A. *J. Biol. Chem.* **1997**, *272*, 32580.
- (52) Selby, C. P.; Sancar, A. *Photochem. Photobiol.* **1999**, *69*, 105.
- (53) Zhao, S.; Sancar, A. *Photochem. Photobiol.* **1997**, *66*, 727.
- (54) Hitomi, K.; Kim, S. T.; Iwai, S.; Harima, N.; Otoshi, E.; Ikenaga, M.; Todo, T. *J. Biol. Chem.* **1997**, *272*, 32591.
- (55) Malhotra, K.; Kim, S. T.; Batschauer, A.; Dawut, L.; Sancar, A. *Biochemistry* **1995**, *34*, 6892.
- (56) Kim, S. T.; Sancar, A.; Essenmacher, C.; Babcock, G. T. *Proc. Natl. Acad. Sci. U.S.A.* **1993**, *90*, 8023.
- (57) Petersen, J. L.; Small, G. D. *Nucleic Acids Res.* **2001**, *29*, 4472.
- (58) Sancar, G. B.; Smith, F. W.; Heelis, P. F. *J. Biol. Chem.* **1987**, *262*, 15457.
- (59) Jorns, M. S.; Sancar, G. B.; Sancar, A. *Biochemistry* **1984**, *23*, 2673.
- (60) Eker, A. P. M.; Kooiman, P.; Hessels, J. K. C.; Yasui, A. *J. Biol. Chem.* **1990**, *265*, 8009.
- (61) Li, Y. F.; Sancar, A. *Nucleic Acids Res.* **1991**, *18*, 4885.
- (62) Heelis, P. F.; Sancar, A. *Biochemistry* **1986**, *25*, 8163.
- (63) Heelis, P. F.; Payne, G. P.; Sancar, A. *Biochemistry* **1987**, *26*, 4634.
- (64) Jorns, M. S.; Wang, B.; Jordan, S. P. *Biochemistry* **1987**, *26*, 6810.
- (65) Johnson, J. L.; Hamm-Alvarez, S.; Payne, G.; Sancar, G. B.; Rajagopalan, K. V.; Sancar, A. *Proc. Natl. Acad. Sci. U.S.A.* **1988**, 2046.
- (66) Kim, S. T.; Malhotra, K.; Ryo, H.; Sancar, A.; Todo, T. *Mutat. Res.* **1996**, *363*, 97.
- (67) Hamm-Alvarez, S.; Sancar, A.; Rajagopalan, K. V. *J. Biol. Chem.* **1989**, *264*, 9649.
- (68) Hamm-Alvarez, S. F.; Sancar, A.; Rajagopalan, K. V. *J. Biol. Chem.* **1990**, *265*, 9850.
- (69) Hamm-Alvarez, S. F.; Sancar, A.; Rajagopalan, K. V. *J. Biol. Chem.* **1990**, *265*, 18656.
- (70) Eker, A. P. M.; Yajima, H.; Yasui, A. *Photochem. Photobiol.* **1994**, *60*, 125.
- (71) Malhotra, K.; Kim, S. T.; Sancar, A. *Biochemistry* **1994**, *33*, 8712.
- (72) Eker, A. P. M.; Hessels, J. K. C.; van de Velde, J. *Biochemistry* **1988**, *27*, 1758.
- (73) Eker, A. P. M.; Dekker, R. H.; Berends, W. *Photochem. Photobiol.* **1981**, *33*, 65.
- (74) Eker, A. P. M.; Hessels, J. K. C.; Dekker, R. H. *Photochem. Photobiol.* **1986**, *44*, 197.
- (75) Massey, V.; Hemmerich, P. *Biochemistry* **1978**, *17*, 9.
- (76) Kiener, A.; Husain, I.; Sancar, A.; Walsh, C. T. *J. Biol. Chem.* **1989**, *264*, 13880.
- (77) Komori, H.; Masui, R.; Kuramitsu, S.; Yokoyama, S.; Shibata, T.; Inoue, Y.; Miki, K. *Proc. Natl. Acad. Sci. U.S.A.* **2001**, *98*, 13560.
- (78) Förster, T. *Discuss. Faraday Soc.* **1959**, *27*, 7.
- (79) Rupert, C. S. *J. Gen. Physiol.* **1960**, *43*, 573.
- (80) Rupert, C. S. *J. Gen. Physiol.* **1962**, *45*, 725.
- (81) Rupert, C. S. *J. Gen. Physiol.* **1962**, *45*, 703.
- (82) (a) Harm, H.; Rupert, C. S. *Mutat. Res.* **1968**, *6*, 355. (b) Harm, H.; Rupert, C. S. *Mutat. Res.* **1970**, *10*, 307.
- (83) Harm, H.; Rupert, C. S. *Mutant Res.* **1976**, *34*, 75.
- (84) Myles, G. M.; Van Houten, B.; Sancar, A. *Nucleic Acids Res.* **1987**, *15*, 1227.
- (85) Svoboda, D. L.; Smith, C. A.; Taylor, J.-S.; Sancar, A. *J. Biol. Chem.* **1993**, *268*, 10694.
- (86) Sancar, G. B.; Smith, F. W.; Sancar, A. *Biochemistry* **1985**, *24*, 1849.
- (87) Husain, I.; Sancar, A. *Nucleic Acids Res.* **1987**, *15*, 1109.
- (88) Jorns, M. S.; Sancar, G. B.; Sancar, A. *Biochemistry* **1985**, *24*, 1986.

- (89) Jordan, S. P.; Alderfer, J. L.; Chandekar, L. P.; Jorns, M. S. *Biochemistry* **1989**, *28*, 8149.
- (90) Kim, S. T.; Sancar, A. *Biochemistry* **1991**, *30*, 8623.
- (91) Baer, M.; Sancar, G. B. *Mol. Cell. Biol.* **1989**, *9*, 4777.
- (92) Baer, M.; Sancar, G. B. *J. Biol. Chem.* **1993**, *268*, 16717.
- (93) Vande Berg, B. J.; Sancar, G. B. *J. Biol. Chem.* **1998**, *273*, 20276.
- (94) Li, Y. F.; Sancar, A. *Biochemistry* **1990**, *29*, 5698.
- (95) (a) Kim, S. T.; Li, Y. F.; Sancar, A. *Proc. Natl. Acad. Sci. U.S.A.* **1992**, *89*, 900. (b) Christine, K. S.; MacFarlane IV, A. W.; Yang, K.; Stanley, R. J. *J. Biol. Chem.* **2002**, *277*, 38339.
- (96) Antony, J.; Medvedev, D. M.; Stuchebrukhov, A. A. *J. Am. Chem. Soc.* **2000**, *122*, 1057.
- (97) Hahn, J.; Michel-Beyerle, M. E.; Rosch, N. *J. Phys. Chem. B* **1999**, *103*, 2001.
- (98) Hahn, J.; Michel-Beyerle, M. E.; Rosch, N. *J. Mol. Model* **1998**, *4*, 73.
- (99) Sander S. D. B.; Wiest, O. *J. Am. Chem. Soc.* **1999**, *121*, 5127.
- (100) Husain, I.; Sancar, G. B.; Holbrook, S. R.; Sancar, A. *J. Biol. Chem.* **1987**, 13188.
- (101) Kim, S. T.; Sancar, A. *Photochem. Photobiol.* **1995**, *61*, 171.
- (102) Sancar, A.; Smith, F. W.; Sancar, G. B. *J. Biol. Chem.* **1984**, *259*, 6028.
- (103) Ramaiah, D.; Kan, Y.; Koch, T.; Orum, H.; Schuster, G. B. *Proc. Natl. Acad. Sci. U.S.A.* **1998**, *95*, 12902.
- (104) Butenandt, J.; Burgdorf, L. T.; Carell, T. *Angew. Chem., Int. Ed.* **1999**, *38*, 708.
- (105) Kim, S. T.; Malhotra, K.; Smith, C. A.; Taylor, J. S.; Sancar, A. *Biochemistry* **1993**, *32*, 7065.
- (106) Pearlman, D. A.; Holbrook, S. R.; Pirkle, D. H.; Kim, S. T. *Science* **1985**, *227*, 1304.
- (107) (a) Husain, I.; Griffith, J. D.; Sancar, A. *Proc. Natl. Acad. Sci. U.S.A.* **1988**, *85*, 2258. (b) Park, H.; Zhang, K.; Ren, Y.; Nadji, S.; Sinha, N.; Taylor, J. S.; Kang, C. *Proc. Natl. Acad. Sci. U.S.A.* **2002**, *99*, 15965.
- (108) Wang, C. I.; Taylor, J. S. *Proc. Natl. Acad. Sci. U.S.A.* **1991**, *88*, 9072.
- (109) Kemmink, J.; Boelens, R.; Koning, T. M. G.; Kaptein, R.; van der Marel, G. A.; van Boom, J. H. *Eur. J. Biochem.* **1987**, *162*, 37.
- (110) Kemmink, J.; Boelens, R.; Koning, T. M. G.; van der Marel, G. A.; van Boom, J. H.; Kaptein, R. *Nucleic Acids Res.* **1987**, *15*, 4645.
- (111) Taylor, J. S.; Garrett, D. S.; Brockie, I. R.; Svoboda, D. L.; Telsler, J. *Biochemistry* **1990**, *29*, 8858.
- (112) Lee, B. J.; Sakashi, H.; Ohkubo, T.; Ikehara, M.; Doi, T.; Morikawa, K.; Kyogoku, Y.; Osafune, T.; Iwai, S.; Ohtsuka, E. *Biochemistry* **1994**, *33*, 57.
- (113) (a) Kim, J. K.; Patel, D.; Choi, B. S. *Photochem. Photobiol.* **1995**, *62*, 44. (b) Miaszkiewicz, K.; Miller, J.; Cooney, M.; Osman, R. *J. Am. Chem. Soc.* **1996**, *118*, 9156. (c) McAteer, K.; Jing, Y.; Kate, J.; Taylor, J. S.; Kennedy, M. A. *J. Mol. Biol.* **1998**, *282*, 1013.
- (114) Roberts, R. J.; Cheng, X. *Annu. Rev. Biochem.* **1998**, *67*, 181.
- (115) Mol, C. D.; Parikh, S. S.; Putnam, C. D.; Lo, T. P.; Tainer, J. A. *Annu. Rev. Biophys. Biomol. Struct.* **1999**, *28*, 101.
- (116) Pearl, L. H. *Mutat. Res.* **2000**, *460*, 165.
- (117) Hollis, T.; Lau, A.; Ellenberger, T. *Mutat. Res.* **2000**, *460*, 201.
- (118) Morikawa, K.; Shirakawa, M. *Mutat. Res.* **2000**, *460*, 257.
- (119) Van Noort, S. J. T.; Orisini, F.; Eker, A. P. M.; Wyman, C.; de Grooth, B.; Greve, J. *Nucleic Acids Res.* **1999**, *27*, 3875.
- (120) MacFarlane IV, A. W.; Stanley, R. J. *Biochemistry* **2001**, *40*, 15203.
- (121) Jordan, S. P.; Jorns, M. S. *Biochemistry* **1988**, *27*, 8915.
- (122) Kim, S. T.; Heelis, P. F.; Okamura, T.; Hirata, Y.; Mataga, N.; Sancar, A. *Biochemistry* **1991**, *30*, 11262.
- (123) Heelis, P. F. *J. Photochem. Photobiol.* **1997**, *38*, 31.
- (124) Okamura, T.; Sancar, A.; Heelis, P. F.; Begley, T. P.; Hirata, Y.; Mataga, N. *J. Am. Chem. Soc.* **1991**, *113*, 3143.
- (125) Kim, S. T.; Heelis, P. F.; Sancar, A. *Biochemistry* **1992**, *31*, 11244.
- (126) Rokita, S. E.; Walsh, C. T. *J. Am. Chem. Soc.* **1984**, *106*, 4589.
- (127) Pac, C.; Miyake, K.; Maasaki, Y.; Yamagichi, S.; Ohno, T.; Yoshimura, A. *J. Am. Chem. Soc.* **1992**, *114*, 10756.
- (128) Heelis, P. F.; Deeble, D. J.; Kim, S. T.; Sancar, A. *Int. J. Radiat. Biol.* **1992**, *62*, 137.
- (129) Kim, S. T.; Volk, M.; Rousseau, G.; Heelis, P. F.; Sancar, A.; Michel-Beyerle, M. E. *J. Am. Chem. Soc.* **1994**, *116*, 3115.
- (130) Deeble, D. J.; Das, S.; Van Sonntag, C. *J. Phys. Chem.* **1985**, *89*, 5784.
- (131) Ogrodnik, A.; Kruger, H. W.; Orthuber, H.; Haberkorn, R.; Michel-Beyerle, M. E. *Biophys. J.* **1982**, *39*, 91.
- (132) Langenbacher, T.; Zhao, X.; Bieser, G.; Heelis, P. F.; Sancar, A.; Michel-Beyerle, M. E. *J. Am. Chem. Soc.* **1997**, *119*, 10532.
- (133) Epple, R.; Wallenborn, E.-U.; Carell, T. *J. Am. Chem. Soc.* **1997**, *119*, 7440.
- (134) Yeh, S. R.; Falvey, D. E. *J. Am. Chem. Soc.* **1991**, *113*, 8557.
- (135) Yeh, S. R.; Falvey, D. E. *J. Am. Chem. Soc.* **1992**, *114*, 7313.
- (136) Kim, S. T.; Sancar, A.; Essenmacher, C.; Babcock, G. T. *J. Am. Chem. Soc.* **1992**, *114*, 442.
- (137) Witmer, M. R.; Altmann, E.; Young, H.; Begley, T.; Sancar, A. *J. Am. Chem. Soc.* **1989**, *111*, 9264.
- (138) McMordie, R. A.; Begley, T. P. *J. Am. Chem. Soc.* **1992**, *114*, 1886.
- (139) McMordie, R. A.; Altmann, E.; Begley, T. P. *J. Am. Chem. Soc.* **1993**, *115*, 10370.
- (140) Burdie, D.; Begley, T. P. *J. Am. Chem. Soc.* **1991**, *113*, 7768.
- (141) Scannell, M. P.; Fenick, D. J.; Yeh, S. R.; Falvey, D. E. *J. Am. Chem. Soc.* **1997**, *119*, 1971.
- (142) Medvedev, D.; Stuchebrukhov, A. A. *J. Theor. Biol.* **2001**, *237*.
- (143) Kay, C. W. M.; Feicht, R.; Schulz, K.; Sadewater, P.; Sancar, A.; Bacher, A.; Möbius, K.; Richter, G.; Weber, S. *Biochemistry* **1999**, *38*, 16740.
- (144) Weber, S.; Möbius, K.; Richter, G.; Kay, C. W. M. *J. Am. Chem. Soc.* **2001**, *123*, 3790.
- (145) Marcus, R. A.; Sutin, N. *Biochim. Biophys. Acta* **1985**, *811*, 265.
- (146) Van Camp, J. R.; Young, T.; Hartman, R. F.; Rose, S. D. *Photochem. Photobiol.* **1987**, *45*, 365.
- (147) Kim, S. T.; Rose, S. D. *Photochem. Photobiol.* **1990**, *52*, 789.
- (148) Hartzfeld, D. G.; Rose, S. D. *Photochem. Photobiol.* **1990**, *52*, 789.
- (149) (a) Pouwels, P. J.; Hartman, R. I.; Rose, S. D.; Kaptein, R. *Photochem. Photobiol.* **1995**, *61*, 575. (b) Ghisla, S.; Massey, V.; Lhoste, J. M.; Mayhew, S. G. *Biochemistry* **1974**, *13*, 589.
- (150) Hartman, R. F.; Rose, S. D. *J. Am. Chem. Soc.* **1992**, *114*, 3559.
- (151) Carell, T.; Epple, R. *Eur. J. Org. Chem.* **1998**, *1245*, 5.
- (152) Epple, R.; Carell, T. *Angew. Chem., Int. Ed.* **1998**, *37*, 938.
- (153) Epple, R.; Carell, T. *J. Am. Chem. Soc.* **1999**, *121*, 7318.
- (154) Lamola, A. A. *Photochem. Photobiol.* **1969**, *9*, 291.
- (155) Helene, C.; Charlier, M. *Biochem. Biophys. Res. Commun.* **1971**, *43*–252.
- (156) Lamola, A. A. *Mol. Photochem.* **1972**, *4*, 107.
- (157) Roth, H. D.; Lamola, A. A. *J. Am. Chem. Soc.* **1972**, *94*, 1013.
- (158) Meistrich, M. L.; Lamola, A. A. *J. Mol. Biol.* **1972**, *66*, 83.
- (159) Jorns, M. S. *J. Am. Chem. Soc.* **1987**, *109*, 3133.
- (160) Carell, T.; Epple, R.; Gramlich, V. *Angew. Chem., Int. Ed. Engl.* **1996**, *35*, 620.
- (161) Okamura, T.; Sancar, A.; Heelis, P. F.; Hirata, Y.; Mataga, N. *J. Am. Chem. Soc.* **1989**, *111*, 5967.
- (162) Heelis, P. F.; Sancar, A.; Okamura, T. *J. Photochem. Photobiol.* **1992**, *16*, 387.
- (163) Gindt, Y. M.; Vollenbrock, E.; Westphal, K.; Sackett, H.; Sancar, A.; Babcock, G. T. *Biochemistry* **1999**, *38*, 3857.
- (164) Heelis, P. F.; Okamura, T.; Sancar, A. *Biochemistry* **1990**, *29*, 5694.
- (165) Kim, S. T.; Heelis, P. F.; Sancar, A. *Methods Enzymol.* **1995**, *258*, 319.
- (166) Essenmacher, C.; Kim, S. T.; Atamian, M.; Babcock, G. T.; Sancar, A. *J. Am. Chem. Soc.* **1993**, *115*, 1602.
- (167) Aubert, C.; Vos, N. H.; Eker, A. P. M.; Brettel, K. *Nature* **2000**, *405*, 586.
- (168) Sancar, G. B.; Smith, F. W.; Lorence, M. C.; Rupert, C. S.; Sancar, A. *J. Biol. Chem.* **1984**, *259*, 6033.
- (169) Li, Y. F.; Heelis, P. F.; Sancar, A. *Biochemistry* **1991**, *30*, 11262.
- (170) Cheung, M. S.; Daizadeh, I.; Stachebrukhov, A. A.; Heelis, P. F. *Biophys. J.* **1999**, *76*, 1241.
- (171) Aubert, C.; Mathis, P.; Eker, A. P. M.; Brettel, K. *Proc. Natl. Acad. Sci. U.S.A.* **1999**, *96*, 5423.
- (172) Weber, S.; Kay, C. W. M.; Mogling, H.; Möbius, K.; Hitomi, K.; Todo, T. *Proc. Natl. Acad. Sci. U.S.A.* **2002**, *99*, 1319.
- (173) Tai, L. A.; Hwang, K. C. *Photochem. Photobiol.* **2001**, *73*, 439.
- (174) Zhong, D.; Zewail, A. H. *Proc. Natl. Acad. Sci. U.S.A.* **2001**, *98*, 11867.
- (175) Tyrrell, R. M.; Webb, R. B.; Brown, M. S. *Photochem. Photobiol.* **1973**, *18*, 249.
- (176) Epple, R.; Carell, T. *J. Am. Chem. Soc.* **1999**, *121*, 7318.
- (177) Sancar, A. *Annu. Rev. Biochem.* **1996**, *65*, 43.
- (178) Wood, R. D. *J. Biol. Chem.* **1977**, *272*, 23465.
- (179) Harm, W.; Hillebrandt, B. *Photochem. Photobiol.* **1962**, *1*, 271.
- (180) Yamamoto, K.; Satake, M.; Shinagawa, H.; Fujiwara, Y. *Mol. Gen. Genet.* **1983**, *190*, 511.
- (181) Sancar, G. B.; Smith, F. W. *Mol. Cell. Biol.* **1989**, *9*, 4767.
- (182) Sancar, A.; Franklin, K. A.; Sancar, G. B. *Proc. Natl. Acad. Sci. U.S.A.* **1984**, *81*, 7397.
- (183) Huang, J. C.; Svoboda, D. L.; Reardon, J. T.; Sancar, A. *Proc. Natl. Acad. Sci. U.S.A.* **1992**, *89*, 3664.
- (184) Selby, C. P.; Sancar, A. *Proc. Natl. Acad. Sci. U.S.A.* **1990**, *87*, 3522.
- (185) Fox, M. E.; Feldman, B. J.; Chu, G. *Mol. Cell. Biol.* **1994**, *14*, 8071.
- (186) Ozer, Z.; Reardon, J. T.; Hsu, D.; Malhotra, K.; Sancar, A. *Biochemistry* **1995**, *34*, 15886.
- (187) Walker, G. C. *Microbial. Rev.* **1984**, *48*, 60.
- (188) Payne, N. P.; Sancar, A. *Mutat. Res.* **1989**, *218*, 207.
- (189) (a) Nishioka, H.; Harm, W. *Mutat. Res.* **1972**, *16*, 121. (b) Mironov, A. S.; Gusarov, I.; Rafikov, R.; Lopez, L. E.; Shatalin, K.; Kreneva, R. A.; Permov, D. A.; Nudler, E. *Cell* **2002**, *111*, 747.
- (190) Sebastian, J.; Kraus, B.; Sancar, G. B. *Mol. Cell. Biol.* **1990**, *10*, 4630.

- (191) Sebastian, J.; Sancar, G. B. *Proc. Natl. Acad. Sci. U.S.A.* **1991**, *88*, 11251.
- (192) Jang, Y. K.; Wang, L.; Sancar, G. B. *Mol. Cell. Biol.* **1999**, *19*, 7630.
- (193) Birell, G. W.; Brown, J. A.; Wu, H. J.; Gidever, G.; Chu, A. M.; Davis, R. W. *Proc. Natl. Acad. Sci. U.S.A.* **2002**, *99*, 8778.
- (194) Yasuhira, S.; Mitani, H.; Shima, A. *Photochem. Photobiol.* **1991**, *53*, 211.
- (195) Mitani, H.; Uchida, N.; Shima, A. *Photochem. Photobiol.* **1996**, *64*, 943.
- (196) Berrocal-Tito, G.; Sametz-Baron, L.; Eichenberg, K.; Horwitz, B. A.; Herrera-Estrella, A. *J. Biol. Chem.* **1999**, *274*, 14288.
- (197) Mitani, H.; Shima, A. *Photochem. Photobiol.* **1995**, *61*, 373.
- (198) Pang, Q.; Hays, J. B. *Plant Physiol.* **1991**, *95*, 536.
- (199) Uchida, N.; Mitani, H.; Shima, A. *Photochem. Photobiol.* **1995**, *61*, 79.
- (200) Suter, B.; Livingstone-Zatche, J. M.; Thoma, F. *EMBO J.* **1997**, *21*, 2150.
- (201) Lamola, A. A. *Photochem. Photobiol.* **1968**, *8*, 601.
- (202) Rahn, R. O.; Hosszu, J. L. *Photochem. Photobiol.* **1969**, *10*, 131.
- (203) Taylor, J.-S.; Cohrs, M. P. *J. Am. Chem. Soc.* **1987**, *109*, 2834.
- (204) Prakash, G.; Falvey, D. E. *J. Am. Chem. Soc.* **1995**, *117*, 11375.
- (205) Brash, D. E.; Franklin, W. A.; Sancar, G. B.; Sancar, A.; Haseltine, W. A. *J. Biol. Chem.* **1985**, *260*, 11438.
- (206) Sancar, A.; Rupp, W. D. *Cell* **1983**, *33*, 249.
- (207) Todo, T.; Takemori, H.; Ryo, H.; Ihara, M.; Matsunaga, T.; Nikaido, O.; Sato, K.; Nomura, T. *Nature* **1993**, *361*, 371.
- (208) Kim, S. T.; Malhotra, K.; Smith, C. A.; Taylor, J.-S.; Sancar, A. *J. Biol. Chem.* **1994**, *269*, 8535.
- (209) Kim, S. T.; Malhotra, K.; Taylor, J.-S.; Sancar, A. *Photochem. Photobiol.* **1996**, *63*, 292.
- (210) Nakajima, S.; Sugiyama, M.; Iwai, S.; Hitomi, K.; Otoshi, E.; Kim, S. T.; Jiang, C. Z.; Todo, T.; Britt, A. B.; Yamamoto, K. *Nucleic Acids Res.* **1998**, *26*, 638.
- (211) Todo, T.; Ryo, H.; Yamamoto, K.; Toh, H.; Inui, T.; Ayaki, H.; Nomura, T.; Ikenaga, M. *Science* **1996**, *272*, 109.
- (212) Sancar, A. *Science* **1996**, *272*, 48.
- (213) Heelis, P. F.; Liu, S. *J. Am. Chem. Soc.* **1997**, 29366.
- (214) Hitomi, K.; Nakamura, H.; Kim, S. T.; Mizukoshi, T.; Ishikawa, T.; Iwai, S.; Todo, T. *J. Biol. Chem.* **2001**, *276*, 10103.
- (215) Wang, Y.; Gasper, P. P.; Taylor, J. S. *J. Am. Chem. Soc.* **2000**, *122*, 5510.
- (216) Joseph, A.; Prakash, G.; Falvey, D. E. *J. Am. Chem. Soc.* **2000**, *122*, 11219.
- (217) Miranda, M. A.; Izquierdo, M. A.; Galindo, F. *Org. Lett.* **2001**, *3*, 1965.
- (218) Cichon, M. K.; Arnold, S.; Carell, T. *Angew. Chem., Int. Ed.* **2002**, *41*, 767.
- (219) Gressel, J. *Photochem. Photobiol.* **1977**, *30*, 749.
- (220) Briggs, W. R.; Huala, E. *Annu. Rev. Cell Dev. Biol.* **1999**, *15*, 33.
- (221) Ahmad, M.; Cashmore, A. R. *Nature* **1993**, *366*, 162.
- (222) Batschauer, A. *Plant J.* **1993**, *4*, 705.
- (223) Lin, C.; Robertson, D. E.; Ahmad, M.; Raibekas, A. A.; Jorns, M. S.; Dutton, P. L.; Cashmore, A. R. *Science* **1995**, *269*, 968.
- (224) Adams, M. D.; Kerlavage, A. R.; Fleischman, R. D.; Fuldner, R. A.; Bult, C. J.; Lee, N. H.; Kirkness, E. F.; Weinstock, K. G.; Gocayne, J. D.; White, O.; et al. *Nature* **1995**, *377*, 3.
- (225) Van der Spek, P. J.; Kobayashi, K.; Bootsma, D.; Takao, N.; Eker, A. P. N.; Yasui, A. *Genomics* **1996**, *37*, 177.
- (226) Miyamoto, Y.; Sancar, A. *Proc. Natl. Acad. Sci. U.S.A.* **1998**, *95*, 6097.
- (227) Yang, H. Q.; Wu, Y. J.; Tang, R. H.; Liu, D.; Liu, Y.; Cashmore, A. R. *Cell* **2000**, *103*, 815.
- (228) Shalitin, D.; Yang, H.; Mockler, T. C.; Maymon, M.; Guo, H.; Whitelam, G. C.; Lin, C. *Nature* **2002**, *417*, 763.
- (229) Cermakian, N.; Pando, M. P.; Thompson, C. L.; Pinchak, A. B.; Selby, C. P.; Gutierrez L.; Wells, D. E.; Cahill, G. M.; Sancar, A.; Sassone-Corsi, P. *Curr. Biol.* **2002**, *12*, 844.
- (230) Stanewsky, R.; Kaneko, M.; Emery, P.; Beretta, B.; Wager-Smith, K.; Kay, S. A.; Rosbash, M.; Hull, J. C. *Cell* **1998**, *95*, 681.
- (231) Helfrich-Forster, C.; Winter, C.; Hofbauer, A.; Hall, J. C.; Stanewsky, R. *Neuron* **2001**, *30*, 249.
- (232) (a) Selby, C. P.; Thompson, C.; Therese, S. M.; Van Gelder, R. N.; Sancar, A. *Proc. Natl. Acad. Sci. U.S.A.* **2000**, *97*, 14697. (b) Van Gelder, R. N.; Gibler, T. M.; Tu, D.; Embry, K.; Selby, C. P.; Thompson, C. L.; Sancar, A. *J. Neurogenet.* **2002**, *16*, 181.
- (233) Thompson, C. L.; Blamer, W. S.; van Gelder, R. N.; Lui, K.; Quadro, L.; Colantuoni, V.; Gottesman, M. E.; Sancar, A. *Proc. Natl. Acad. Sci. U.S.A.* **2001**, *98*, 11708.
- (234) Thresher, R. J.; Vitaterna, M. H.; Miyamoto, Y.; Kazantsev, A.; Hsu, D. S.; Petit, C.; Selby, C. P.; Dawut, L.; Smithies, O.; Takahashi, J. S.; Sancar, A. *Science* **1998**, *282*, 1490.
- (235) (a) Vitaterna, M. H.; Selby, C. P.; Todo, T.; Niwa, H.; Thompson, C.; Fruechte, E. M.; Hitomi, K.; Thresher, R. J.; Ishikawa, T.; Miyazaki, J.; Takahashi, J. S.; Sancar, A. *Proc. Natl. Acad. Sci. U.S.A.* **1999**, *96*, 12114. (b) Palmer, J. D. *The Living Clock*; Oxford University Press: New York, **2002**.
- (236) Ronneberg, T.; Foster, R. G. *Photochem. Photobiol.* **1997**, *66*, 549.
- (237) Czeisler, C. A.; Shanahan, T. L.; Klerman, E. B.; Martens, H.; Brotman, D. J.; et al. *N. Engl. J. Med.* **1995**, *332*, 6.
- (238) Yanovsky, M. Y.; Mazella, M. A.; Casal, J. J. *Curr. Biol.* **2000**, *10*, 1013.
- (239) Van der Horst, G. T.; Muijtjens, M.; Kobayashi, K.; Takano, R.; Kanno, S.; Takao, M.; de Wit, J.; Verkerk, A.; Eker, A. P. M.; van Leenen, D.; Buijs, R.; Bootsma, D.; Hoeijmakers, J. H. J.; Yasui, A. *Nature* **1999**, *398*, 627.
- (240) Kume, K.; Zylka, M. J.; Sriram, S.; Shearman, L. P.; Weaver, D. R.; Jin, X.; Maywood, E. S.; Hastings, M. H.; Reppert, S. M. *Cell* **1999**, *98*, 193.
- (241) (a) Miyamoto, Y.; Sancar, A. *Mol. Brain Res.* **1999**, *71*, 248. (b) Van Gelder, R. N.; Wee, R.; Lee, J.; Tu, D. C. *Science* **2003**, *299*, 222.
- (242) Provencio, I.; Jiang, G.; DeGrip, V. J.; Hayes, W. P.; Rollag, M. D. *Proc. Natl. Acad. Sci. U.S.A.* **1998**, *95*, 340.
- (243) Provencio, I.; Rodriguez, I. R.; Jiang, G.; Hayes, W. P.; Moreira, E. F.; Rollag, M. D. *J. Neurosci.* **2000**, *20*, 600.
- (244) Gooley, J. J.; Lu, J.; Chou, T. C.; Scammell, T. E.; Saper, C. B. *Nat. Neurosci.* **2001**, *12*, 1165.
- (245) Hannibal, J.; Hindersson, P.; Knudsen, S. M.; Georg, B.; Fahrenkrug, J. *J. Neurosci.* **2002**, *22*, RC191:1.
- (246) Berson, D. M.; Dunn, F. A.; Takao, M. *Science* **2002**, *295*, 1070.
- (247) Hattar, S.; Liao, H. W.; Takao, M.; Berson, D. M.; Yau, K. W. *Science* **2002**, *295*, 1065.
- (248) Provencio, I.; Rollag, M. D.; Castrucci, A. M. *Nature* **2002**, *145*, 4.
- (249) Barinaga, M. *Science* **2002**, *295*, 955.
- (250) Ruby, N. F.; Brennan, T. J.; Xie, X.; Cao, V.; Franken, P.; Heller, H. C.; O'Hara, B. F. *Science* **2002**, *298*, 2211.
- (251) Panda, S.; Sato, T. K.; Castrucci, A. M.; Rollag, M. D.; DeGrip, W. J.; Hogenesch, J. B.; Provencio, I.; Kay, S. A. *Science* **2002**, *298*, 2213.
- (252) Ceriani, M. F.; Darlington, T. K.; Staknis, D.; Mas, P.; Petti, A. A.; Weitz, C. J.; Kay, S. A. *Science* **1994**, *285*, 553.
- (253) Rosato, E.; Codd, V.; Mazzotta, G.; Piccin, A.; Zordan, M.; Costa, R.; Kyriacou, C. P. *Curr. Biol.* **2001**, *11*, 909.
- (254) Folta, K. M.; Spalding, E. P. *Plant J.* **2001**, *28*, 333.

CR0204348

